Passive Earth Pressure of Overconsolidated Cohesionless Backfill Overlaying Natural Deposit

Mousa Ibraheem Bani Baker

A Thesis

In

The Department

Of

Building, Civil, and Environmental Engineering

Presented in Partial Fulfillment of the Requirements

for the Degree of Master of Applied Science of Civil Engineering at

Concordia University

Montreal, Quebec, Canada

August 2003

Your file Votre référence
ISBN: 0-612-83861-7
Our file Notre référence
ISBN: 0-612-83861-7

ABSTRACT

Passive Earth Pressure of Overconsolidated Cohesionless Backfill Overlaying Natural Deposit

Mousa Bani Baker

This work presents a theoretical study of passive earth pressure exerted behind a retaining structure, for homogeneous normally consolidated and overconsolidated sands, then for normally and overconsolidated cohesionless backfill overlaying natural deposit. The theoretical data were compared with the available test results for both homogeneous and layered sands.

It was found that the coefficient of passive earth pressure in the case of homogeneous overconsolidated cohesionless soil increases while increasing the internal frictional angle of the sands (ϕ), soil-wall frictional angle (δ_P) and overconsolidation ratio (OCR).

For the case of two layers of different types of cohesionless soils it was found that coefficients of passive earth pressure of strong homogeneous are more than that of strong overlaying weak sands. For the case of weak sand layer overlying a very strong layer, the coefficient of passive earth pressure remains as that of the weak layer and the failure plane will not go through the strong layer. Results are given in terms of design charts, which are simple and easy to use.

Dedication

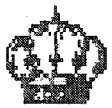

To the Spirit of His Majesty

Al-Sharif Al-Hussein Bin Talal

(The Late King of the H. Kingdom of Jordan)

To His Majesty King Abdullah The Second

The King of Jordan.

To my Parents

"Ibraheem and Rasmyah"
Al-Kattab

My family, and to all people of Peace and

Freedom.

ACKNOWLEDGMENTS

I would like to express my deepest warm thanks to my supervisor

Professor Adel. M. Hanna

"The Distinguished Scholar in Geotechnical Engineering."

For his calm patience and devout help during my research work with his valuable guidance and strong cooperation.

I wish him a great success in continuing his enduring research legacy, which began with the very well known scholar "G. G. Mayerhof". I am deeply indebted for his dedicated support.

Thanks are extended to all friends especially: Salim, Rashad and Khalid, for their moral sincere support.

TABLE OF CONTENTS

LIST OF FIGURES

CHAPTER 2

CHAPTER 3

LIST OF TABLES

LIST OF SYMBOLS

α_i =Angle between the horizontal and the failure surface for each slice.

α_n =The angle at which the logarithmic spiral will depart from the bottom of the wall.

α_o= Inclination of Rankine zone base with horizontal.

β =Backfill inclination with horizontal.

c= Soil cohesion .

ϕ = Angle of shearing resistance.

γ =Unit weight of the soil.

H =Height of the wall.

i =Wall inclination with vertical.

K_{pm} =Passive earth pressure coefficient for Khoury proposed method.

k_i = Passive earth pressure coefficient for the i^{th} slice of the proposed method.

K_{nc} = Coefficient of earth pressure at-rest under normally consolidated state.

K_p= Coefficient of passive earth pressure.

K_o= Coefficient of earth pressure at rest.

k_{PR} =Passive earth pressure coefficient of Rankine zone of the proposed method.

k_i = Passive earth pressure coefficient of the i^{th} slice of the proposed method.

k_{i-1} = Passive earth pressure coefficient of the previous slice $(i-1)$.

K_{nc} = Coefficient of lateral earth pressure at rest under normally consolidation state.

K_o (oc) =The respective values of (K_o) for normally and overconsolidated soils.

$K_{P\gamma E}$, K_{pqE}, K_{PCE} = Seismic passive earth pressure coefficients due to soil density, surcharge load and cohesion of the soil.

λ =Scaling parameter to describe the distribution of interslice force inclinations.

OCR=Overconsolidation ratio.

P_p =Total passive earth pressure.

q=Surcharge load.

δ = Angle of wall-soil friction.

δ_{i-1} = Interslice frictional angle of the previous slice $(i-1)$.

τ = Shear stress.

θ_i = Angle of slice (i) from the backfill surface.

θ_{i-1} = Angle of the previous slice $(i-1)$ from the backfill surface.

θ_o= The angular coordinate of the edge $\overline{OA_o}$ (figure3.2) of the passive Rankine zone.

W= Weight of soil.

CHAPTER 1

INTRODUCTION

1.1 Preface:

Soil can be retained on walls, sheet pile walls, braced cuts, and other similar structures. The design of these structures requires the estimation of the lateral earth pressure, which is a function of the type and amount of wall movement; shear strength of soil, unit weight of the soil, and the drainage condition of the backfill. The prediction of lateral earth pressure has occupied a paramount position in the field of Geotechnical Engineering.

The development of active lateral earth pressure has received a considerable amount of attention. This is due to the fact that the majority of these retaining structures are made to support active earth pressure. However design of many structures requires the evaluation of passive earth pressure.

In the literature, several theoretical and experimental studies are reported to investigate the magnitude and distribution of passive earth pressure behind a retaining wall. Most of these studies considered the shear strength of the soil (the cohesion c and the angle of shearing resistance ϕ) as the only parameters affecting the value of earth pressure, and none of these consider the stress history of the soil as a viable parameter, furthermore no attempts were made to study the layered soils effect on the passive earth pressure.

1.2 Research objectives:

The objectives of this study are to:

1. To develop a theory to predict the passive earth pressure behind walls retaining overconsolidated cohesionless soil.

2. To develop a theory for passive earth pressure for walls retaining overconsolidated backfill overlying natural deposits.

4. To extend the theories developed for the case of inclined backfill material of normally consolidated and overconsolidated cohesionless homogeneous soil and two layers of different types of sands.

5. To compare the results with available experimental test results.

CHAPTER TWO

LITERATURE REVIEW

2.1 General

Passive earth pressures play an important role in soil-structure interaction problems. They provide stabilizing forces for anchor blocks, retaining walls and laterally loaded pile foundations. Quite often passive earth pressures are used to resist lateral movement of structures.

The determination of soil characteristics and accordingly an appropriate coefficient of passive earth pressure is one of the major obstacles in geotechnical engineering. In the literature, several reports can be found dealing with the subject matter, nevertheless, little or none has reported with respect to passive earth pressure of overconsolidated cohessionless soils and the effects of the natural deposit below the backfill.

2.2 HISTORICAL REVIEW

Coulomb (1776) suggested a mathematical solution for the calculation of earth pressure behind a retaining wall, taking into consideration the wall-soil friction angle δ. He assumed that the failure surface was a plane, and the friction forces were uniformly distributed along this rupture surface, he further assumed that the soil is isotropic and homogeneous. Thus, he stated the so-called Coulomb's law, as follows:

$$P_P = \frac{1}{2}\gamma H^2 K_P \quad \text{..... (2.1)}$$

Where,

$$K_p = \frac{1}{\cos\delta} \times \left(\frac{1}{(1/\cos\phi) - (\tan^2\phi + \tan\phi\tan\delta)^{0.5}} \right)^2 \quad \text{.....................} \quad (2.2)$$

Further,

P_P=Total passive earth pressure

γ =Unit weight of the soil (Lb/ft^3).

H =Height of the wall (ft).

K_p= Coefficient of passive earth pressure

δ = Angle of wall-soil friction, and,

ϕ = Angle of shearing resistance.

Rankine (1875) introduced a mathematical solution assuming that the earth mass is in a state of plastic equilibrium. He used the condition of failure defined by the Mohr-Coulomb criterion of the soil to develop a formula for predicting passive earth pressure behind smooth retaining walls ($\delta = 0$) as follows:

$$K_p = \tan^2(45^\circ + \frac{\phi}{2}) \quad \text{..} \quad (2.3)$$

Terzaghi (1941) adopted a method for predicting the passive earth pressure assuming the failure surface consists of two parts, logarithmic spiral and straight plane. Figure 2.1 represents a section through wall face (AB) the location of the point (C) is not known. The curved lower portion (BC) of the failure surface is assumed to be an arc of a logarithmic spiral, the center of which lies on line (CA), the equation of the spiral curve is:

$$r = r_o e^{\theta . \tan \phi} \quad \text{..... (2.4)}$$

Where;

r: Radius of the spiral.

r_o: Starting radius at $\theta=0$.

θ: Angle between r and r_o ,and,

ϕ: Angle of shearing resistance.

The upper straight portion (CD) is a straight plane that makes an angle of $(45-\phi/2)$ with the horizontal. The soil in the zone (KCD) is in Rankine's passive state. A few trials have to be executed in order to determine the lowest value of "Pp".

Caquot and Kerisel (1948) presented a solution for the passive earth pressure acting on the face of a wall, showing that the mobilized value of the wall frictional angle δ depends on the type of wall movement. They developed charts for the values of the passive earth pressure coefficient (K_p) utilizing curved failure surface for granular soil (c = 0) for the case of $\phi = \delta$.

Brinch Hansen (1966) developed a method for correcting the results of conventional passive earth pressure theories for the case of three-dimensional case, based on Ovesen's test results. As a result the passive earth pressure of the 3D may be twice as much as that computed from conventional theory. Consequently, the shape of the wall is an important factor that should be included in the analysis of passive earth pressure resistance.

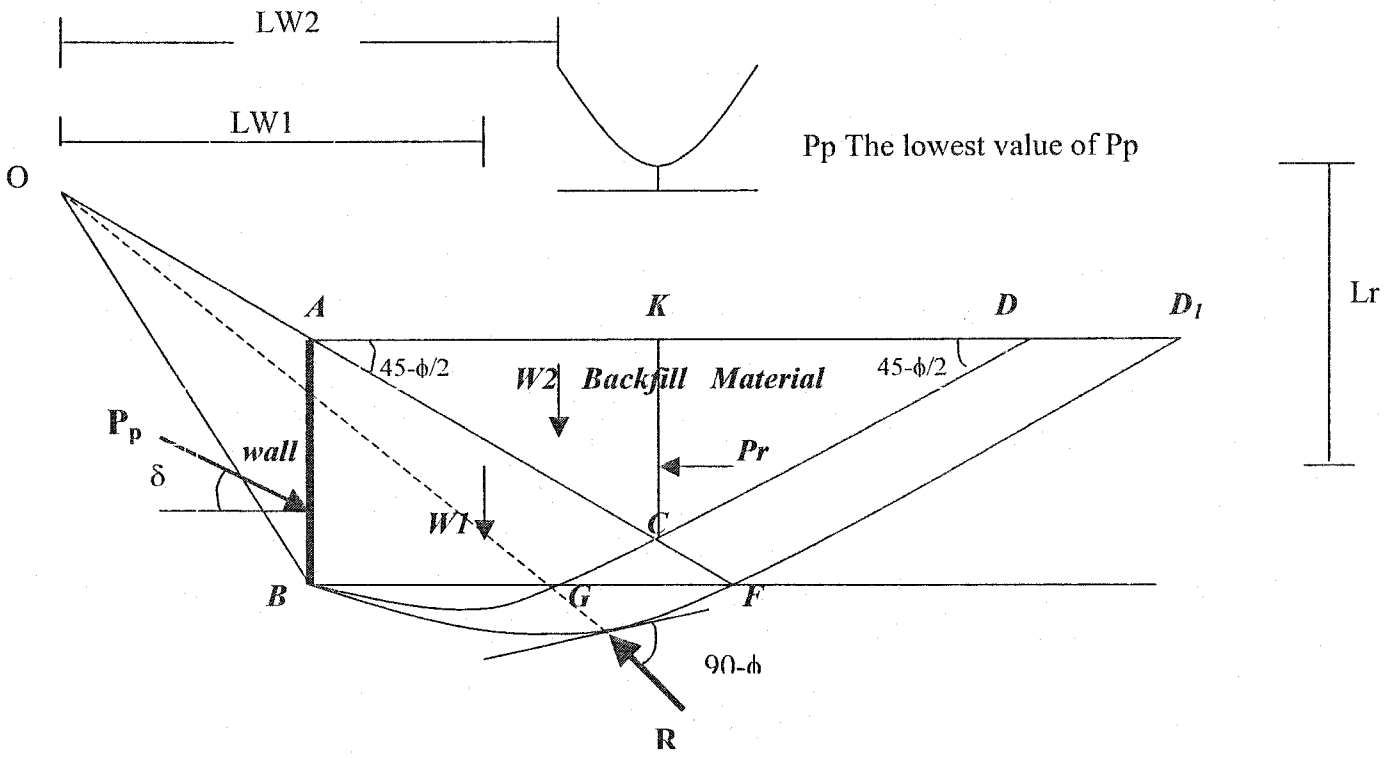

Figure 2.1: Passive earth pressure- Terzaghi's Logarithmic Spiral Method

Narain (1969) investigated experimentally the determination of the rupture surface behind a retaining wall subjected to translation or rotation around its bottom or top for the case of loose or dense sand conditions. He reported that the magnitude of passive earth pressure reached the maximum values when the wall was rotated around its bottom and reached the minimum value when the wall rotated about its top.

James and Brensby (1970) studied the distribution of normal and shear stresses on a rough plane wall rotating about its toe into a mass of dry sand with a horizontal surface. They reported that the earth pressure reaches first its peak value nears the top of the wall where the rupture surfaces were first observed. Furthermore, the magnitude of the passive earth pressures measured in the case of dense sand are much greater than those measured for loose sands.

Shields and Tolunay (1972) adopted Terzaghi's failure mechanism, which is composed of the logarithmic spiral and a plane part. They used the method of slices similar to that of Bishop for slope stability analysis to compute the values of passive earth pressure P_p. They proposed the following equation:

$$P_p = \frac{Pr + \sum W \tan(\alpha + \phi)}{1 - \tan\delta \times \tan(\alpha_n + \phi)} \quad \ldots\ldots\ldots\ldots\ldots\ldots\ldots\ldots (2.5)$$

Where,

$$P_r = \tfrac{1}{2}\gamma H^2 \tan^2(45^\circ + \phi/2) \quad \ldots\ldots\ldots\ldots\ldots\ldots\ldots\ldots (2.6)$$

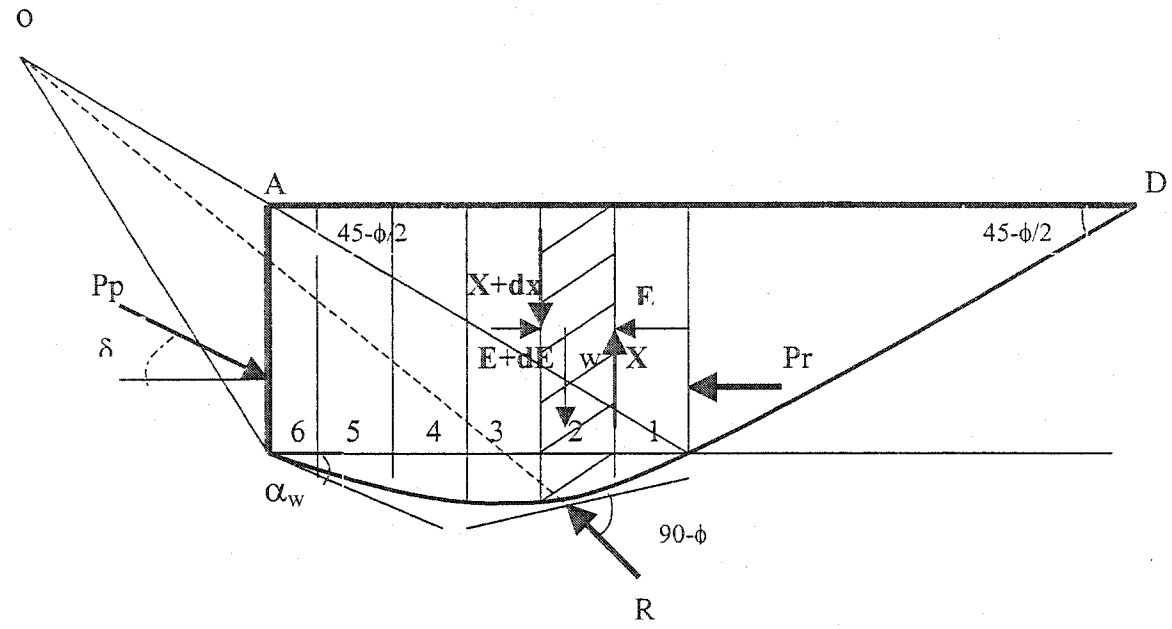

Figure 2.2: Passive earth pressure behind a retaining wall by Shields' and Tolunay slices method.

Where,

Pr = Rankine passive force.

δ = Soil-wall frictional angle.

α_n = Angle between the horizontal and the failure surface for each slice

W =Weight of the slice.

H = Height of the wall.

Worth (1975) proposed the following relationship to calculate the coefficients of earth pressure at rest for over consolidated soils K_o (oc):

$$K_o(oc) = K_o(nc) \times OCR - \left(\frac{\mu}{1-\mu}\right)(OCR-1) \quad \ldots\ldots\ldots\ldots\ldots\ldots (2.7)$$

Where [K_o (nc)] and {K_o (oc)] are the respective values of (K_o) for normally and over consolidated soils, (μ) is the Poisson's ratio, ranging between 0.254 and 0.371. Worth stated that this correlation is only valid for lightly overconsolidated soils; i.e., (OCR) $\leq$ (5).

Meyerhof (1976) proposed a semi-empirical formula for predicting K_o values for over consolidated soils; as follows:

$$K_o\,(oc) = (1 - \sin\phi)\,(OCR)^{0.5} \quad \ldots\ldots\ldots\ldots\ldots\ldots\ldots\ldots\ldots (2.8)$$

Hanna and Ghaly (1990) conducted experimental and theoretical investigations on the effect of (K_o) and (OCR) on the uplift capacity of anchors in sand. They found that the sand placing technique affects the stress level within the sand layer. They presented a

mathematical formula for predicting the coefficients of the earth pressure at rest (K_o). The parameters used are: the angle of shearing resistance ϕ, shape and interlocking of soil particles, soil porosity, modulus of elasticity, elastic and sliding, aging, dilation, compaction effort, stress history and applied stress level.

Khoury (1994) studied the passive earth pressure of overconsolidated homogeneous and layered cohesionless soil experimentally. A wall was tested under horizontal movements, where no rotation was permitted. He proposed the following formula:

$$K_{pm}=K_{pr}.b.\sqrt{OCR} \quad \ldots\ldots\ldots\ldots\ldots\ldots\ldots\ldots (2.9)$$

Where,

Kpm: coefficient of passive earth pressure.

Kpr: coefficient of passive earth pressure by Rankine method for normally consolidated sand.

b : constant

b=1.00 when OCR=1.00

b=2.50 when OCR>1.00

He produced sets of experimental test results for different values of ϕ, δ, and OCR.

Kumar and Subba (1997) developed comprehensive charts based on an assumed failure surface consisted of a logarithmic spiral and a plane parts to determine the magnitudes of passive earth pressure coefficients. They found that the statically admissible inclination of the failure surface with the wall depends on the values of the angles of wall-soil friction (δ), angle of vertical inclination of the wall (ι), and the angle

of shearing resistance (ϕ). They reported that the angle of the failure surface with the horizontal would control the curvature of the failure surface.

They presented the passive earth pressure coefficient for the critical surface as follows;

$$K_P = \frac{P_P \cos\delta}{\left(\frac{\gamma D^2}{2}\right)} \quad \ldots\ldots\ldots\ldots\ldots\ldots (2.10)$$

Where,

P_p = Resultant of passive earth pressure resistance.

D = Height of the wall, and

γ = Unit weight of the soil.

Soubra (2000) investigated the static and seismic passive earth pressure problems using the upper-bound method of limit analysis of a transitional failure mechanism. This mechanism allows the slip surface to develop more freely; hence it leads to smaller upper-bound solutions of the passive earth pressure.

The upper-bound theorem, which considers a perfectly plastic soil model with an associated flow rule, states that the rate of energy dissipation in any kinematically admissible velocity field can be equated with the rate of work done by the external forces. It should be noted that the upper-bound theorem provides an overestimate of passive earth pressure.

He assumed that the failure mechanism is composed of a radial shear zone including "n" triangular rigid blocks. He proposed that the wall is translated horizontally and all the

triangles moved as rigid bodies in the direction, which make an angle ϕ with the discontinuity lines d_ι (ι =1,2,.....n) .

He presented the following equation:

$$P_{P\gamma E} = K_{P\gamma E}(\theta_i, \beta_i)\frac{\gamma H^2}{2} + K_{PqE}(\theta_i, \beta_i)qH + K_{PCE}(\theta_i, \beta_i)cH \quad \ldots\ldots\ldots (2.11)$$

Where,

$K_{P\gamma E}$, K_{pqE}, K_{PCE} = the seismic passive earth pressure coefficients due to soil density, surcharge load and cohesion of the soil. At a static passive earth pressure coefficient with no surcharge load and cohesionless sand then K_{pqE}= K_{PCE} = 0. Then the passive earth pressure is equal to $K_{P\gamma E}$.

q = Surcharge load (Lb/ft^2).

H = Length of the wall (ft).

γ = Unit weight of the soil (Lb/ft^3).

C = Cohesion factor (PSF).

In which the seismic earth pressure coefficients $K_{p\gamma E}$, K_{pqE}, and K_{PCE} can be expressed in terms of angles θ_ι and β_ι as shown in Figure 2.3.

Furthermore, he found that the most critical passive earth pressure coefficients could be obtained by minimization of these coefficients with regard to the mechanism parameters.

The upper–bound solution can be improved by increasing the number of rigid blocks, the reduction in the Kpγ value decreases with an increase in "n" value. The same trend for the coefficients K_{pq} and K_{pc} was observed.

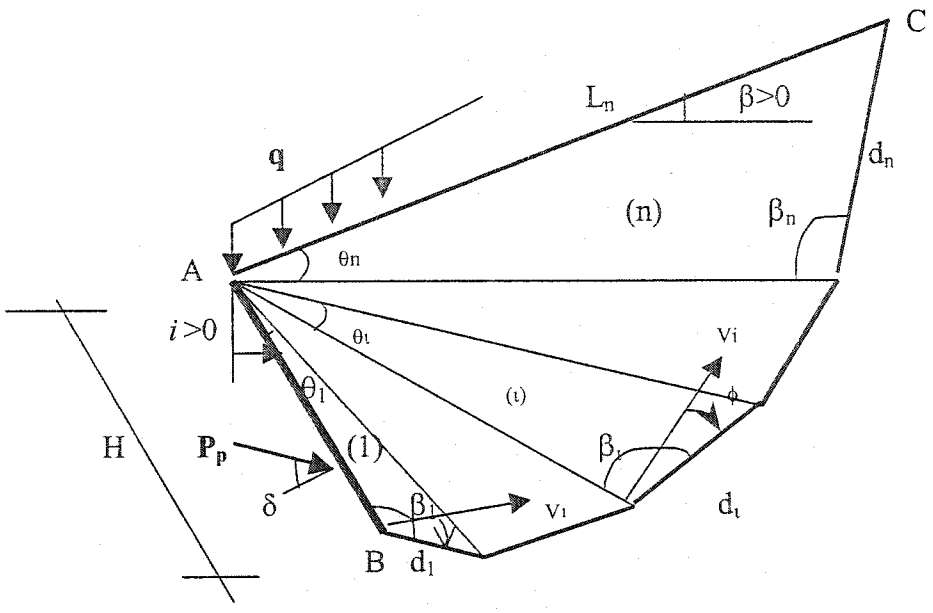

Figure 2.3: Failure mechanism for static and seismic earth pressure analysis.

(Soubra, 2000).

Yong and Qian (2000) proposed a procedure for determining the passive earth pressure coefficients using triangular slices within the framework of the limit equilibrium method. The soil mass behind the wall is divided into a series of triangular slices. The interslice forces are expressed in terms of a force coefficient. They derived equations for solving the interslice coefficients, and then the passive earth pressure coefficient is determined by using the principle of optimality (the critical inclinations of the slice bases, minimum interslice force coefficients).

They considered a wall inclined at an angle ι to the vertical, retaining cohesionless backfill having a slope angle of β and stated that ι is positive when the wall is inclined toward the backfill, and β is positive when the surface of the backfill slope upwards from the top of the wall, as shown in Figure 2.4.

They divided the failure zone into two zones, the passive Rankine zone and the deformation zone as the shear deformation generally occurs within this zone, which is divided into n triangular slices .The overall location of the failure surface is dependent on the inclinations of these slice bases.

They considered force equilibrium for the passive Rankine zone, as follows:

$$k_{PR} = \frac{\sin(\theta_o + \alpha_o)\sin(\theta_o)\sin(\alpha_o + \phi)}{\sin(\alpha_o)\sin(\theta_o + \alpha_o + 2\phi)} \quad \ldots\ldots\ldots\ldots (2.12)$$

Selecting the *ith* slice as a typical slice, then the force P_i is expressed as:

$$P_\iota = \tfrac{1}{2}\, k_i\, \gamma\, \overline{OA_i}^2 \quad \ldots\ldots\ldots\ldots\ldots\ldots\ldots\ldots (2.13)$$

Where;

$$k_i = \left(\frac{\sin(\theta_i + \alpha_i)}{\sin(\theta_{i-1} + \alpha_i)\sin(\theta_i + \alpha_i + \delta_i + \phi)} \right) \times$$

$$\left(k_{i-1} \frac{\sin(\theta_i + \alpha_i)\sin(\theta_{i-1} + \alpha_i + \delta_{i-1} + \phi)}{\sin(\theta_{i-1} + \alpha_i)} + \sin(\theta_i - \theta_{i-1})\sin(\alpha_i + \phi) \right) \quad \ldots. (2.14)$$

For the last slice, i.e, the soil wall interface, the resultant passive earth pressure, $P_p = P_n$, is calculated as:

$$Pp = (½)\, k_n \gamma\, \overline{OA}_n^2 \quad \ldots\ldots\ldots\ldots\ldots\ldots\ldots\ldots\ldots\ldots\ldots\ldots (2.15)$$

Then

$$K_P = \frac{P_P}{0.5\gamma H^2} \quad \ldots\ldots\ldots\ldots\ldots\ldots\ldots\ldots\ldots\ldots\ldots\ldots\ldots\ldots (2.16)$$

Where H is the vertical wall height.

It can be noted that K_p for the three mentioned theories in Table 2.1 are almost the same when soil-wall frictional angle is 0, and the difference increases with the increase of angle of shearing resistance and the soil-wall frictional angle.

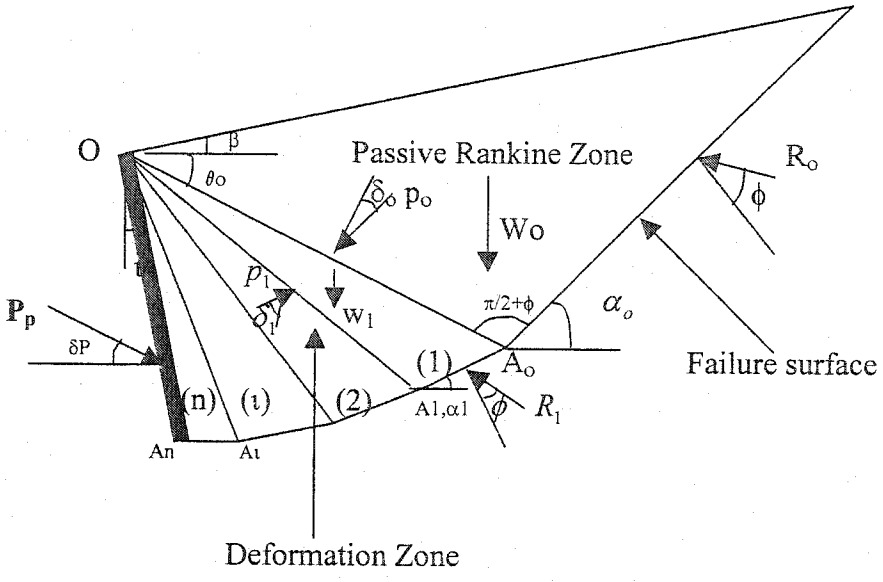

Figure 2.4: Discretization of the sliding mass and related forces.

(Yong and Qian, 2000)

Table 2.1: Comparison between the values of the coefficients of passive earth pressure as deduced by different theories

(horizontal backfill, vertical or inward-inclined wall)

($\beta = 0°$, $Kp = P_p/0.5\gamma H^2$)

(After Yong and Qian, 2000)

ϕ (°)	δ (°)	$\iota = 0°$			$\iota = 10°$			$\iota = 20°$		
		Coulomb	Sokolovski	Yong	Coulomb	Sokolovski	Yong	Coulomb	Sokolovski	Yong
10	0	1.42	1.42	1.42	1.36	1.35	1.36	1.36	1.34	1.35
	5	1.57	1.56	1.55	1.48	1.47	1.48	1.46	1.46	1.45
	10	1.73	1.66	1.66	1.6	1.57	1.57	1.58	1.53	1.53
20	0	2.04	2.04	2.04	1.84	1.83	1.83	1.75	1.71	1.72
	10	2.64	2.55	2.56	2.27	2.26	2.26	2.08	2.08	2.08
	20	3.52	3.04	3.06	2.86	2.65	2.66	2.49	2.42	2.41
30	0	3	3	3	2.54	2.46	2.51	2.27	2.16	2.21
	15	4.98	4.62	4.61	3.8	3.73	3.73	3.16	3.16	3.16
	30	10.1	6.55	6.59	6.45	5.19	5.2	4.76	4.3	4.3
40	0	4.6	4.6	4.59	3.59	3.47	3.53	3.02	2.84	2.89
	20	11.77	9.69	9.66	7.36	6.98	6.95	5.34	5.32	5.3
	40	92.58	18.2	18.24	25.65	12.68	12.72	12.82	9.32	9.34

Wang (2000) used the same concept of Coulomb, namely that the earth pressure against the back of retaining wall is due to the thrust exerted by a sliding wedge of soil between the back of the wall and a plane which passes through the bottom edge of the wall and has an inclination of θ. A differential equation of first order is set up by considering the equilibrium of the forces on an element of the wedge, and then he obtained a theoretical result for the unit earth pressure on a retaining wall given in the following formula:

$$P_Y = \left[q - \frac{\gamma H}{ak-2}\right]\left[\frac{H-y}{H}\right]^{aK-1} + \left[\frac{\gamma H}{ak-2}\right]\left[\frac{H-y}{H}\right] \quad \text{.....(2.17)}$$

And $P_X = KP_Y$

Where,

K = lateral pressure coefficient, and,

$$a = \frac{\cos(\theta-\phi-\delta)\tan\theta}{\sin(\theta-\phi)\cos\delta} \quad \text{..... (2.18)}$$

The resultant earth pressure on the wall is:

$$P = \sqrt{\left(P_X^2 + T_1^2\right)} = \left[qH + \frac{1}{2}\gamma H^2\right]\left[\frac{\sin(\theta-\phi)\cot\theta}{\cos(\theta-\phi-\delta)}\right] \quad \text{..... (2.19)}$$

Where, $T1 = \int_0^H \tau_1 dy$.

Also he found that the height of application of resultant earth pressure in case where the earth pressure is linearly distributed is:

$$H_P = \frac{1}{3}H\left(\frac{3q+\gamma H}{2q+\gamma H}\right) \quad \text{..... (2.20)}$$

If q = 0 then $H_p = \frac{H}{3}$

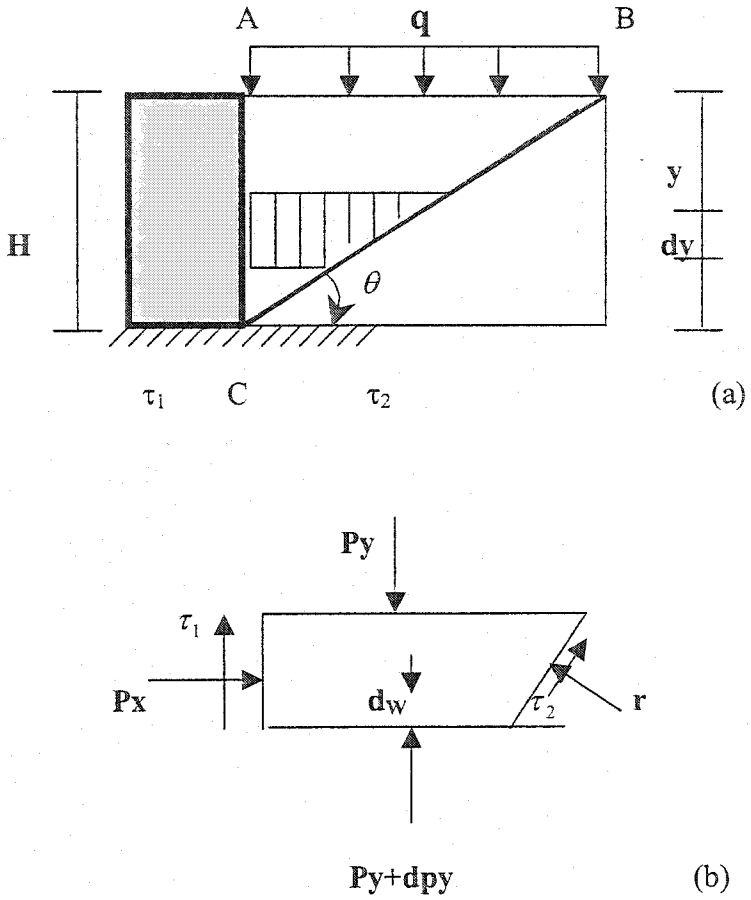

Figure 2.5: Failure mechanism proposed by Wang (2000) subjected to passive earth pressure.

Soubra and Regenass (2000) investigated the 3D nature of the passive earth pressure problem by upper-bound method of the limit analyses theory. Three kinematically admissible failure mechanisms are considered for the calculation schemes referred to as M_1, Mn, and M_{nt}. They investigated the increase of the passive pressures due to the decrease of the wall breadth using the kinematical approach of the limit analyses theory. The following assumptions were considered:

1. The wall of the dimensions b×h (b= breadth; h= height) is vertical, and the backfill is horizontal.

2. A transnational soil-wall movement is assumed.

3. The soil is homogenous and isotropic.

4. The angle of friction δ at the soil structure interface is assumed to be constant.

5. A tangential adhesive force P_a is assumed to act at the soil structure interface the intensity of this force is c ($\tan\delta/\tan\phi$) bh.

6. The velocity at the soil-structure interface is assumed to be tangential to the wall.

By equating the total rate of external work to the total rate of energy dissipation along the different velocity discontinuities, they obtained the following equation:

$$P_p = K_{p\gamma} . \gamma . (h^2/2) . b + K_{pq} . q . h . b + K_{pc} . c . h . b \quad \ldots\ldots\ldots\ldots\ldots\ldots\ldots\ldots\ldots\ldots (2.21)$$

Where $K_{p\gamma}$, K_{pq}, and K_{pc} are the passive earth pressure coefficients due to soil weight, surcharge loading, and cohesion, respectively. These coefficients are functions of ϕ, δ, and b/h.

Yung, Ying and Tsang (2002) present experimental data of earth pressure acting against a vertical rigid retaining wall, which moved toward a mass of dry sand. The backfill had been placed in lifts to achieve relative densities of 38, 63, and 80%, and they found based on the experimental results that Coulomb and Terzaghi solutions calculated with the peak internal friction angle significantly had overestimated the ultimate passive thrust for the retaining wall filled with dense sand. They inferred that the passive earth pressure is related to the shearing resistance of the soil along the rupture surface. Then they concluded that for the wall with loose backfill, the earth pressure increased with increasing wall movement and eventually reached a limiting passive earth pressure .For the wall with dense backfill, the earth pressure coefficient increased with increasing wall movement, after reaching a peak value, the earth pressure coefficient decreased with increasing wall movement, and finally reached an ultimate value.

2.3 Discussion and scope of research:

It can be reported that here is little or no research can be found to solve the problem stated. There are evidences that overconsolidation of the soil, has a significant effect on the passive earth pressure, as the value of K_p increases considerably due to an increase of OCR. Furthermore, the presence of the natural deposit below the backfill may change drastically the produced coefficient of passive earth pressure.

Chapter 3

Theoretical Model

3.1 General

In practice, Coulomb's (1776) and Rankine's (1857) theories are widely used in for predicting the passive earth pressure on retaining walls. The logarithmic spiral theory is less popular due to its complexity; however, it provides predictions that are more accurate than those given by the empirical formulas. A number of investigators have developed alternative procedures using the logarithmic spiral theory for evaluating the coefficient of passive earth pressure (K_P). The results confirmed the accuracy of the logarithmic spiral theory for a wide range of the angle of shearing resistance ϕ, and the angle of wall-soil friction, δ_p.

Table 3.1 presents the coefficients of passive earth pressure as deduced from different theories. It can be noted that the theory of Soubra (2000) and theory of Yong (2000) have almost produced the same results. Also, the results of Rankine's theory which is valid for smooth retaining walls ($\delta_p = 0$) were given. Caqout and Kerisel's theory gives good estimates for the case of $\phi = \delta_p$ and the theory of Shield and Tolunay (1973) for the case of $\delta_p / \phi < 1.0$ are given. It can be noted that, when the ratio δ_p/ϕ becomes closer to 1.0 Shield's and Tolunay's method underestimates the coefficient of the passive earth pressure. As the value of δ_p increases, Coulomb's theory predicts increasingly erroneous values of passive earth pressure coefficients. It can be noted that Yong and Qian's theory provide better predictions under all these conditions, as it takes into consideration the effects of all these variables.

Table 3.1: Coefficients of passive earth pressure, K_p for normally consolidated cohesionless soils.

ϕ	δ	Caqout and Kerisel (1948)	Rankine (1857)	Coulomb (1776)	Shields and Tolunay (1973)	Soubra (2000)	Yong and Qian (2000)
20	0	------	2.040	2.040	2.040	2.040	2.040
	10	------	-----	2.640	2.520	2.580	2.560
	20	3.000	-----	3.520	2.880	3.120	3.060
30	0	-----	3.000	3.000	3.000	3.000	3.000
	15	-----	-----	4.980	4.450	4.690	4.610
	30	6.450	-----	10.10	5.770	6.860	6.590
40	0	-----	4.599	4.600	4.600	4.600	4.590
	20	-----	-----	11.770	9.080	9.990	9.660
	40	17.500	-----	92.580	14.420	19.620	18.240

"The application of vibratory densification produce an overconsolidation effect on the sand, so the produced sand bed may not be as normally consolidated or homogeneous, it will be most likely an overconsolidated, nonhomogeneous." After Hanna and Saad. ASTM "Geotechnical Testing Journal (2001)."

This confirms that the coefficient of passive earth pressure will not remain the same after compaction. This case appears when there is an excavation and a bridge is needed to be constructed, then the soil which is behind the bridge to be replaced and compacted in layers which will produce a new case of overconsolidated sand overlaying deep natural deposit as shown in figure (3.1).

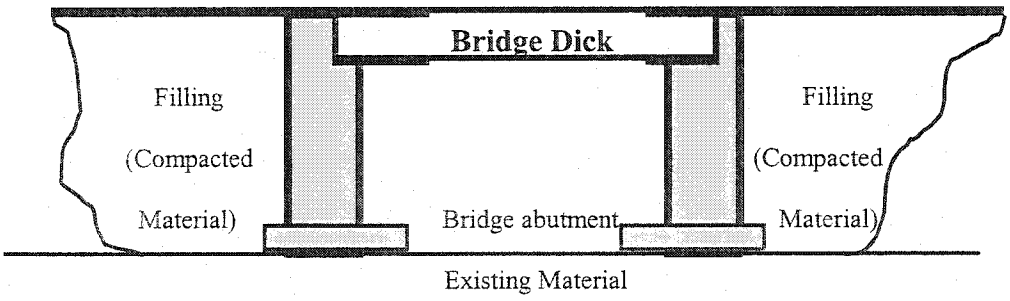

Figure 3.1: Filling behind retaining walls in bridges.

In this chapter, the theoretical model developed by Yong and Qian (2000) to predict the coefficient of passive earth pressure of normally consolidated cohesionless soils is modified for the case of overconsolidated cohesionless horizontal and inclined backfills behind walls. Furthermore, the theoretical model is further extended to predict the coefficient of passive earth pressure for the case of normally consolidated or overconsolidated cohesionless backfill overlaying deep deposit.

3.2 Homogeneous Cohesionless Soil Behind Retaining Walls:

3.2.1 Method of Triangular Slices:

Consider a vertical wall with horizontal backfill made of cohesionless soil as shown in Figure 3.2. The angle of shearing resistance of the backfill is ϕ, the unit weight of the backfill is γ, and the frictional angle of the soil-wall interface is δ_p. Under the passive stress condition, it is assumed that the backfill will develop a failure plane, which consists of curved and plane portions. As the wall is being pushed toward the backfill, the sliding surface is developed, making an angle of 45°-$\phi/2$ with the horizontal as shown in Figure 3.3. The failure plane, the backfill surface and the wall itself are bounding the sliding mass. In this analysis, the sliding mass is divided into two zones, the deformation zone and the Rankine zone and they are well described in Figures 3.2 and 3.3. The deformation zone will be subdivided into (n) number of triangular slices, where each will be analyzed using the limit equilibrium method of analysis. The Rankine zone will be regarded as one solid mass, which behaves as one rigid body. The angular coordinate of the edge $\overline{OA_o}$

(Figure3.3) of the Rankine zone, θ_o, and the inclination of the base α_o can be determined according to Rankine, as follows:

$$\theta_o = 45^o - \frac{\phi}{2} \quad \text{.....(3.1)}$$

$$\alpha_o = \frac{\pi}{2} - \theta_o - \phi \quad \text{..... (3.2)}$$

Yong and Qian (2000) have developed Equation 3.3 to predict the coefficient of passive earth pressure for homogeneous normally consolidated sand by considering force equilibrium for the passive Rankine zone, as follows:

$$k_{PR} = \frac{\sin(\theta_o + \alpha_o)\sin(\theta_o)\sin(\alpha_o + \phi)}{\sin(\alpha_o)\sin(\theta_o + \alpha_o + 2\phi)} \quad \text{..... (3.3)}$$

Where,

ϕ : Angle of shearing resistance of the soil of the backfill.

The boundary conditions of Rankine zone were evaluated and used to calculate the stresses on the first slice in the deformation zone. Thus, by considering force equilibrium for the first slice in the deformation zone, the coefficient of passive earth pressure is given as:

$$k_1 = \left(\frac{\sin(\theta_1 + \alpha_1)}{\sin(\theta_0 + \alpha_1)\sin(\theta_1 + \alpha_1 + \delta_1 + \phi\ )} \right) \times$$

$$\left(k_{PR} \frac{\sin(\theta_1 + \alpha_1)\sin(\theta_0 + \alpha_1 + \delta_1 + \phi)}{\sin(\theta_0 + \alpha_1)} + \sin(\theta_1 - \theta_0)\sin(\alpha_1 + \phi) \right) \quad \text{.....(3.4)}$$

Where;

ϕ : Angle of shearing resistance of the soil.

α_1 : First slice base inclination

δ_1 : Interslice frictional angle for the first slice.

θ_1 : Angle of the first slice from the backfill surface.

Then the stresses will be transformed to the rest of the slices one after another, until it reaches the last slice (n). A typical slice (i) is given in Figure 3.4 in which the forces were applied, that take into consideration all the body forces on the slice. The point of action of force R_i acting on the slice base is assumed to be at the centroid of the slice base, which makes an angle of ϕ with the normal to the slice base

The point of action of the force P_i and P_{i-1} should lie at the lower one-third point of the radial lines $\overline{OA_i}$ and $\overline{OA_{i-1}}$ respectively according to the theory of plasticity. Then the magnitudes of forces P_i, R_i, and w_i, the locations of their points of action and the magnitude of the lateral force P_p and its location can be determined by satisfying the moment equilibrium condition of the deformation zone.

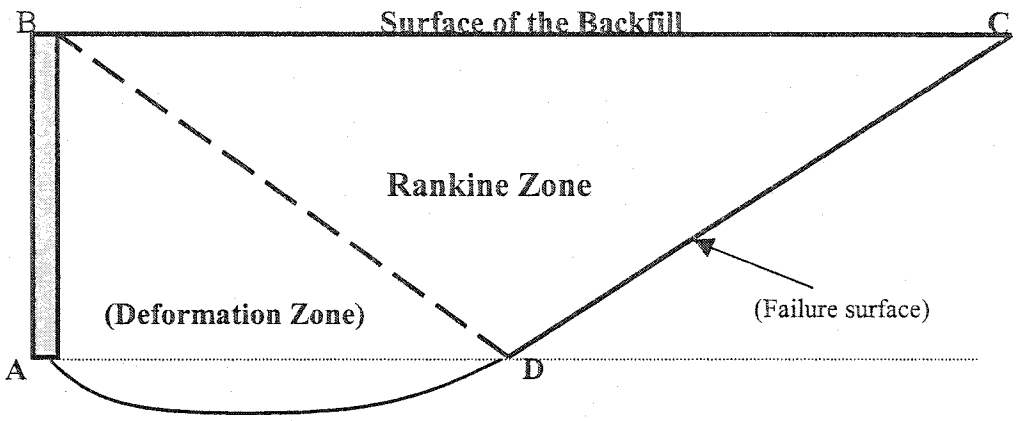

Figure 3.2: Failure mechanism behind a retaining wall subjected to passive conditions, showing Rankine and the Deformation zones.

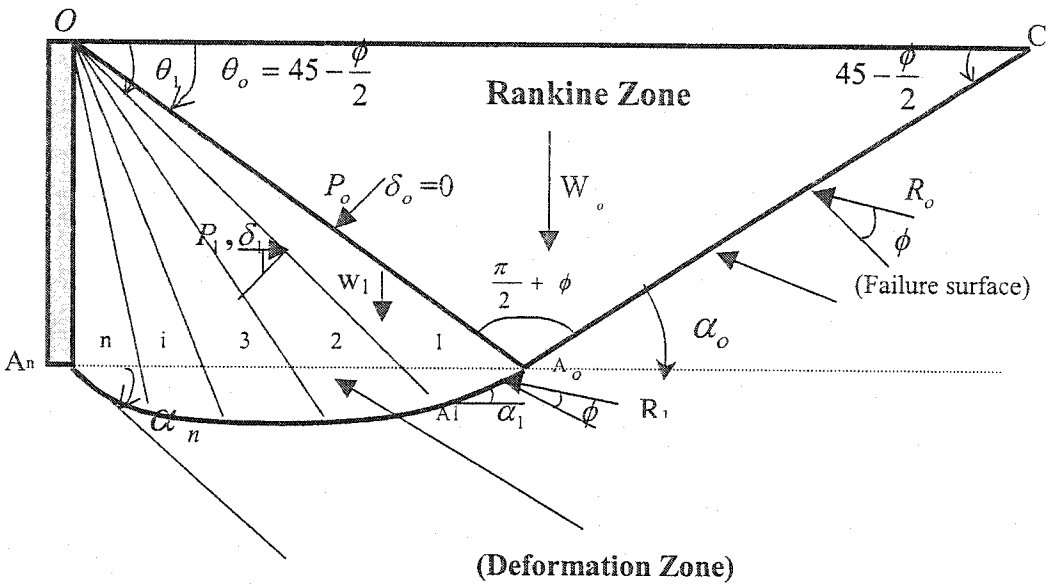

Figure 3.3: Failure mechanism behind a retaining wall subjected to passive conditions.

For the last slice (n) the passive earth pressure, K_n, will be the same applied on the wall itself, K_p. There are unknowns for the optimization problem i.e., (n) slice base inclinations, α_1, α_2... α_n. The process of determining slice base inclination and the interslice force coefficients may be regarded as a multistage decision problem, in which $k_{\iota's}$ are state variables and $\alpha_{\iota's}$ are decision variables. It could be noticed that k_ι is related to the immediately previous coefficient $k_{\iota-1}$ and current slice base inclination α_ι, and independent of all the other coefficients and slice base inclinations. That means each decision in the above process only influences the next decision.

With the value of k_{PR} known, the minimization of k_1 with respect to α_1 may be readily achieved by a procedure of trial and error or some simple optimization techniques that will be used in the proposed method using mathematical formulas that will give the minimum passive earth pressure coefficient.

The process is repeated for k_2, α_2 ..... k_n, α_n. With α_n , α_{n-1},....., α_1 , α_o known the critical failure surface is immediately traced from the toe of the wall out to the backfill surface. Such minimization of K_p along with determination of the critical failure surface is straightforward; since it consists of n stages of minimization of k_ι involving only one unknown, say α_ι at each stage in order that K_n or K_p achieves a minimum.

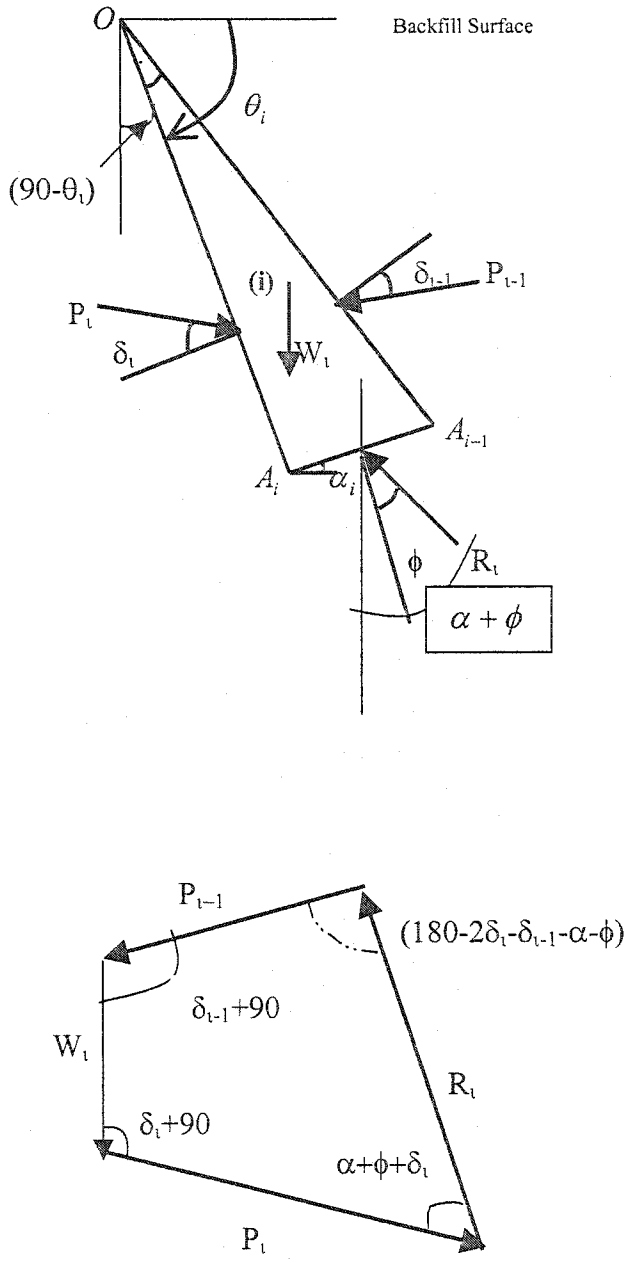

Figure 3.4: Slice forces hodograph for a typical slice (i).

For the remaining slices the coefficient of passive earth pressure is given as the following:

$$k_i = \left(\frac{\sin(\theta_i + \alpha_i)}{\sin(\theta_{i-1} + \alpha_i)\sin(\theta_i + \alpha_i + \delta_i + \phi)} \right) \times$$

$$\left(k_{i-1} \frac{\sin(\theta_i + \alpha_i)\sin(\theta_{i-1} + \alpha_i + \delta_{i-1} + \phi)}{\sin(\theta_{i-1} + \alpha_i)} + \sin(\theta_i - \theta_{i-1})\sin(\alpha_i + \phi) \right) \quad \ldots\ldots\ldots (3.5)$$

For ι = 2, 3, 4...n.

Where;

ϕ : Angle of shearing resistance of the soil.

α_i : *ith* Slice base inclination.

δ_i : Interslice frictional angle of slice (i).

δ_{i-1} : Interslice frictional angle of the previous slice ($i-1$).

θ_i : Angle of slice (i) from the backfill surface.

θ_{i-1} : Angle of the previous slice ($i-1$) from the backfill surface.

k_{i-1} : Passive earth pressure coefficient of the previous slice ($i-1$).

The procedure followed by Yong and Qian (2000) is illustrated in the following steps:

A. Before determining the location of the critical failure surface, the inclinations of the slice bases are assumed to be known (the overall failure surface is dependent on the inclinations of these slice bases the determination of which is a primary part of the problem) denoted by α_o, α_1, α_2, α_i,.....α_n. The inclinations of interslice forces P_o, P_1, ..., P_i , ..., P_n ($P_n = P_p$, which is the resultant of lateral earth force) on the slice boundaries are assumed to be δ_o,δ_1 ,...δ_i..... ,δ_n (the angle between the interslice force direction and the normal to the slice boundary).

B. Considering force equilibrium for the passive Rankine's zone, the force P_r is immediately obtained in the following form:

$$P_r = \tfrac{1}{2} k_r \gamma \overline{OA_n}^2 \quad \text{..... (3.6)}$$

C. The coefficient of passive earth pressure K_p can be determined by calculating the interslice force coefficient (k_i) step by step. Assuming that inclinations of interslice forces are specified, the purpose is to locate the critical failure surface in order that K_p achieves a minimum. It could be seen that K_p is independent of the wall height, H.

As in slope stability analysis by the method of slices, calculating the lateral earth force using triangular slices is also an indeterminate problem. In this method a function $\delta(\theta)$ is

employed which includes a scaling parameter λ to describe the distribution of interslice force inclinations:

$$\delta(\theta_i) = \frac{(\delta_p - \phi)(\theta_i - \theta_o)}{(\theta_n - \theta_o)} + \phi + \lambda \sin\left[\frac{\pi(\theta_i - \theta_o)}{(\theta_n - \theta_o)}\right] \quad \ldots\ldots\ldots\ldots\ldots\ldots (3.7)$$

Where;

ϕ : Angle of shearing resistance of the soil.

θ_i : Angle of slice (i) from the backfill surface.

θ_n : Angle of the last slice (n) from the backfill surface.

λ : A scaling parameter.

θ_o : Previously determined. π =3.14.

The scaling parameter λ is used to enable the condition of moment equilibrium for the sliding soil mass to be satisfied. In the solution process, an initial value of λ must be assumed and then the interslice force inclinations are specified. Then the critical inclinations of the slice bases and the interslice force coefficients are determined systematically by the procedure of trial and error to get Kp minimum.

The above method of triangular slices is implemented into a computer program of MATLAB 6.1 (which is given in the appendix) using some changes that will facilitate and speed up the process of calculating Kp instead of the long procedure of trial and error. These changes are:

1. Due to the wall roughness, vertical shear stress was applied on the soil close to the wall; this shear stress will dissipate in between the first slice and Rankine zone along the radial line $\overline{OA_o}$. By definition, this zone ($\overline{OA_o}$C) as shown in figure (3.2) is in Rankine passive state .The interslice angle of friction varied between values of zero at Rankine's zone to the maximum of wall-soil friction angle behind the wall, δ_p. The relationship was assumed to be linear as follows:

$$\delta_{(i)} = \delta_{(o)} + \frac{i}{n} \times \delta_{(p)} \quad \text{..... (3.8)}$$

2. The deformation zone $\overline{OA_o}A_n$ is subdivided into (n) number of slices that have equal sub-angles, then, taking the horizontal backfill as a datum, the values of $\theta_{(i)}$ increase linearly according to the following proposed formula:

$$\theta_{(i)} = \left(\frac{\pi}{2} - \theta_{(o)}\right) \times \frac{i}{n} + \theta_{(o)} \quad \text{..... (3.9)}$$

Value of θ_o was given in Equation 3.1, ($\theta_o = \pi/4 - \phi/2$).

In order to determine the minimum coefficient of passive earth pressure, the angle θ_o was varied over a wide range.

For the last slice, n (next to the wall), the angle at which the logarithmic spiral will depart from the bottom of the wall is calculated using Shield's and Tolunay's formula method as follows:

$$\alpha_n = \left(\frac{1}{2}\right)\left[\arccos\left\{\cos(\phi - \delta_p) - \frac{\sin(\phi - \delta_p)}{\tan\phi}\right\} - \phi - \delta_p\right] \quad \text{..... (3.10)}$$

4. The spiral logarithmic curve in the deformation zone itself is subdivided into two parts by assuming the base of each slice in the deformation zone is a part of parabolic function, which is close to the second order function. That means the slice base inclinations are the tangents of that function, that gives a tangent somewhere else which is equal to zero, meaning it is horizontal. In this way two assumptions are made due to some simple optimization techniques and by means of trial and error, many iterations are done. Results obtained here are compared with those given by Yong and Qian (2000) in order to use them to minimize the work that is needed to find out the coefficient of passive earth pressure instead of the long iteration procedure that is used by Yong and Qian. These formulas give the best fit for the passive earth pressure coefficients along the curved plane zone, after this failure plane could be traced.

5. The first one is these angles in the right side of the horizontal tangent of the curve *ED* (Figure 3.4), these angles are related to Rankine failure plane inclination with horizontal $\alpha_{(o)}$, and are given in the following formula:

$$\alpha_{(r,i)} = \left(\frac{i-10}{0.5\times n}\right)^2 \times \alpha_{(o)} \qquad (3.11)$$

The second one is that angles are in the left side of the horizontal tangent of the curve *EA* (Figure 3.4), these angles are related to last slice (n) base inclination $\alpha_{(n)}$, and are given in the following formula:

$$\alpha_{(l,i)} = \left(\frac{i-10}{0.5\times n}\right)^2 \times \alpha_{(n)} \quad \text{..... (3.12)}$$

These formulas are dependent on the number of slices that are used in the optimization. Many trials were done to find the passive earth pressure coefficients by comparing the results with the results given by Yong and Qian (2000), as the number of slices changes while the horizontal tangent in the lower portion remains in the same position. But the formula could change due to change on the number of slices so we have to determine the slice number that will make the horizontal tangent, until we get proper results that match the given ones.

Table 3.2 shows the results of these two formulas for a case of soil backfill with angle of shearing resistance equal to 10 and frictionless wall. The deformed zone is sub-divided into 12 slices and all base inclination angles were given in Radians.

It was assumed that the minimum passive earth pressure was obtained when the passive Rankine zone makes an angle of $\theta_o = 45 - \frac{\phi}{2}$, which was also assumed by Yong and Qian (2000) and already assumed by Rankine (1857). In this study this assumption is tested, by letting the failure plane move due to the increase and decrease of the angle θ_o. That will result in a change of the failure plane shape, as illustrated in Figure 3.5. A specific sub-code is written using the computer program to do this task, and some of these results are illustrated in Figure 3.6 where, ϕ =10, δ_p=10. Then it could be seen that the minimum passive earth pressure coefficient is obtained when θ_o is equal to 40° which gives K_p

equal to 1.66 which is equal to that value given by Yong and Qian (2000). That means at a value of $\theta_o = \frac{\pi}{4} - \frac{\phi}{2}$, the passive earth pressure coefficient is at its minimum value. In this modification it can be verified that k_{PR} has already been minimized with respect to α_o by equation 3.3.

Table 3.3 shows a comparison of both the new study and Yong's and Qian's method for a wide range of soil-wall friction angles, and internal friction angles. Figure 3.7 represents this comparison for the case of internal friction angle equal of 20 and soil-wall frictional angles ranges from 0 to 20. It can be seen that the new study is in good agreement with Yong's and Qian's results.

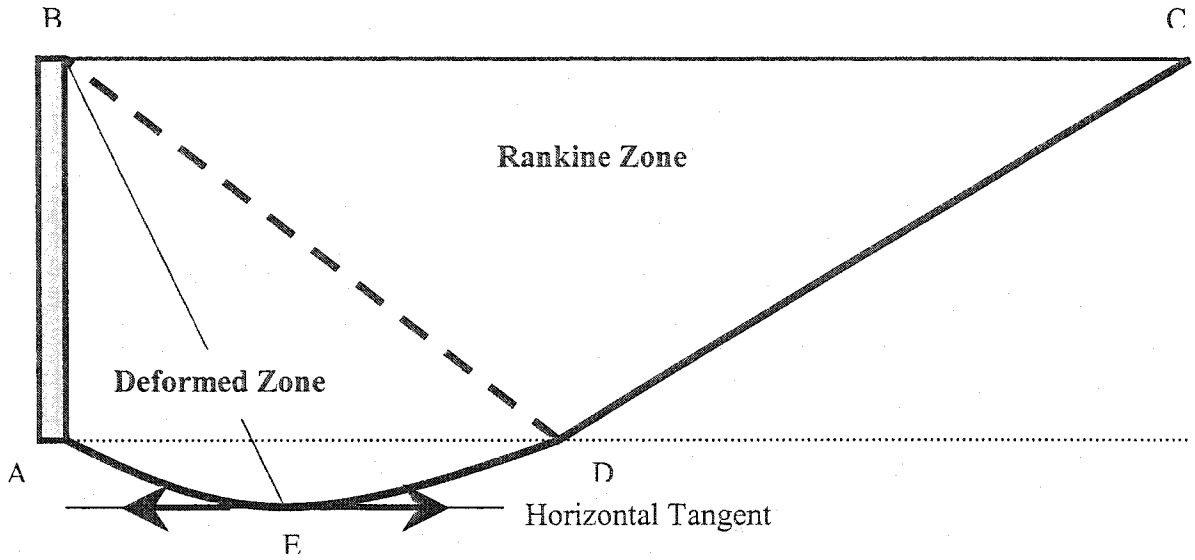

Figure 3.5: The Deformation Zone divided it into two parts by the horizontal tangent.

Table 3.2: Trial calculation for a number of slices (n) =12, ϕ^o =10, and $\delta_p{}^o$ =0, using the proposed formulas.

Slice No.	ϕ^o	δ_P	$\alpha_{(r,i)} = \left(\frac{i-10}{0.5\times n}\right)^2 \times \alpha_{(o)}$ Radians	$\alpha_{(l,i)} = \left(\frac{i-10}{0.5\times n}\right)^2 \times \alpha_{(n)}$ Radians
1	10	0.0	0.9817	
2			0.7757	
3			0.5939	
4			0.4363	
5			0.3030	
6			0.1939	
7			0.1091	
8			0.0485	
9			0.0121	
10			**0.0000**	
11				0.0121
12				0.4363
K_p =1.4823				

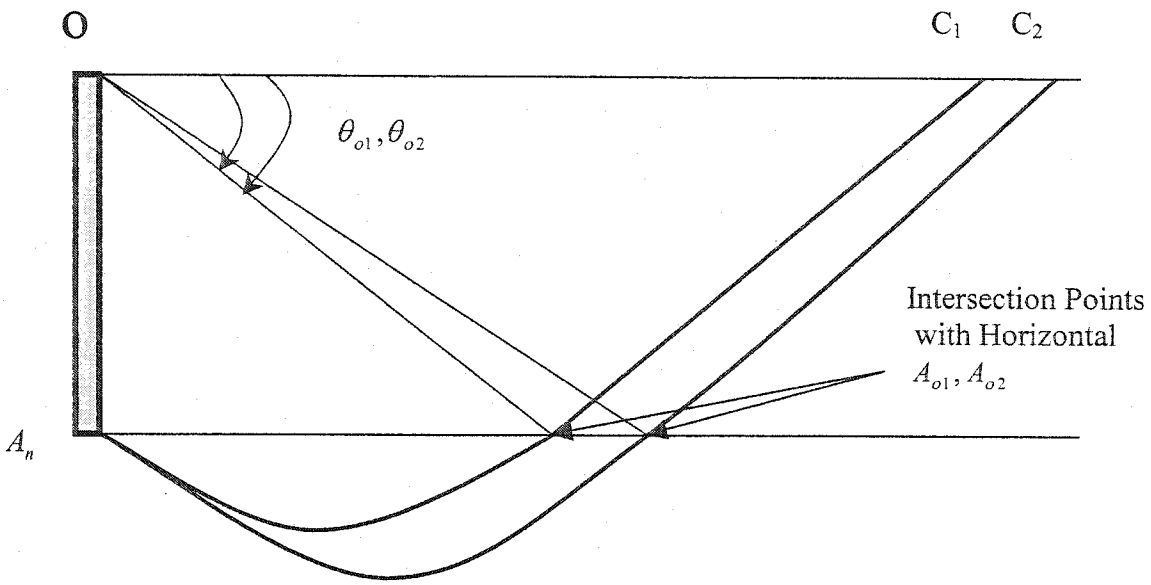

Figure 3.6: Illustration of different assumed failure planes due to change in θ_o.

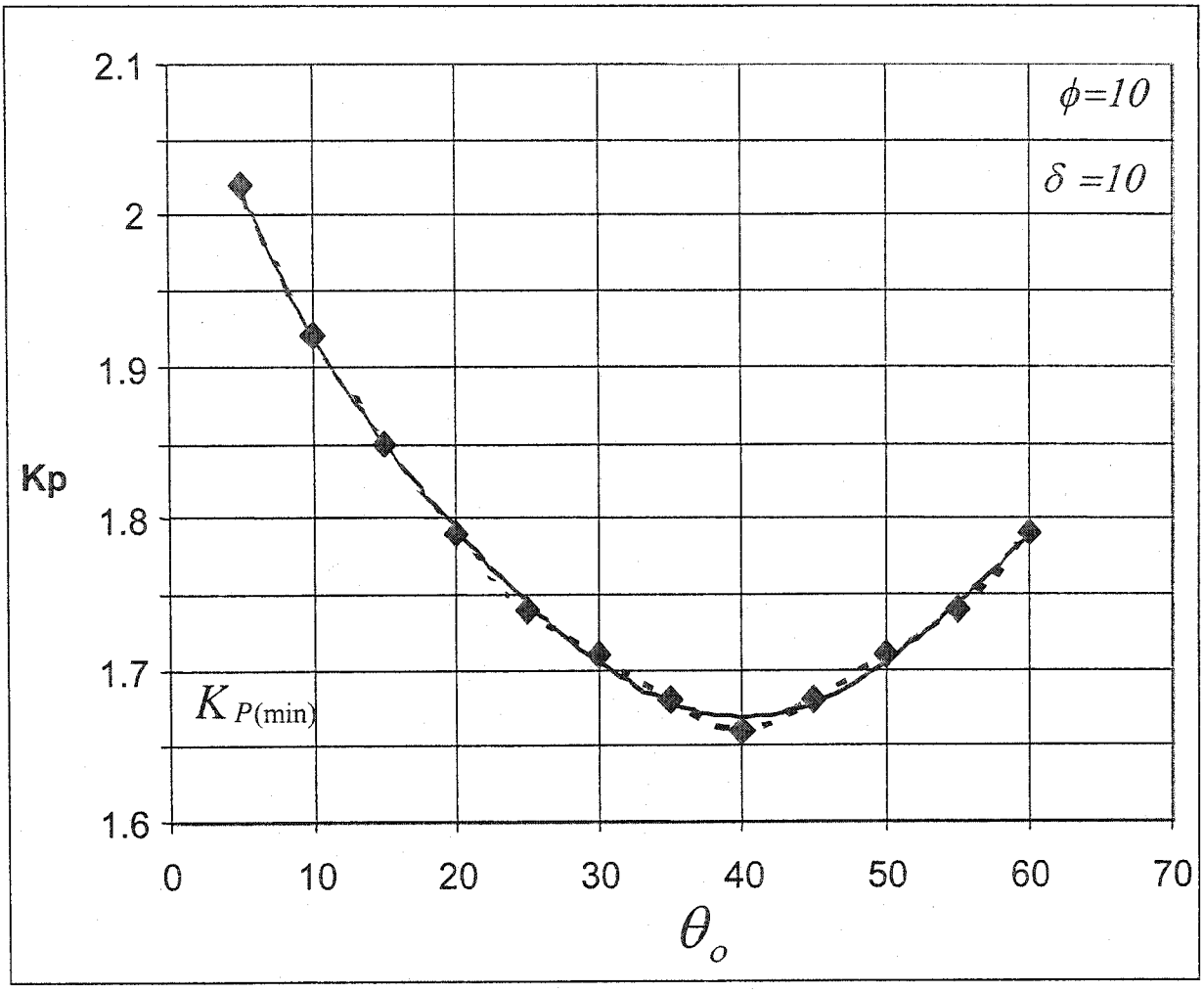

Figure 3.7: Typical Kp minimum for the case of ϕ=10°, δ_p=10.

Table 3.3: Coefficients of passive earth pressure as deduced by the present study and Yong and Qian (2000) Method.

ϕ	δ_p	K_P	
		Present study	Yong and Qian 2000
10	0	1.48	1.42
	5	1.57	1.56
	10	1.67	1.66
20	0	2.18	2.04
	10	2.51	2.56
	20	2.99	3.06
30	0	3.27	3.00
	15	4.29	4.61
	30	6.24	6.59
40	0	5.16	4.59
	20	8.25	9.66
	40	18.39	18.24

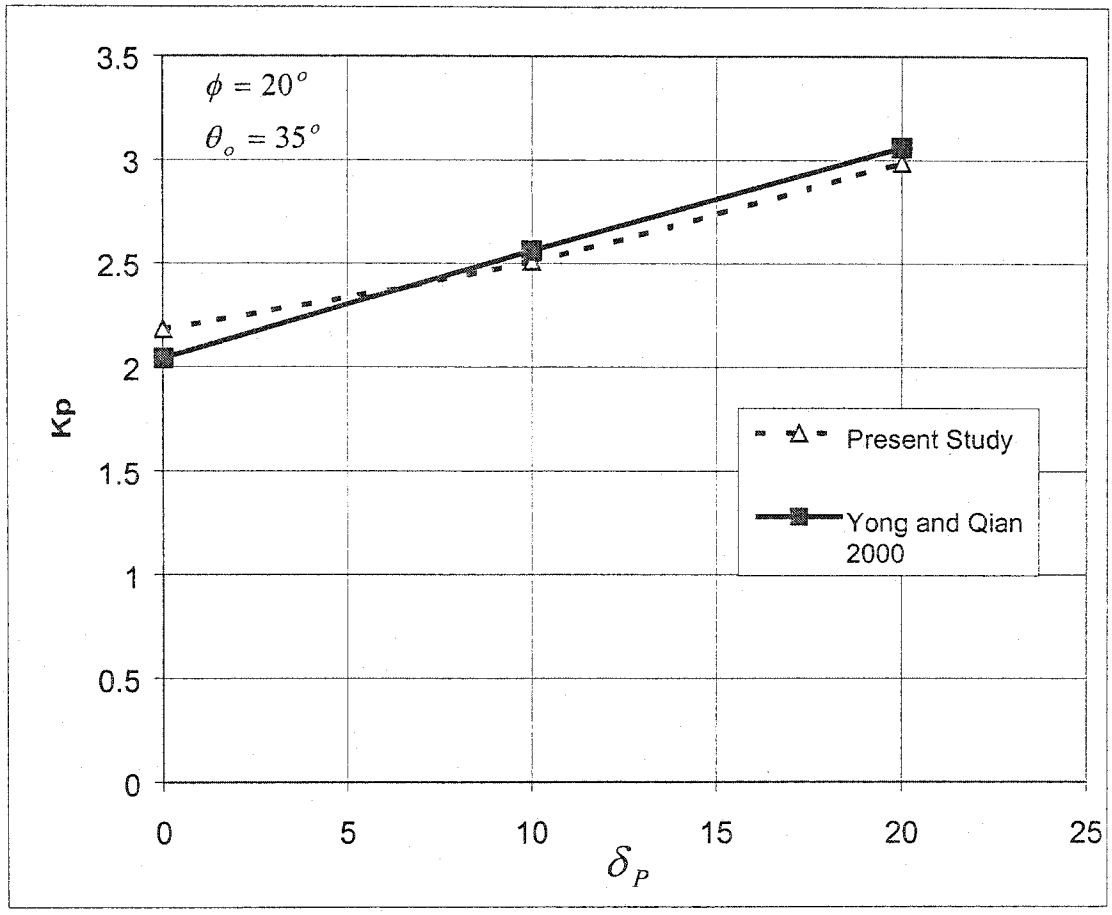

Figure 3.8: Coefficients of passive earth pressure versus the angle of soil-wall frictional angle.

3.3: Passive Earth Pressure of Homogeneous Overconsolidated Sands:

In the previous section, Yong's and Qian's (2000) method was validated to predict the coefficients of passive earth pressure of homogeneous normally consolidated sand. Herein the proposed method will be extended for the case of overconsolidated cohesionless soils. Referring to Figure 3.2, the coefficient of passive earth pressure in the Rankine zone, k_{PR} will be replaced by the following semi-empirical formula, which takes into account the effect of overconsolidation in terms of overconsolidation ratio (OCR) as follows:

$$k_{PR} = \frac{b\sqrt{OCR}\sin(\theta_o + \alpha_o)\sin(\theta_o)\sin(\alpha_o + \phi)}{\sin(\alpha_o)\sin(\theta_o + \alpha_o + 2\phi)} \quad \text{..... (3.13)}$$

Where;

OCR = Overconsolidation ratio.

ϕ = Angle of shearing resistance of the soil of the backfill.

b = Factor, which depends on the angle of shearing resistance of the soil backfill.

θ_o and α_o as previously defined.

The experimental data reported by Khoury (1994) was used extensively to develop the empirical formula given in Equation (3.14). Trial calculations were performed for the experimental set-up used by Khoury with the objective to determine the passive earth pressure produced in Rankine zone, and accordingly the Factor, b.

In case b = 1 for OCR =1, and for OCR>1 and $\phi < 45^{o}$ then, the following Equation is proposed;

$$b = \frac{1.25}{\cos(45 - \phi)} \quad \text{..... (3.14)}$$

Where;

ϕ : Angle of shearing resistance of the soil of the backfill.

Then, the effect of overconsolidation will transform to next slices in the deformation zone using equations 3.4 and 3.5.

The computer program was adjusted to take into consideration the effect of overconsolidation to calculate the passive earth pressure behind the retaining wall using the same previous assumptions.

In this analysis, wide ranges of the parameters were used with the objective to develop design charts for practicing use. The results of this analysis are given in the next section of the design charts.

3.4 : Passive Earth Pressure of Normally and Overconsolidated Cohesionless Soils Overlaying Deep Deposit:

It is often the case that a foundation rests on a soil consisting of a thin, strong layer overlaying a weak sand deposit. The strong sand layer may naturally exist or be artificially provided to increase the bearing capacity to a desired design value based on the fact that the failure strain of the upper sand layer is less than that of the lower layer. Simultaneous occurrence of the shearing failure in both layers could not take place and more strain is required in the upper layer to reach the lower layer failure strain value and then decrease the settlement.

This section of the thesis is a trial to solve the problem of layered soils. The problem of layered soils arises, for example while building a retaining wall along the shores of a river, or when constructing a bridge whose abutments rest on one type of soil and backfill material is of a different density.

In this section two layers are assumed, the top layer with ϕ_1 is overlaying a lower layer of sand with ϕ_2 .The failure plane will start at the toe of the wall going through the lower layer forming the deformation zone, then after it goes to the upper layer forming passive Rankine zone in the case of strong sand overlaying weak sand which was approved by the experimental work of Khoury (1994) and showed in figure (3.8). It appears that the failure plane is consisted of two parts: the curved part, and the straight plane. It will not be the same story for the case of weak sand overlaying very strong deposit, because the

failure plane will be formed only in between the two layers and will not go through the very strong sand layer, which was approved by Khoury's (1994) test results, as shown in figure (3.9).

The proposed method is extended to find the passive earth pressure coefficient for this case, by adding new assumptions as shown in figure 3.10. Rankine Zone will occur within the upper layer so that the upper layer internal frictional angle (ϕ_1) will be considered to calculate the passive earth pressure coefficient for Rankine Zone.

$$k_{PR} = \frac{b\sqrt{OCR}\sin(\theta_o + \alpha_o)\sin(\theta_o)\sin(\alpha_o + \phi_1)}{\sin(\alpha_o)\sin(\theta_o + \alpha_o + 2\phi_1)} \quad \ldots\ldots\ldots\ldots\ldots\ldots\ldots (3.15)$$

Where;

OCR: Overconsolidation ratio.

ϕ_1 : Angle of shearing resistance of the soil of the backfill for the upper layer.

Factor b was previously determined.

$\theta_o = \pi/4 - \phi_1/2$,

$\alpha_o = \pi/2 - \theta_o - \phi_1$.

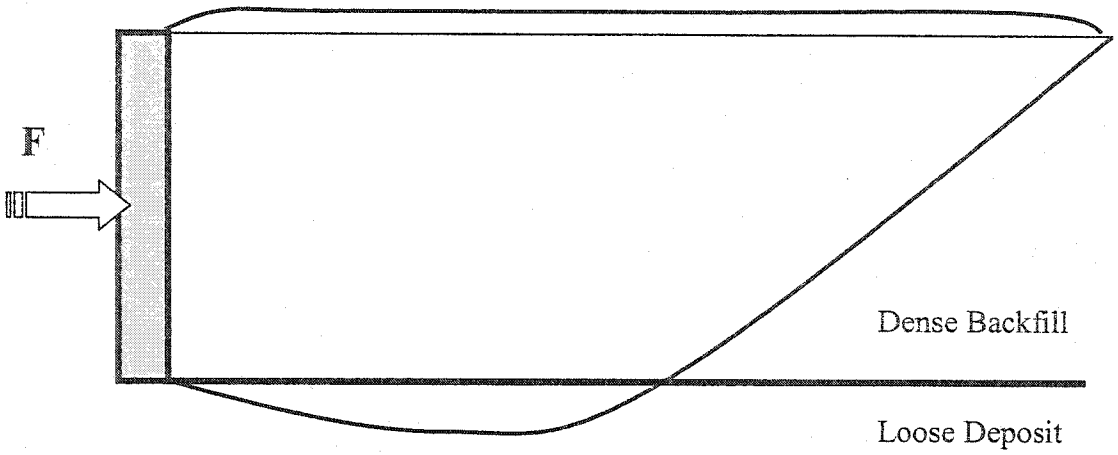

Figure 3.9: Failure plane for two layers of dense sand overlaying loose sand. (Khoury, 1994).

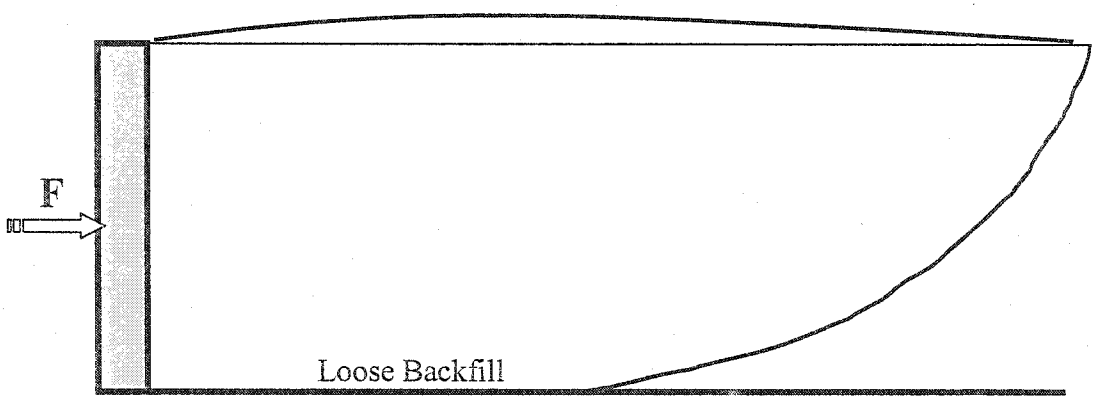

Figure 3.10: Failure plane for two layers of loose sand overlaying dense sand.

(Khoury, 1994).

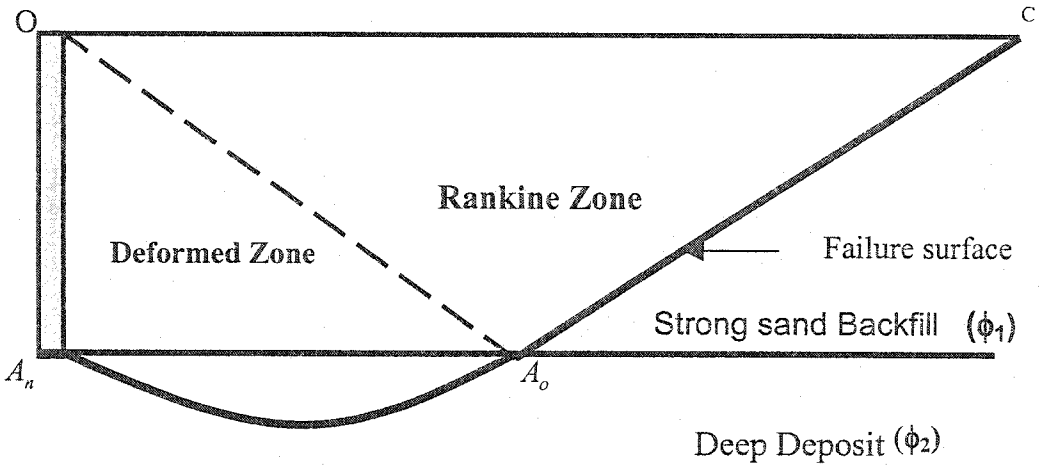

Figure 3.11: Failure plane for the case of strong sand backfill overlaying deep deposit.

The deformed zone will occur in both layers in the upper one and in the lower layer, then, a new internal frictional angle will be composed of the two layers, considering the weight as a proportionate combination of the weights of the respective layers within the slice. This new proposed angle is given in the following formula:

$$\phi_{new} = \tan^{-1}\left(\frac{\tan\phi_1 + \tan\phi_2}{2}\right) \quad \text{(3.16)}$$

Where;

ϕ_1: Upper layer soil friction angle

ϕ_2: Lower layer soil friction angle

This angle will be replaced instead of internal friction angle of the homogeneous backfill for the deformation zone in equations (3.4) and (3.5), and in equation (3.10) for the last slice base inclination α_n.

The computer program will be adjusted to take the previous assumptions into consideration. In this analysis, wide ranges of the parameters were used also, with the objective to develop design charts for practicing use.

3.5: Design Charts for the Cases of Normally Consolidated and Overconsolidated of Homogeneous and Two Layers of Sands:

The results of the mentioned analysis were put into design charts, which are simple and easy to use for practical purposes, taking into consideration all the cases mentioned above with wide ranges of internal frictional angles and soil-wall frictional angles.

These results show that all values of passive earth pressure of strong homogeneous sands are higher than that of strong sand overlaying weak sand; this can be explained by the fact that with decreasing lower layer strength it will result in a decrease in the passive pressure all over the system because the stress needed for the weak layer to fail is much less than that for the strong layer.

In the next step the modified method is checked for weak sand overlaying very dense sand and the results were close to that for the weak homogeneous layer. In this case for medium sand (ϕ=40°) overlaying dense sand (ϕ=45°) for wall-soil frictional angle (δ_p=0), then the coefficient of passive earth pressure (OCR=2) was 9.2830, and 10.4799 for homogeneous medium sand, and 14.1626 for homogeneous dense sand. It could be noticed that for homogeneous dense sand the passive earth pressure coefficient is the highest value among all, followed by homogenous medium sand, then medium sand overlaying dense sand. This shows that for the weak sand overlaying strong sand the passive earth pressure will remain the same as of weak homogeneous sand when the lower layer is very dense and much stronger than the upper layer.

passive earth pressure will remain the same as of weak homogeneous sand when the lower layer is very dense and much stronger than the upper layer.

The following design charts will be introduced in terms of lower layer internal frictional angle (ϕ_2) in the X-axis, upper layer internal friction angle (ϕ_1) that is represented by the curve itself, and passive earth pressure coefficients in the Y-axis.In these design charts, $\delta_P \leq \phi_2$.

In order to use these charts, the wall roughness should be determined first in terms of $\frac{\delta_P}{\phi_1}$, then the overconsolidation ratio (OCR) .The lower layer internal frictional angle is determined in the X- axis then we go vertically to the curve that gives the internal frictional angle of the upper layer after that going horizontally to find the coefficient of passive earth pressure in the Y-axis. These charts give the choice for homogeneous and strong sand overlaying deep deposit of normally and overconsolidated sand.

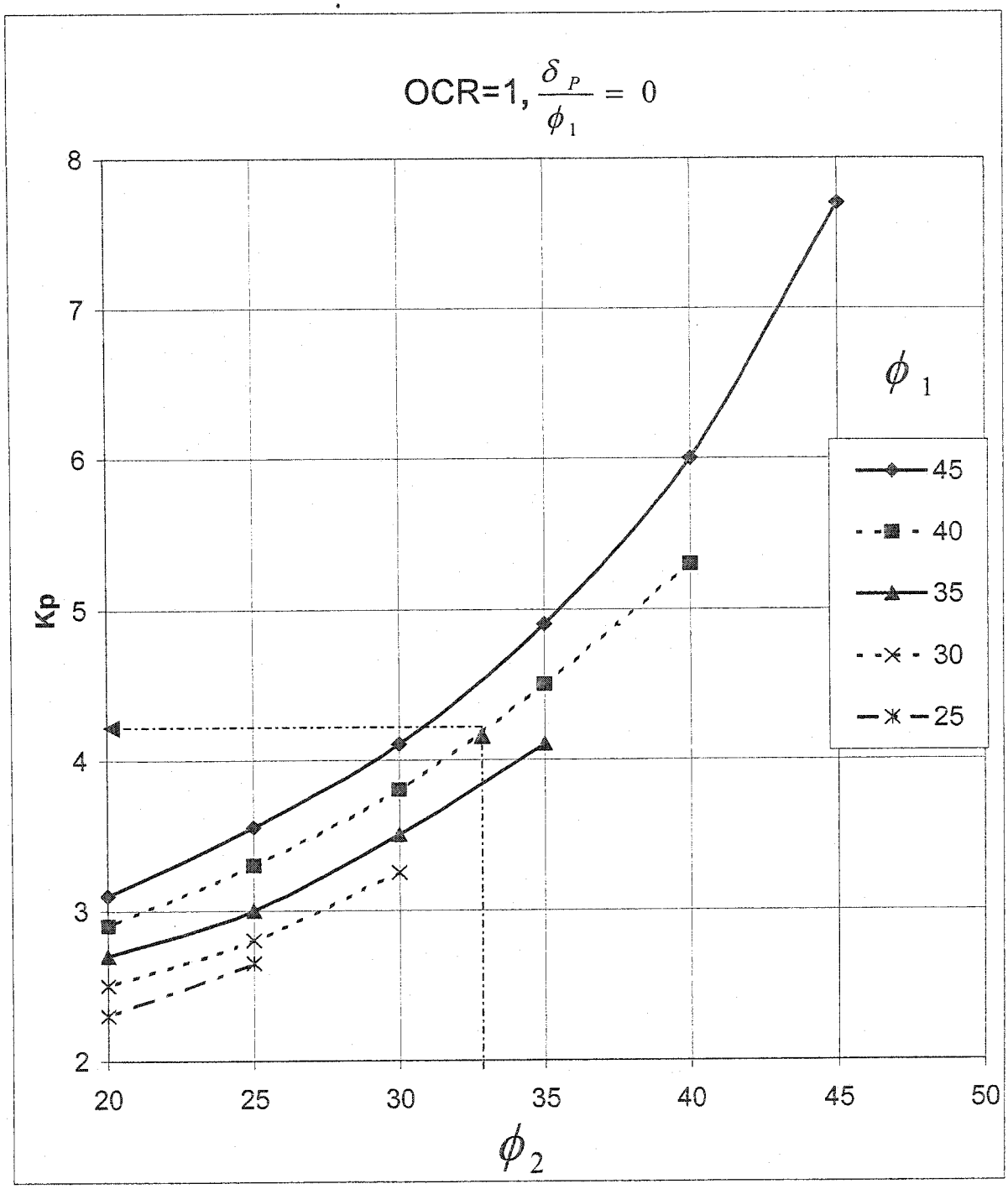

Figure 3.12: Coefficient of passive earth pressure for normally consolidated sands. $\frac{\delta_P}{\phi_1} = 0$.

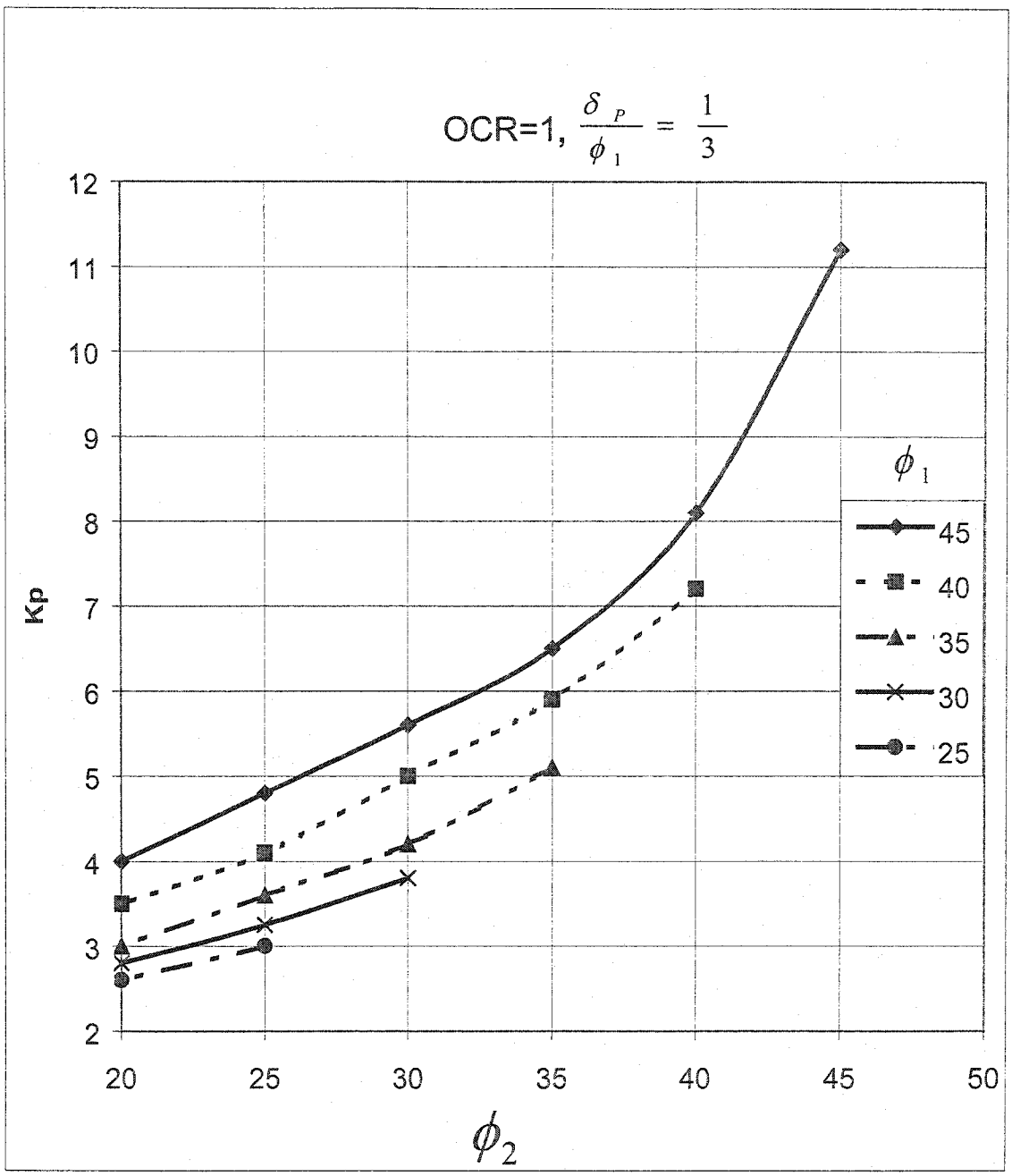

Figure 3.13: Coefficient of passive earth pressure for normally consolidated sands. $\frac{\delta_P}{\phi_1} = \frac{1}{3}$

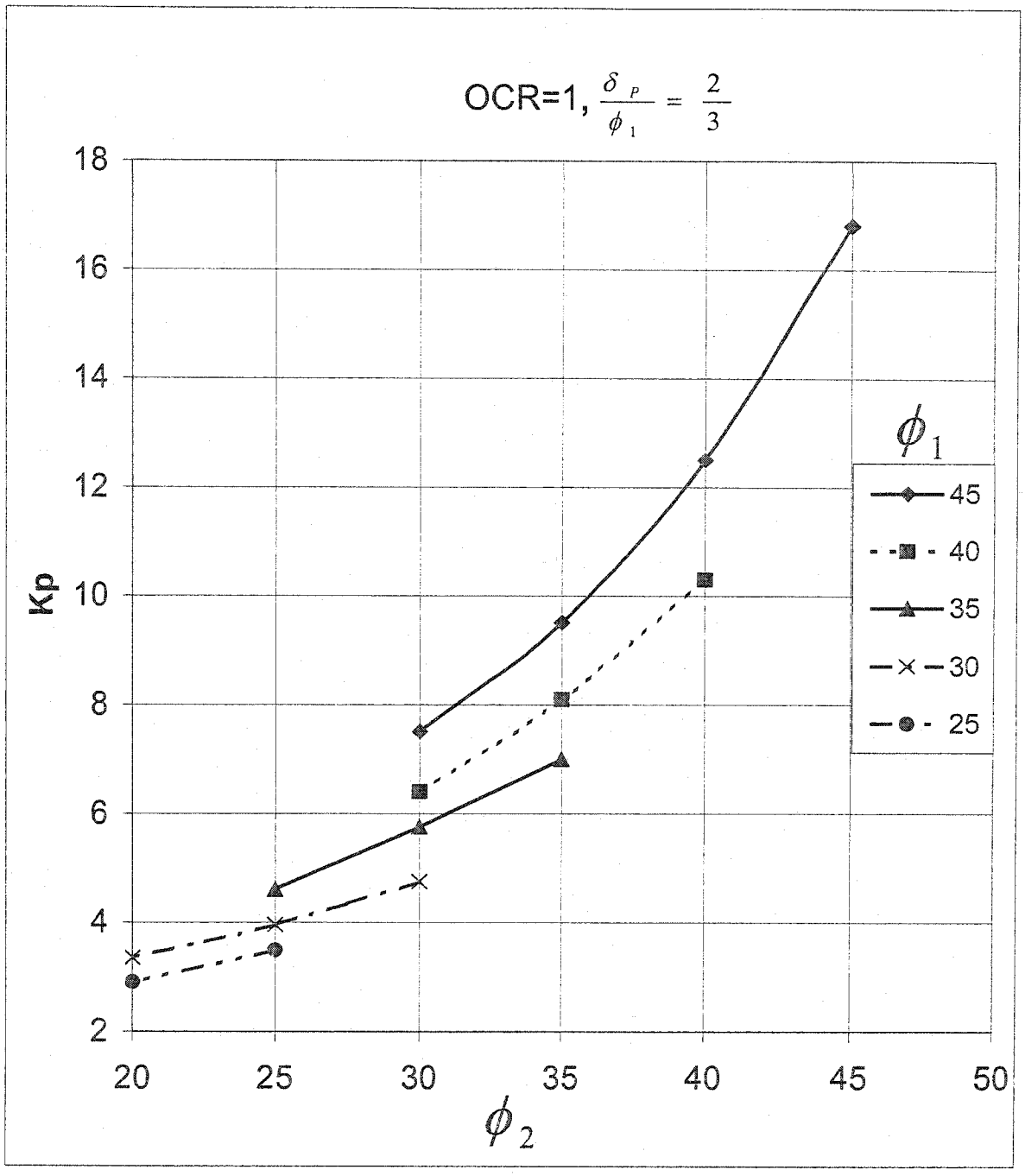

Figure 3.14: Coefficient of passive earth pressure for normally consolidated sands. $\frac{\delta_P}{\phi_1} = \frac{2}{3}$.

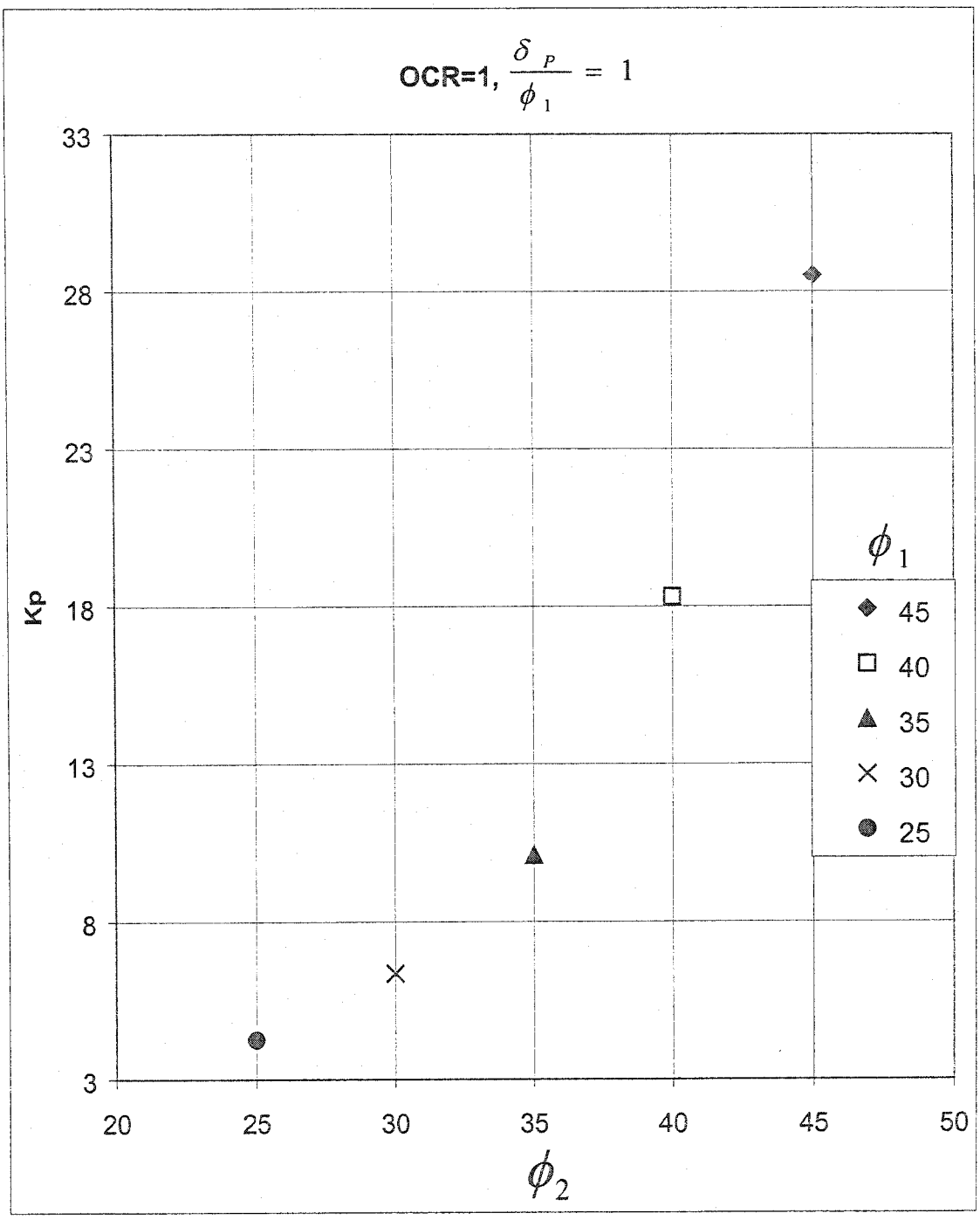

Figure 3.15: Coefficient of passive earth pressure for normally consolidated sands. $\frac{\delta_P}{\phi_1} = 1$

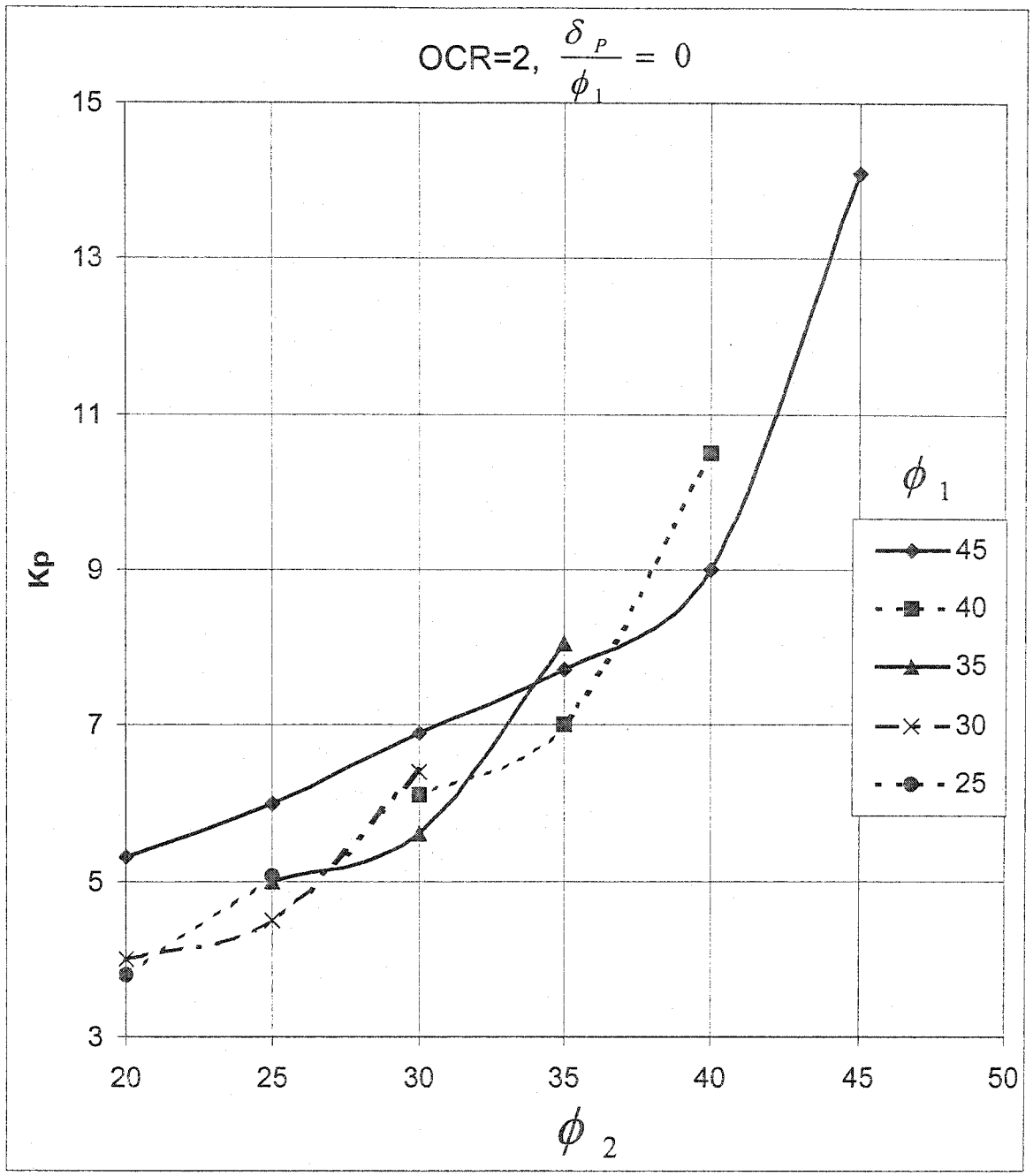

Figure 3.16: Coefficient of passive earth pressure for OCR =2, $\frac{\delta_P}{\phi_1} = 0$

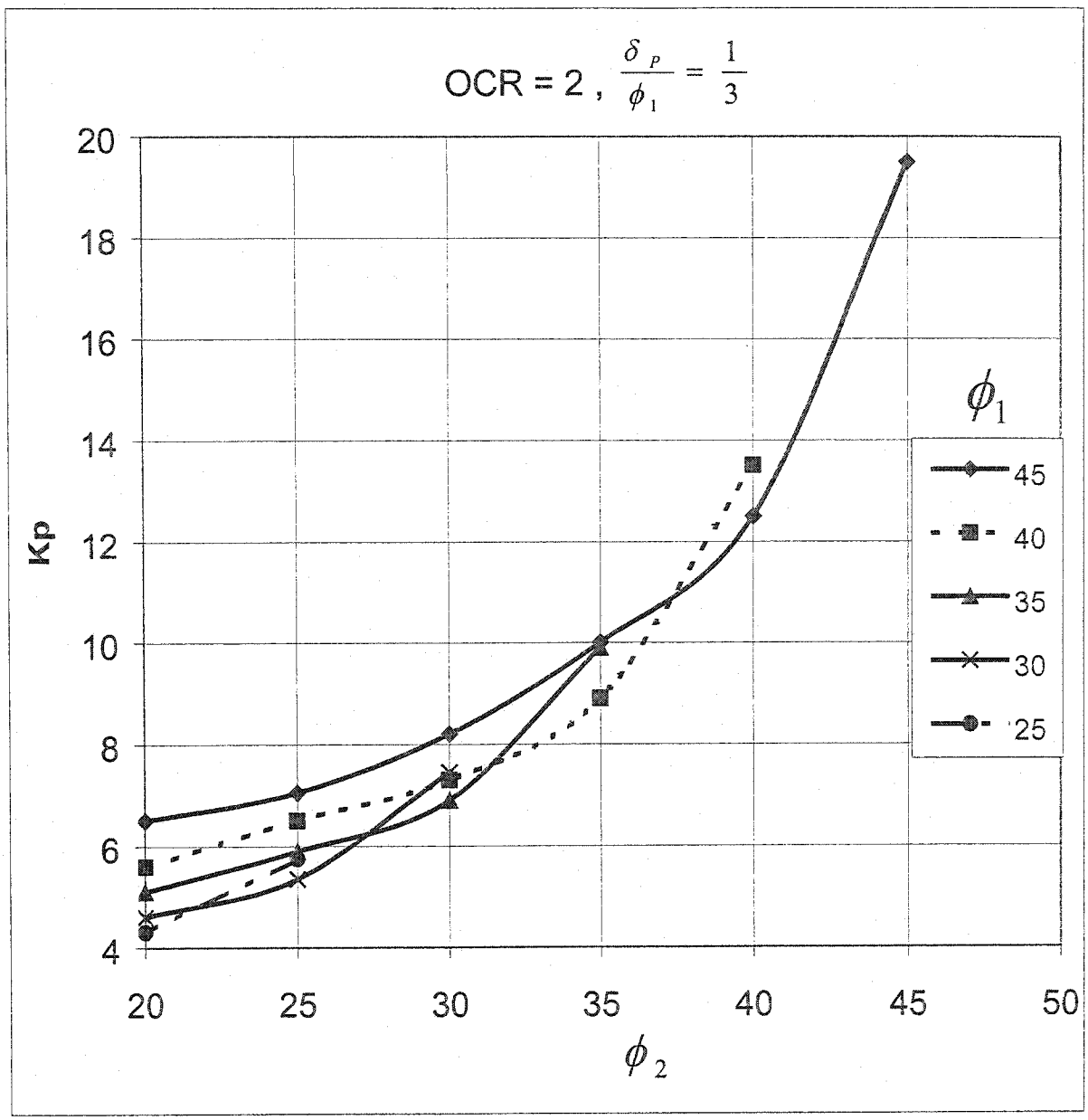

Figure 3.17: Coefficient of passive earth pressure for OCR =2, $\frac{\delta_P}{\phi_1} = \frac{1}{3}$

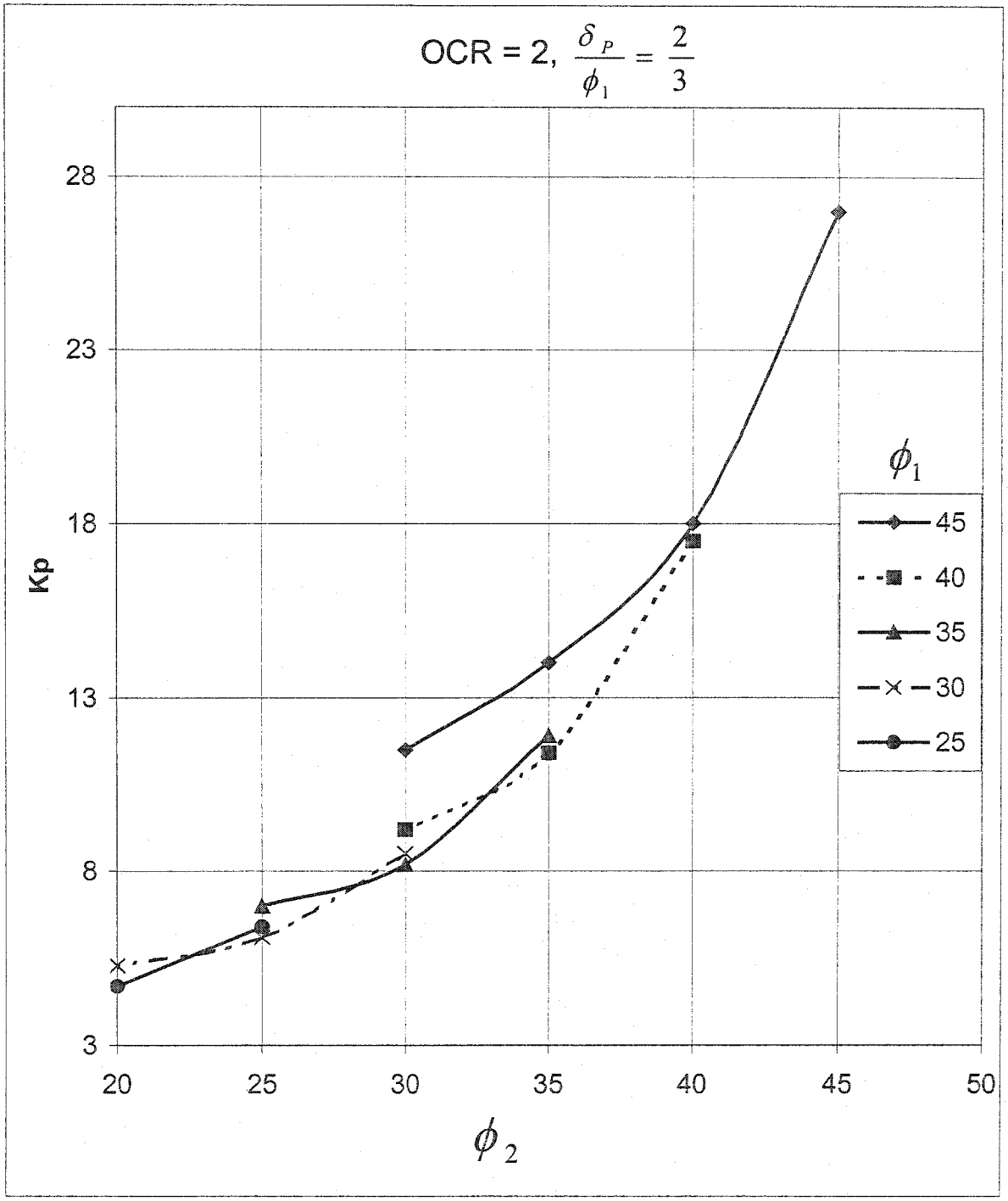

Figure 3.18: Coefficient of passive earth pressure for OCR =2, $\frac{\delta_P}{\phi_1} = \frac{2}{3}$

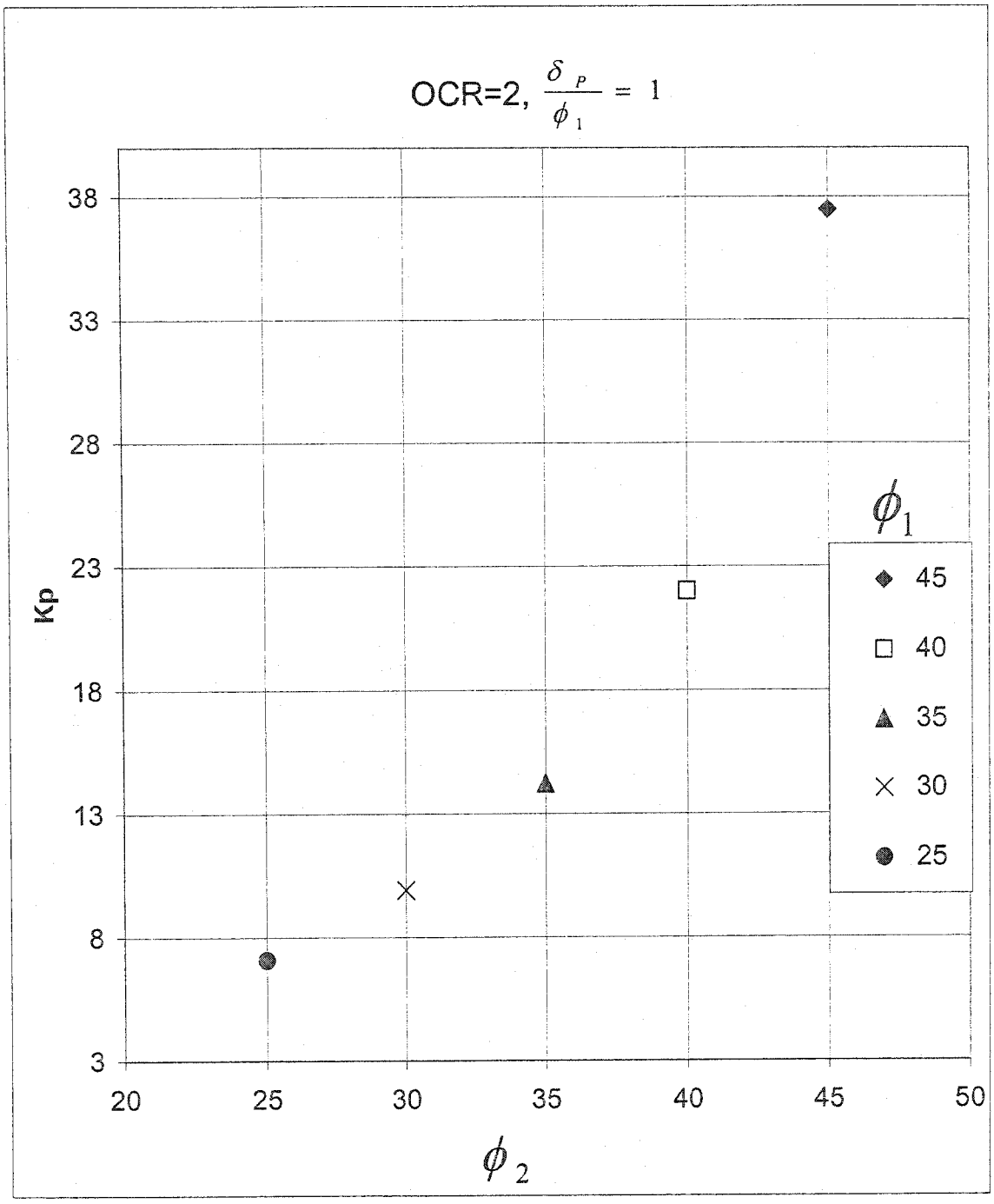

Figure 3.19: Coefficient of passive earth pressure for OCR =2, $\frac{\delta_P}{\phi_1} = 1$

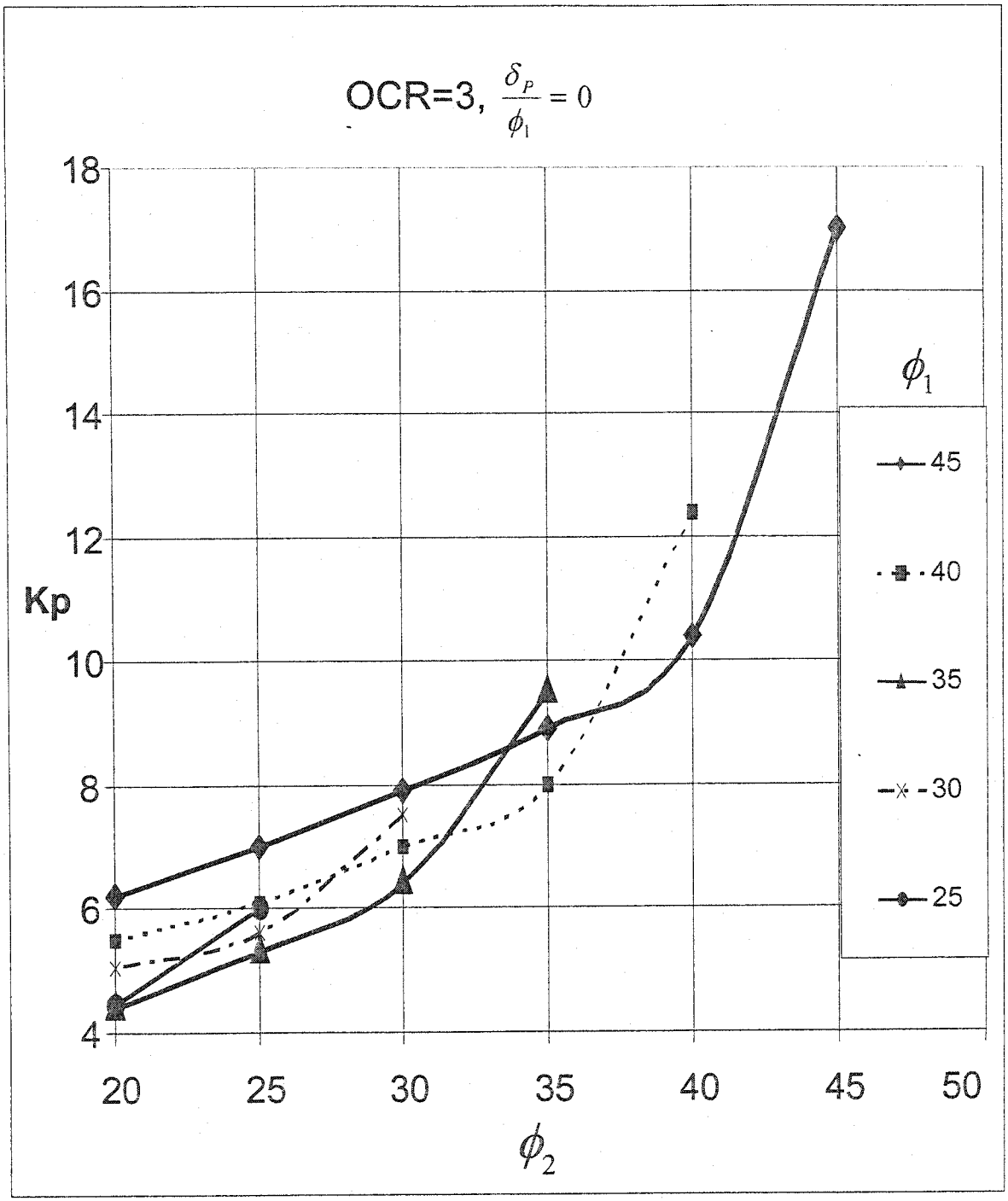

Figure 3.20: Coefficient of passive earth pressure for OCR =3, $\frac{\delta_P}{\phi_1} = 0$

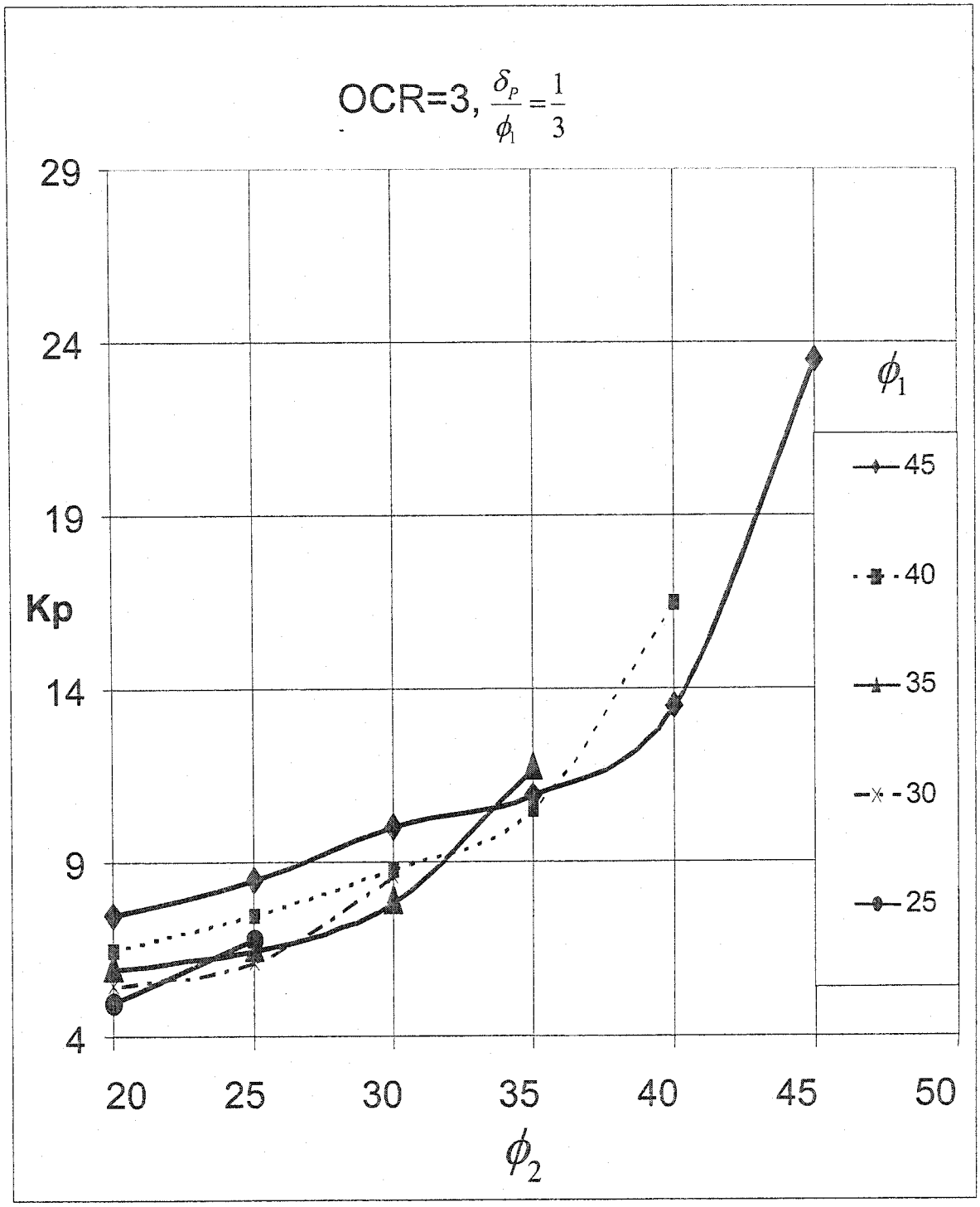

Figure 3.21: Coefficient of passive earth pressure OCR =3, $\frac{\delta_P}{\phi_1}=\frac{1}{3}$

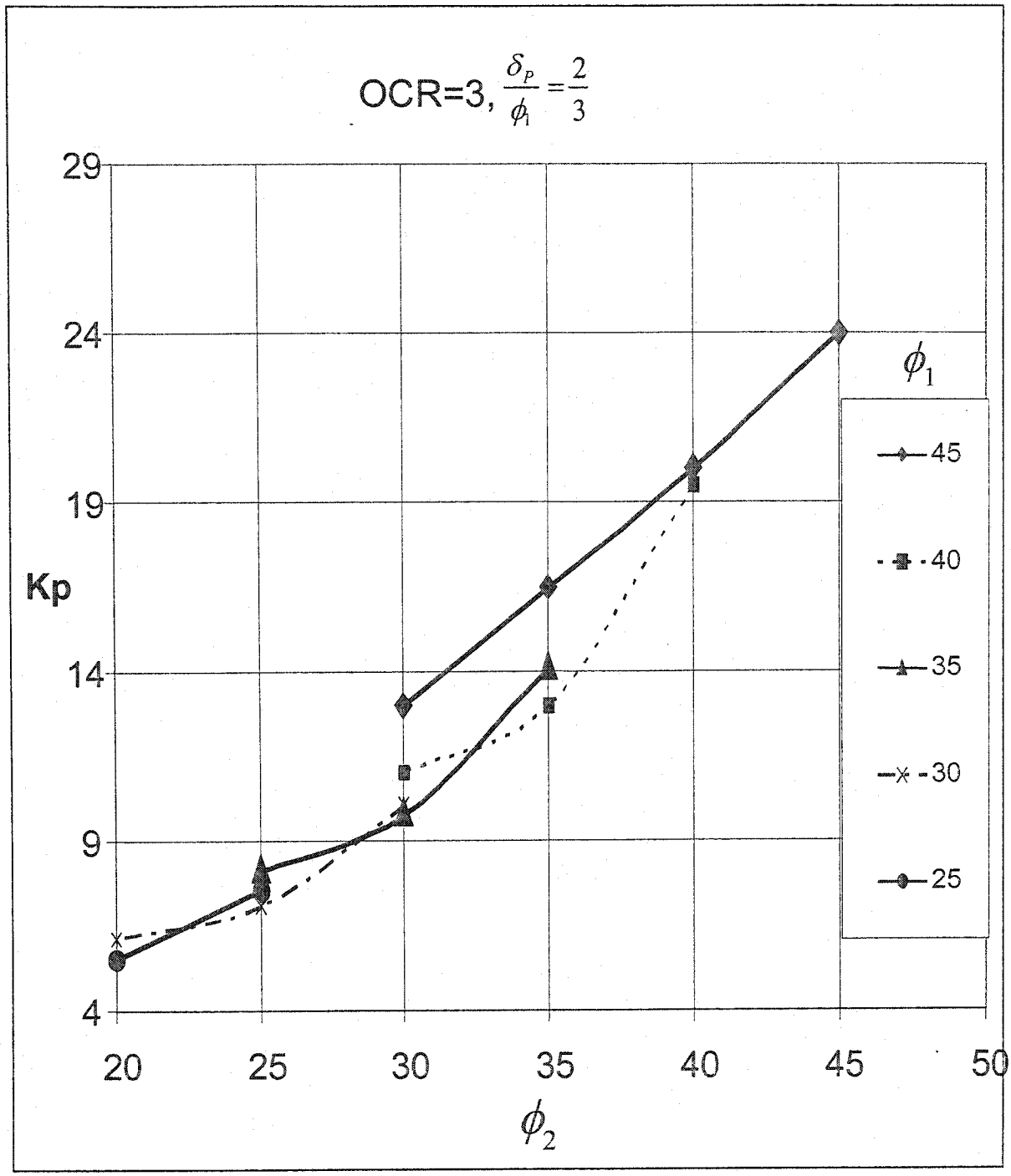

Figure 3.22: Coefficient of passive earth pressure for OCR =3, $\frac{\delta_P}{\phi_1}=\frac{2}{3}$

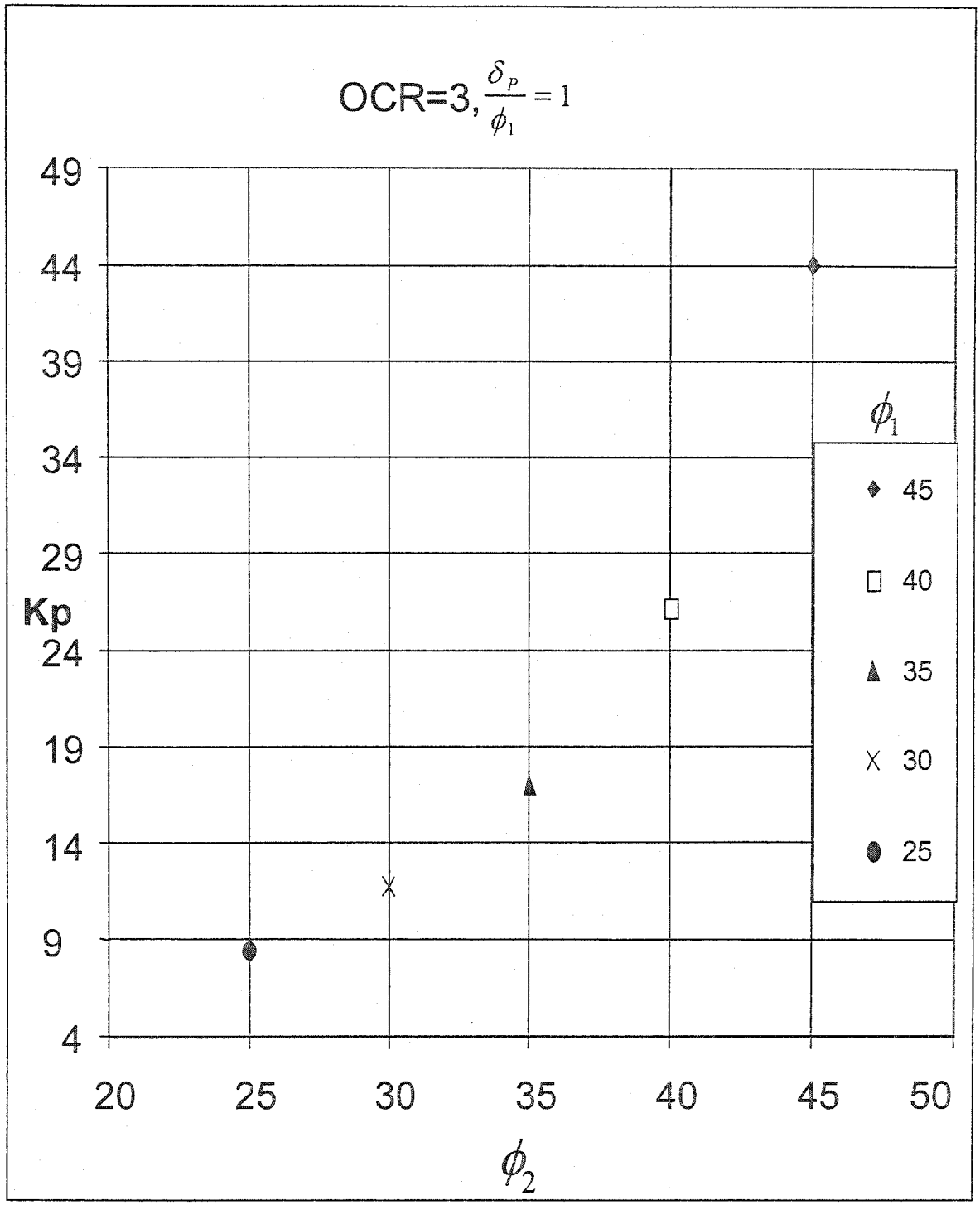

Figure 3.23: Coefficient of passive earth pressure for OCR =3, $\frac{\delta_P}{\phi_1}=1$

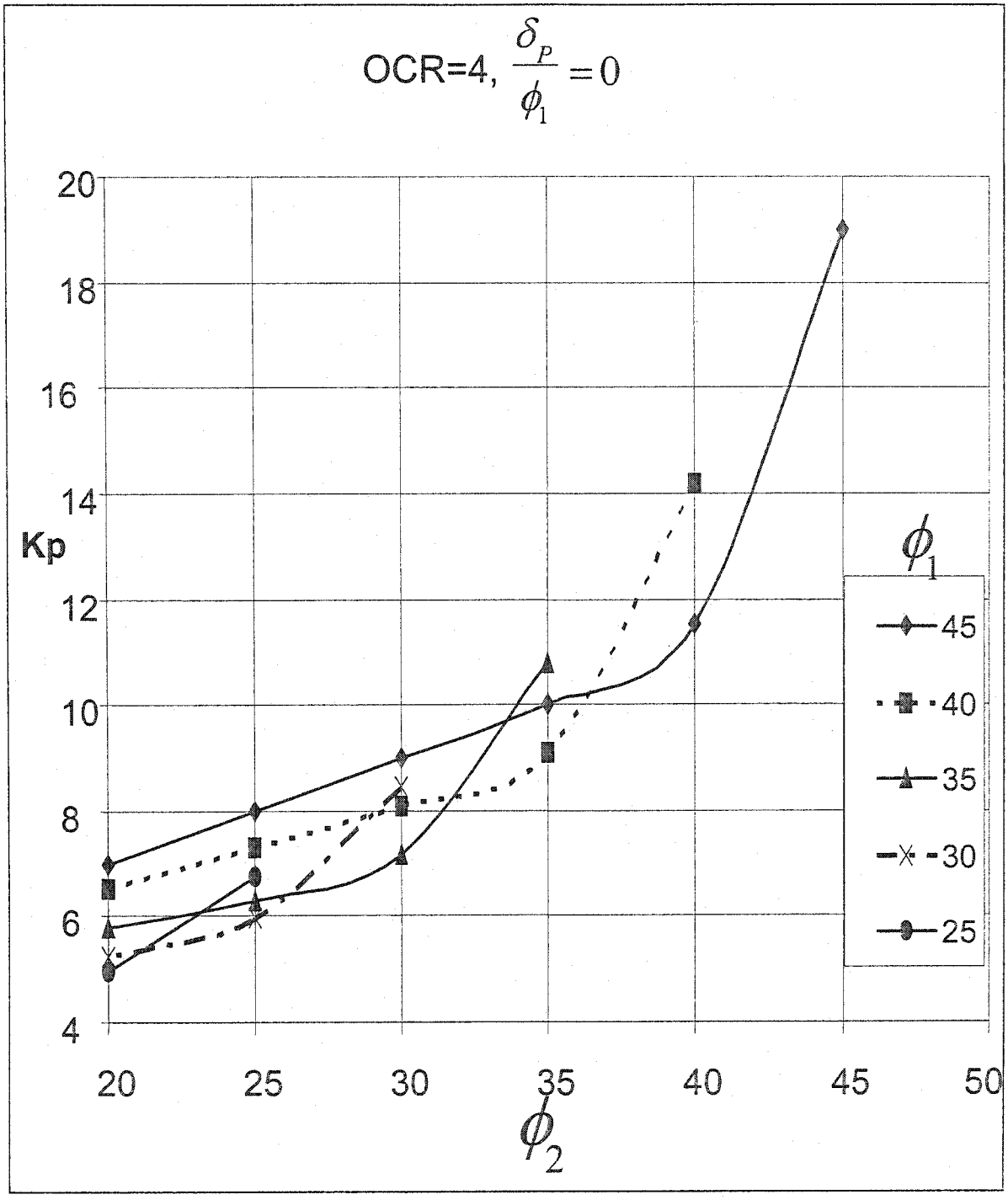

Figure 3.24: Coefficient of passive earth pressure for OCR =4, $\frac{\delta_P}{\phi_1}=0$

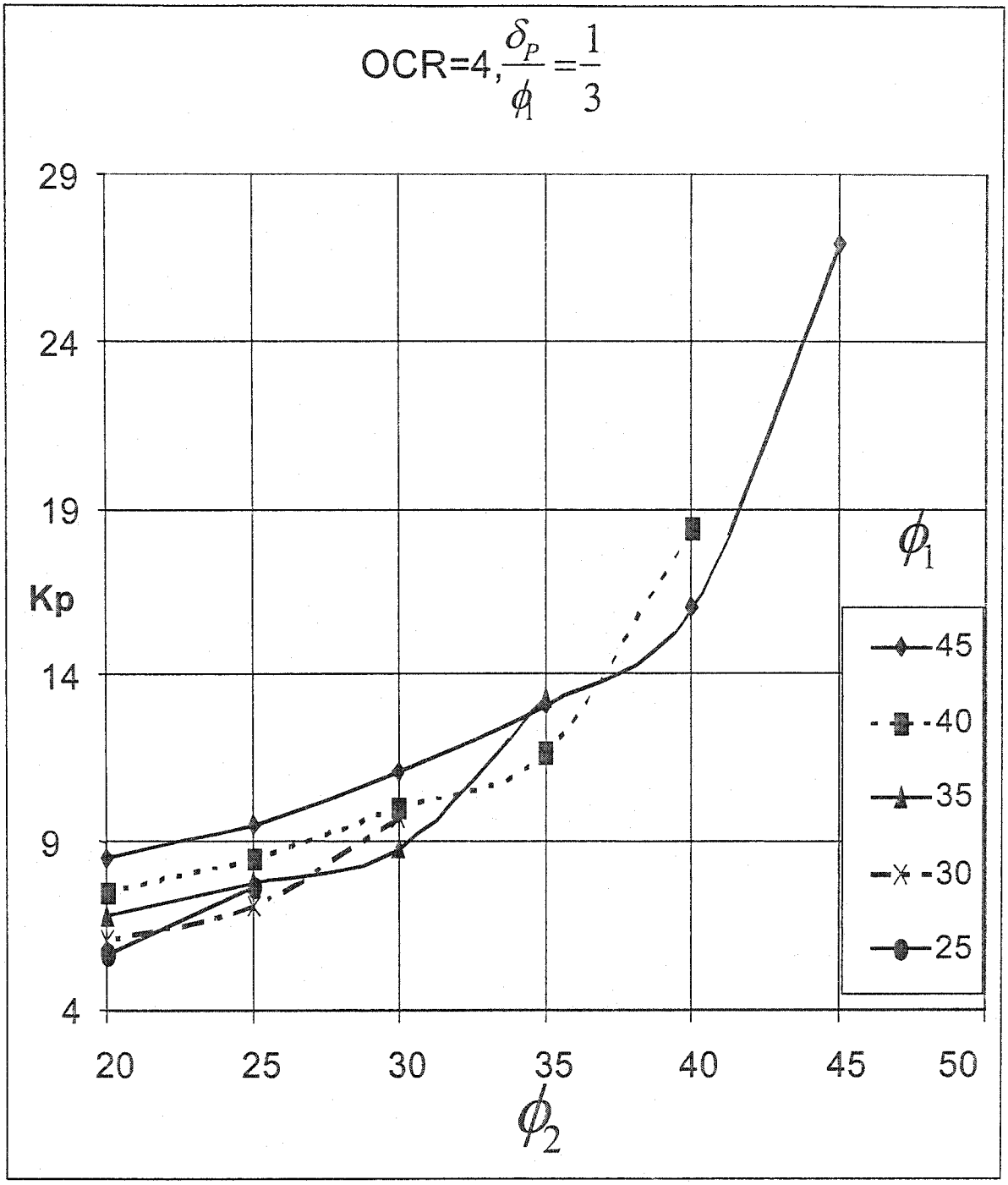

Figure 3.25: Coefficient of passive earth pressure for OCR =4, $\frac{\delta_P}{\phi_1} = \frac{1}{3}$

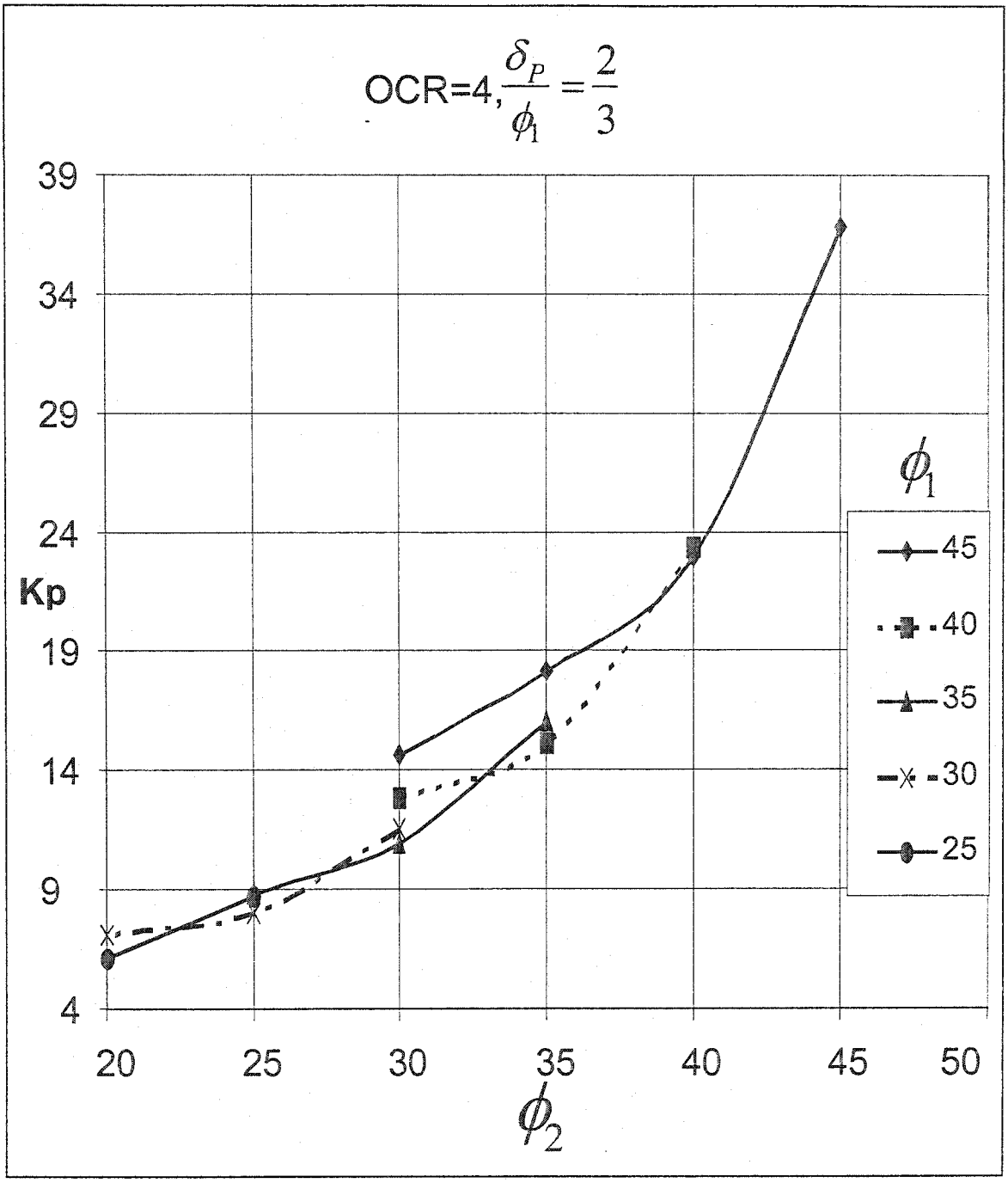

Figure 3.26: Coefficient of passive earth pressure for OCR =4, $\frac{\delta_P}{\phi_1} = \frac{2}{3}$

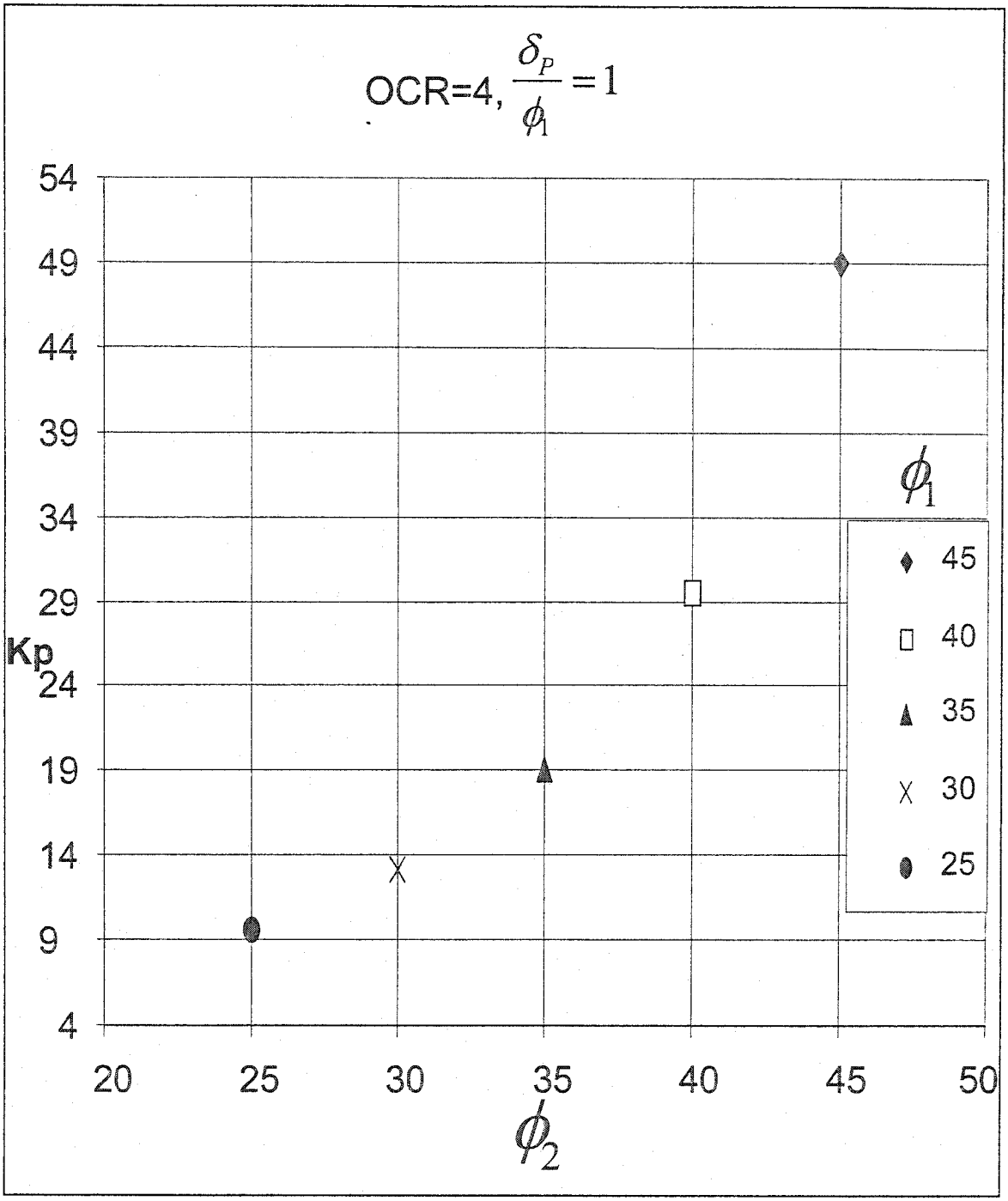

Figure 3.27: Coefficient of passive earth pressure for OCR =4, $\frac{\delta_P}{\phi_1}=1$

3.6: Theoretical Model for Inclined Backfill:

In this case a vertical rigid retaining wall with a cohesionless backfill of slope in an angle of β is considered (Figure 3.27), which is positive when the surface of the backfill slopes upwards from the top of the wall. The internal frictional angle of the backfill is ϕ for the case of homogeneous backfill. ϕ_1, for the upper layer, ϕ_2 for the lower layer in the case of strong backfill overlaying deep deposit. This backfill inclination will be included in passive Rankine zone; as well the overcosolidation for the case of overconsolidated cohesionless soil backfill, and is introduced in the following formula:

$$k_{PR} = \frac{b \times \sqrt{OCR}\sin(\theta_o + \alpha_o)\sin(\theta_o + \beta)\sin(\alpha_o + \phi_1)}{\sin(\alpha_o - \beta)\sin(\theta_o + \alpha_o + 2\phi_1)} \quad \text{..... (3.17)}$$

ϕ_1 : Internal frictional angle of the upper layer, which is equal to the internal frictional angle of the lower layer for the case of homogeneous backfill.

b: A factor, previously determined. b=1 for OCR=1.

$$\theta_o = \frac{\pi}{4} - \frac{\phi}{2} - \frac{\beta}{2} - \frac{1}{2}\arcsin\left(\frac{\sin\beta}{\sin\phi_1}\right) \quad \text{..... (3.18)}$$

Then, equations (3.4) and (3.5) will be used to transfer the stresses to the slices in the deformation zone and then to calculate the coefficient of passive earth pressure behind the retaining wall, by considering the two cases of homogeneous backfill, which means ($\phi_1 = \phi_2$) and the case of two different layers, and at this case the composite internal frictional angle ϕ_{new} will be used for the calculations of the deformed zone.

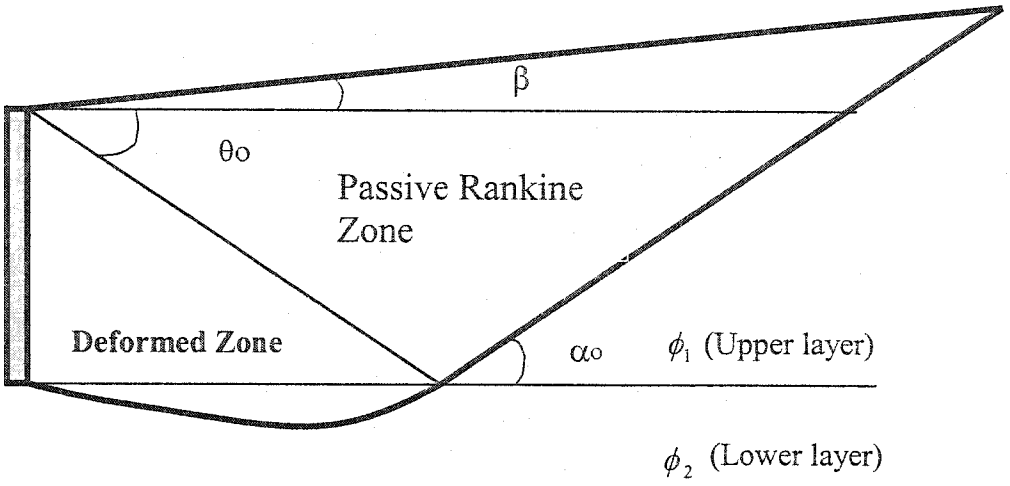

Figure 3.28: Failure plane for inclined backfill material of an angle behind a retaining wall.

3.7: Design Charts for Inclined Backfill:

The computer program will be adjusted to take the previous assumptions into consideration. In this analysis, wide ranges of the parameters were used with the objective to develop design charts for practicing use. These charts will take the soil conditions parameters that affect the coefficient of passive earth pressure into consideration which are given in terms of overconsolidation ratio (OCR), internal friction angle of the backfill ϕ, the ratio of soil-wall friction angle over internal friction angle of the soil backfill $\frac{\delta_P}{\phi}$, and the backfill inclination β^o.

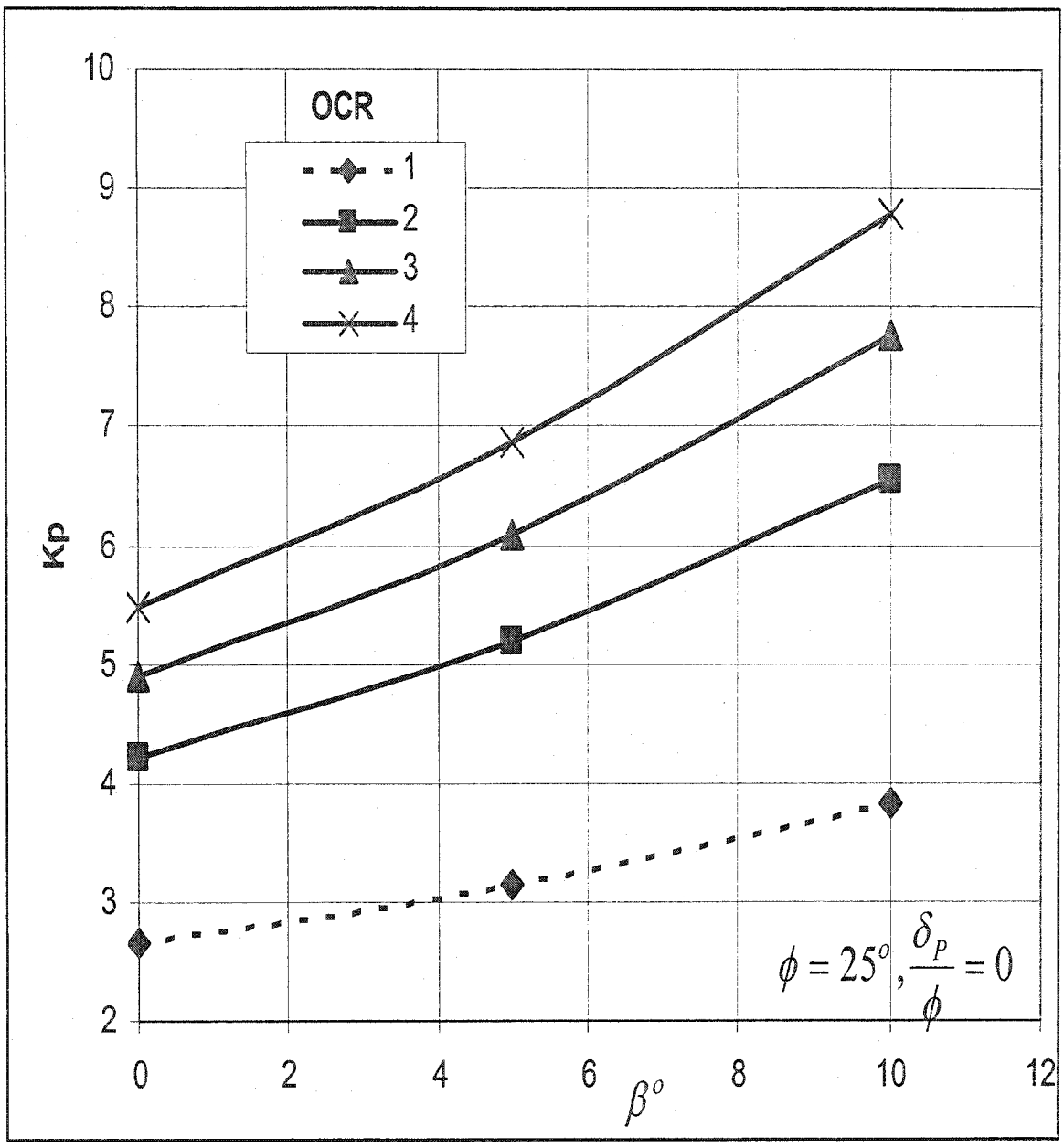

Figure 3.29: Coefficient of passive earth pressure for inclined homogeneous normally and overconsolidated backfill sand. $\phi = 25^o, \frac{\delta_P}{\phi} = 0$.

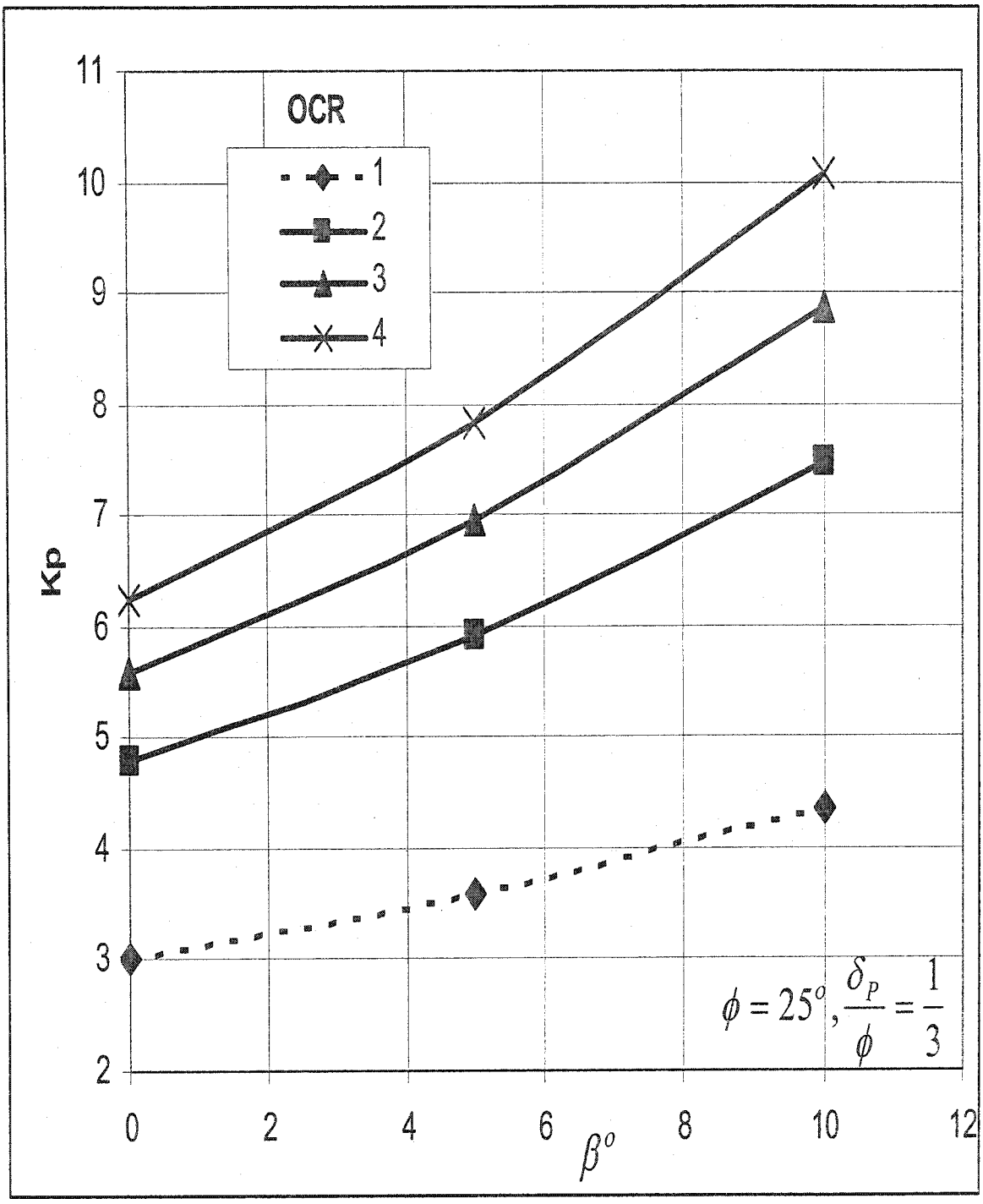

Figure 3.30: Coefficient of passive earth pressure for inclined homogeneous normally and overconsolidated backfill sand. $\phi = 25^o, \frac{\delta_P}{\phi} = \frac{1}{3}$.

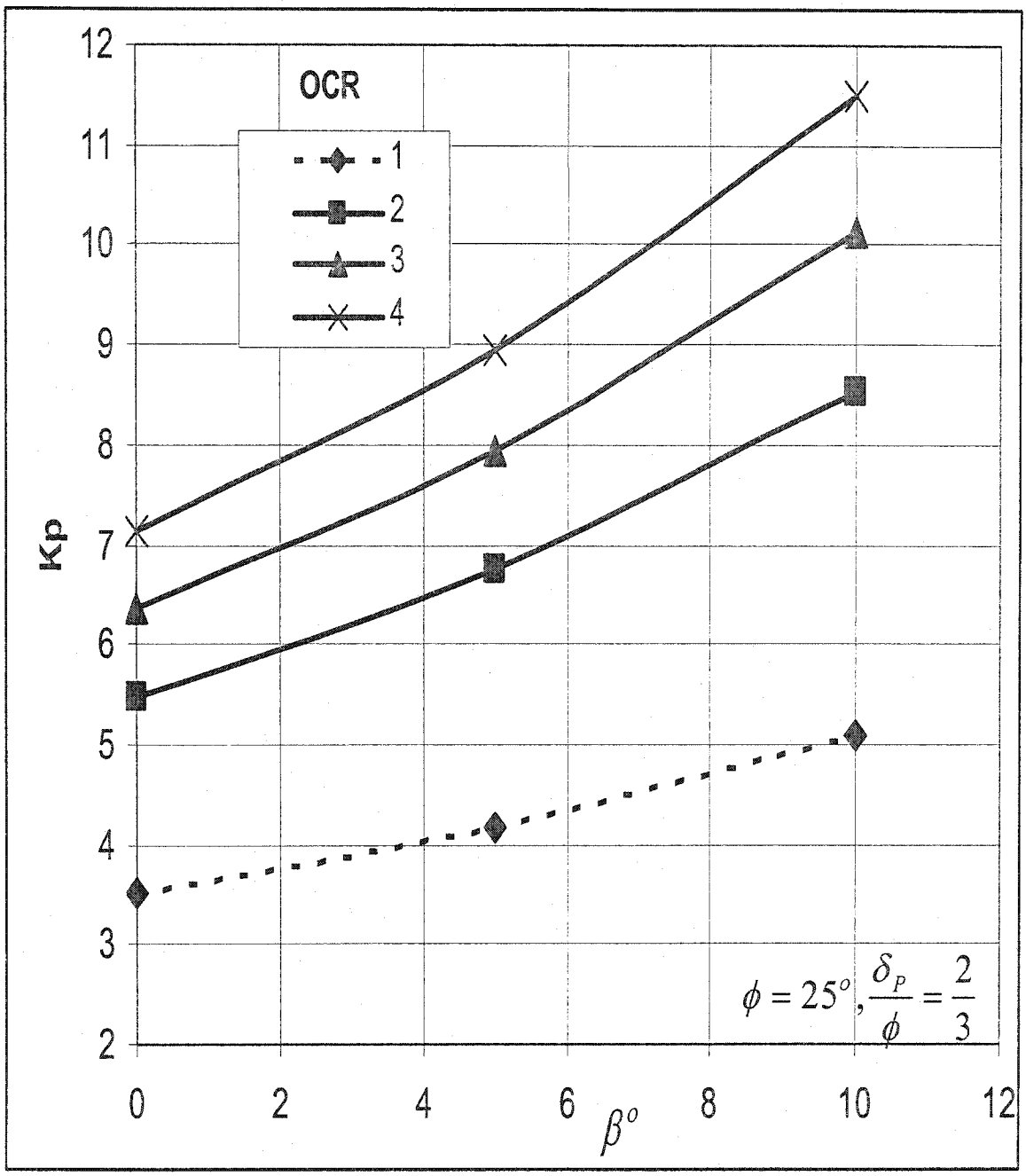

Figure 3.31: Coefficient of passive earth pressure for inclined homogeneous normally and overconsolidated backfill sand. $\phi = 25^o, \frac{\delta_P}{\phi} = \frac{2}{3}$.

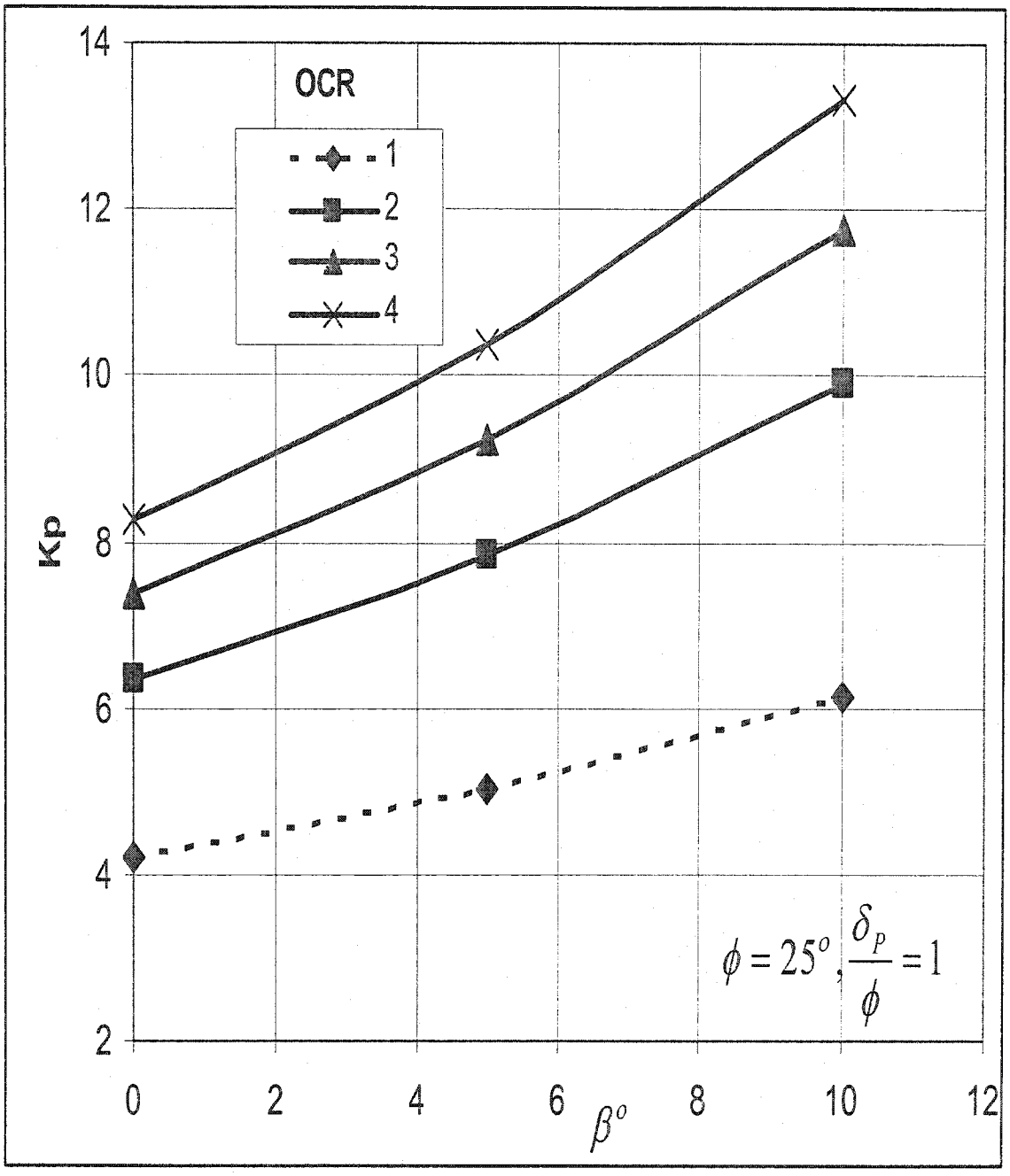

Figure 3.32: Coefficient of passive earth pressure for inclined homogeneous normally and overconsolidated backfill sand. $\phi = 25^o, \frac{\delta_P}{\phi} = 1$.

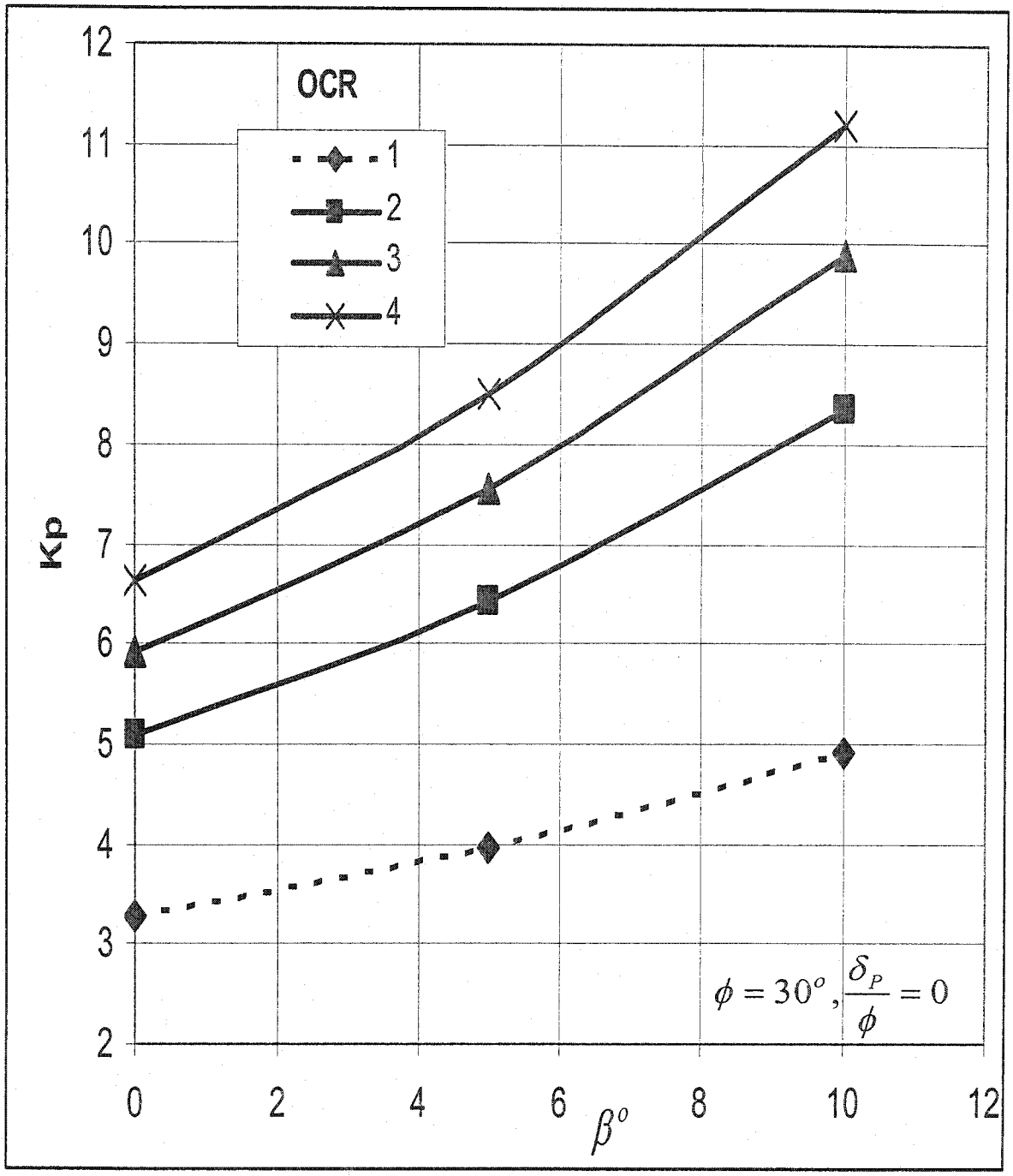

Figure 3.33: Coefficient of passive earth pressure for inclined homogeneous normally and overconsolidated backfill sand. $\phi = 30^\circ, \frac{\delta_P}{\phi} = 0$.

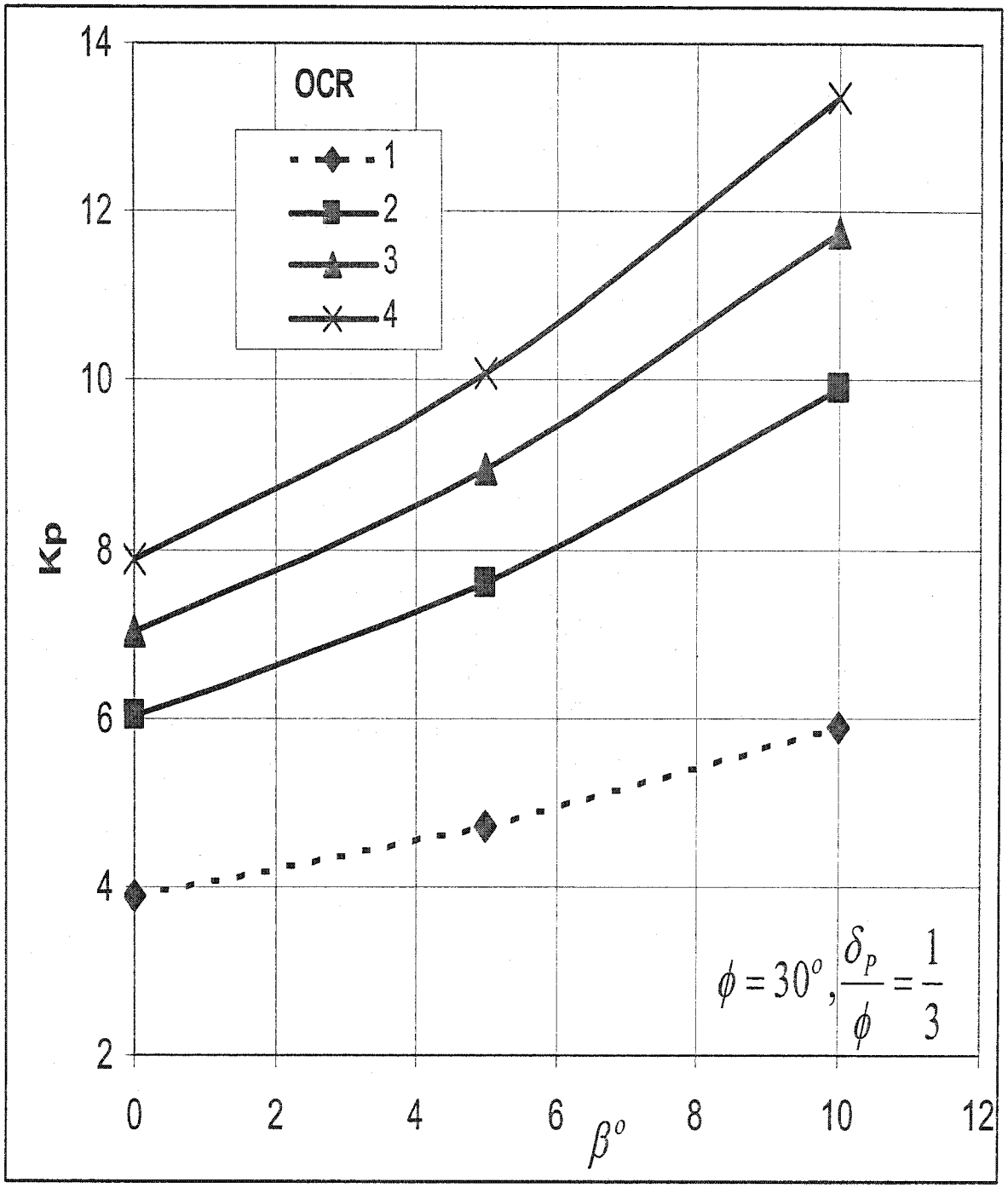

Figure 3.34: Coefficient of passive earth pressure for inclined homogeneous normally and overconsolidated backfill sand. $\phi = 30^o, \frac{\delta_P}{\phi} = \frac{1}{3}$.

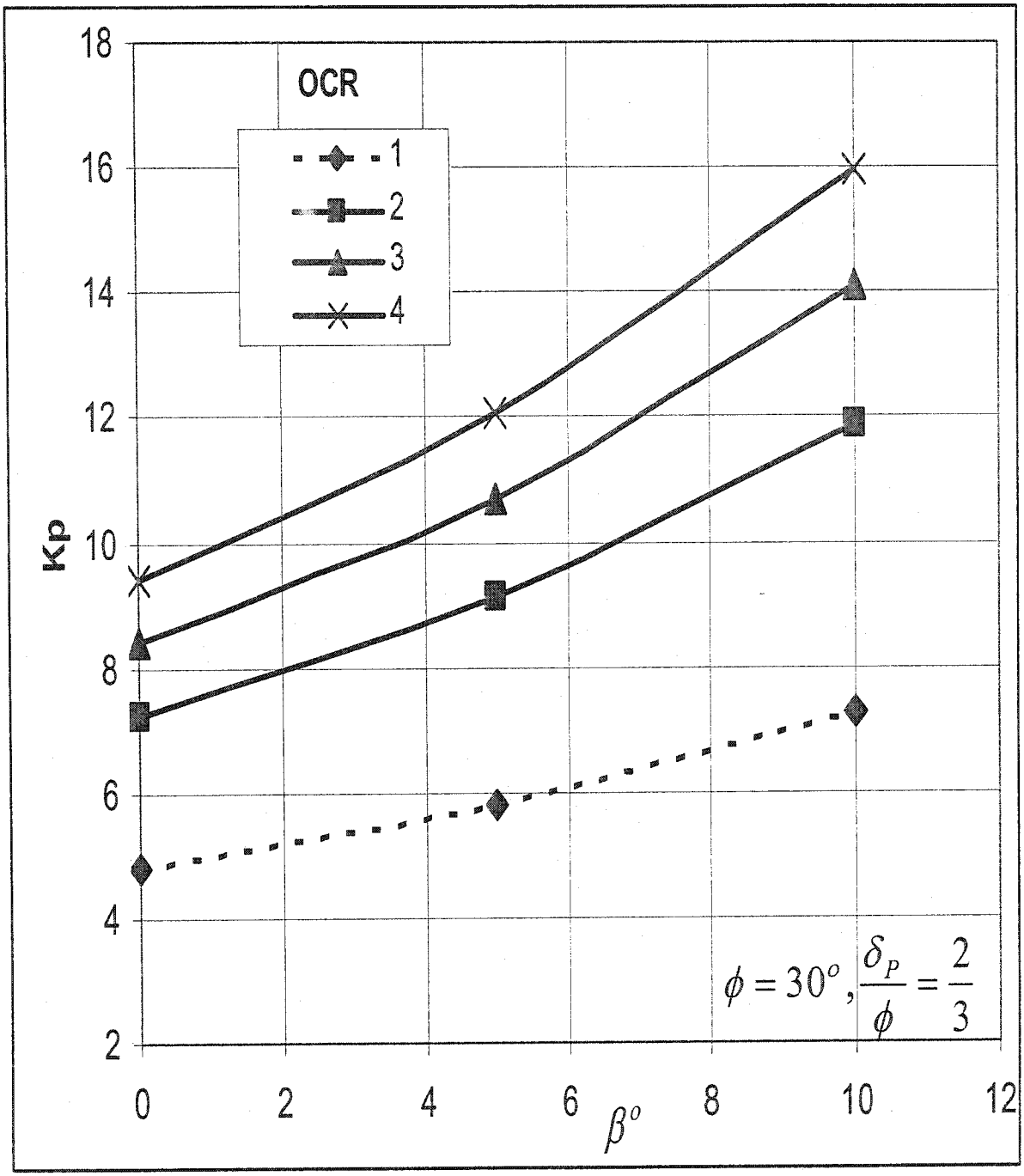

Figure 3.35: Coefficient of passive earth pressure for inclined homogeneous normally and overconsolidated backfill sand. $\phi = 30^o, \frac{\delta_P}{\phi} = \frac{2}{3}$.

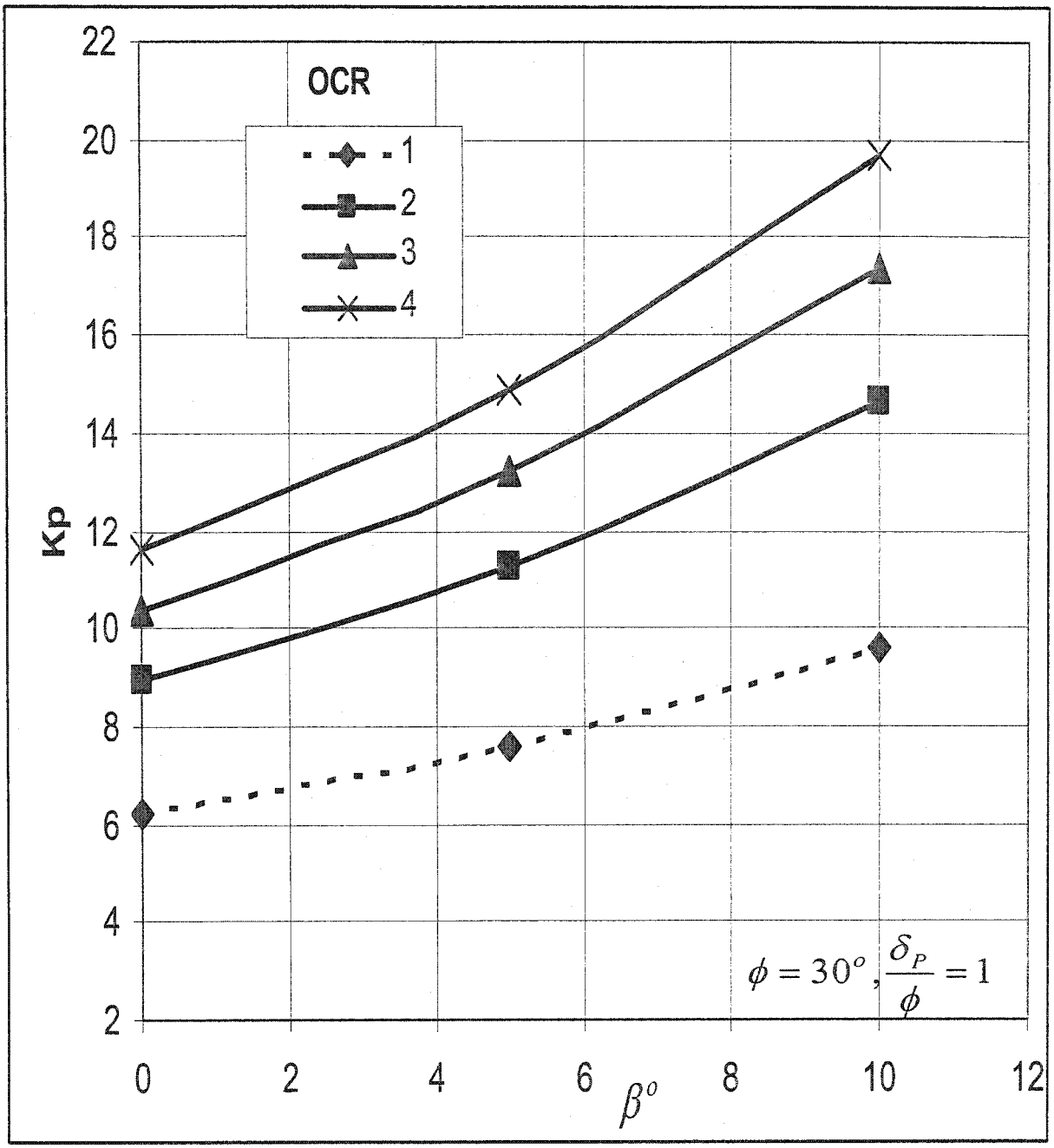

Figure 3.36: Coefficient of passive earth pressure for inclined homogeneous normally and overconsolidated backfill sand. $\phi = 30^o, \frac{\delta_P}{\phi} = 1$.

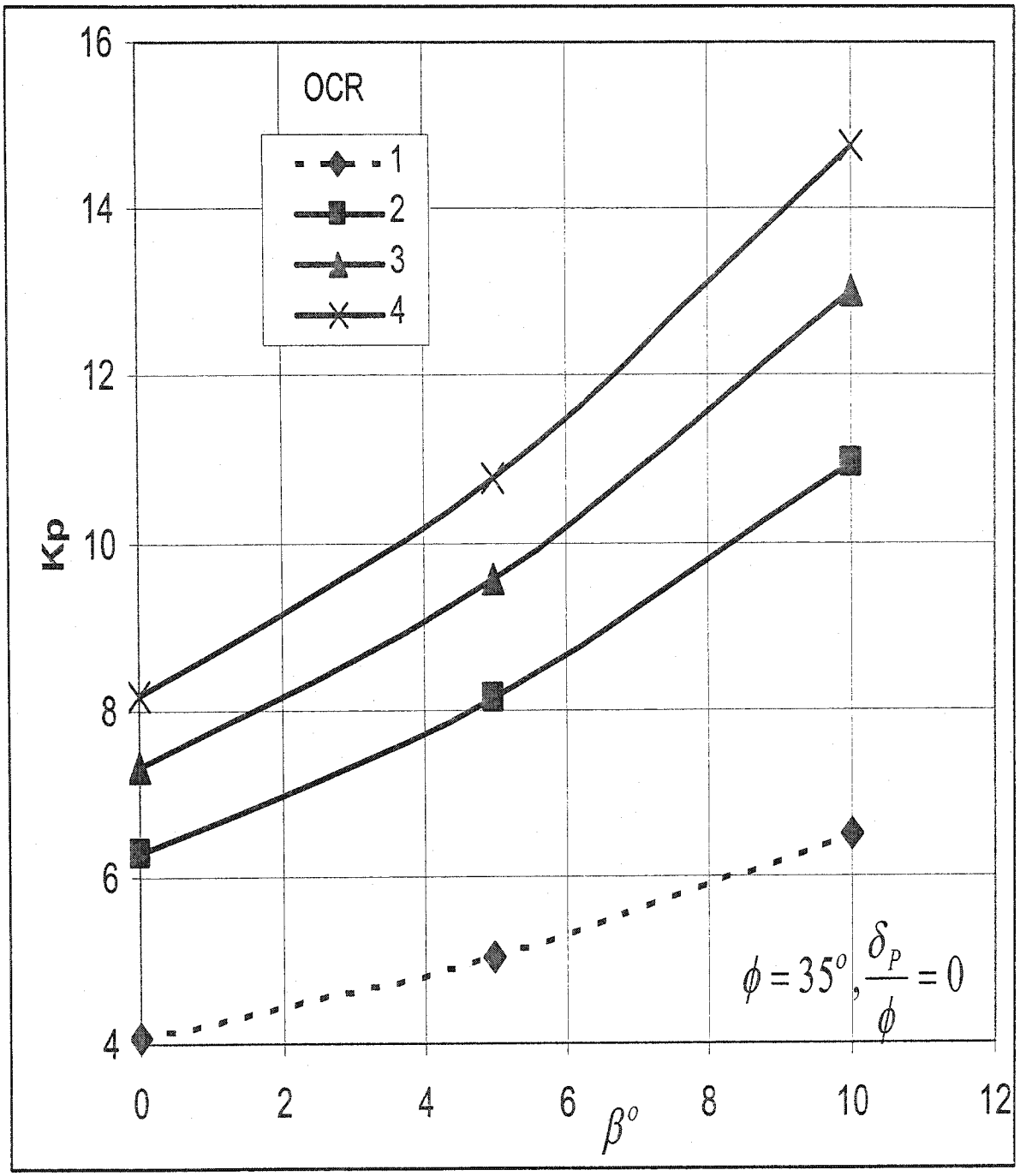

Figure 3.37: Coefficient of passive earth pressure for inclined homogeneous normally and overconsolidated backfill sand. $\phi = 35^o, \frac{\delta_P}{\phi} = 0$.

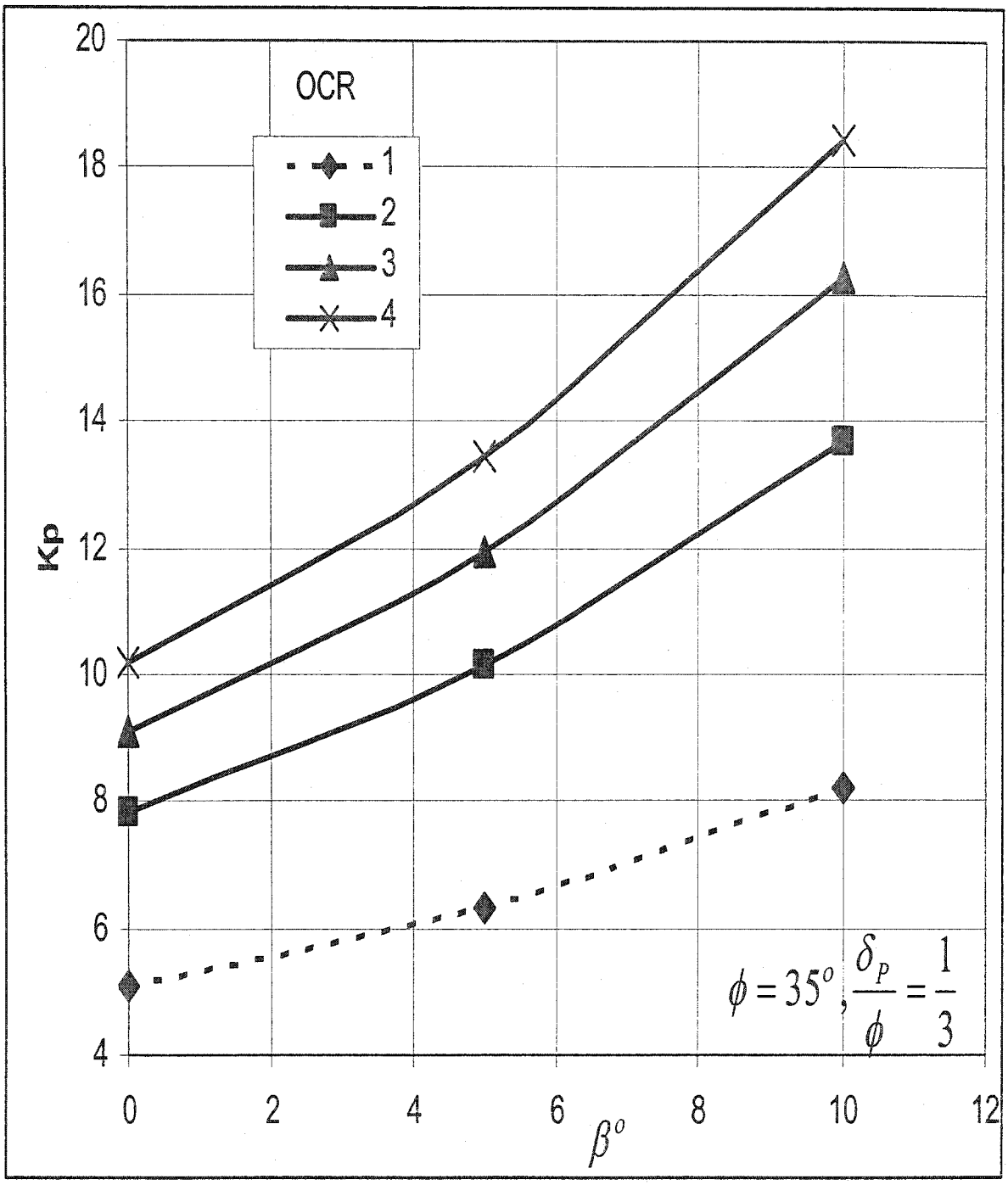

Figure 3.38: Coefficient of passive earth pressure for inclined homogeneous normally and overconsolidated backfill sand. $\phi = 35^o, \frac{\delta_P}{\phi} = \frac{1}{3}$.

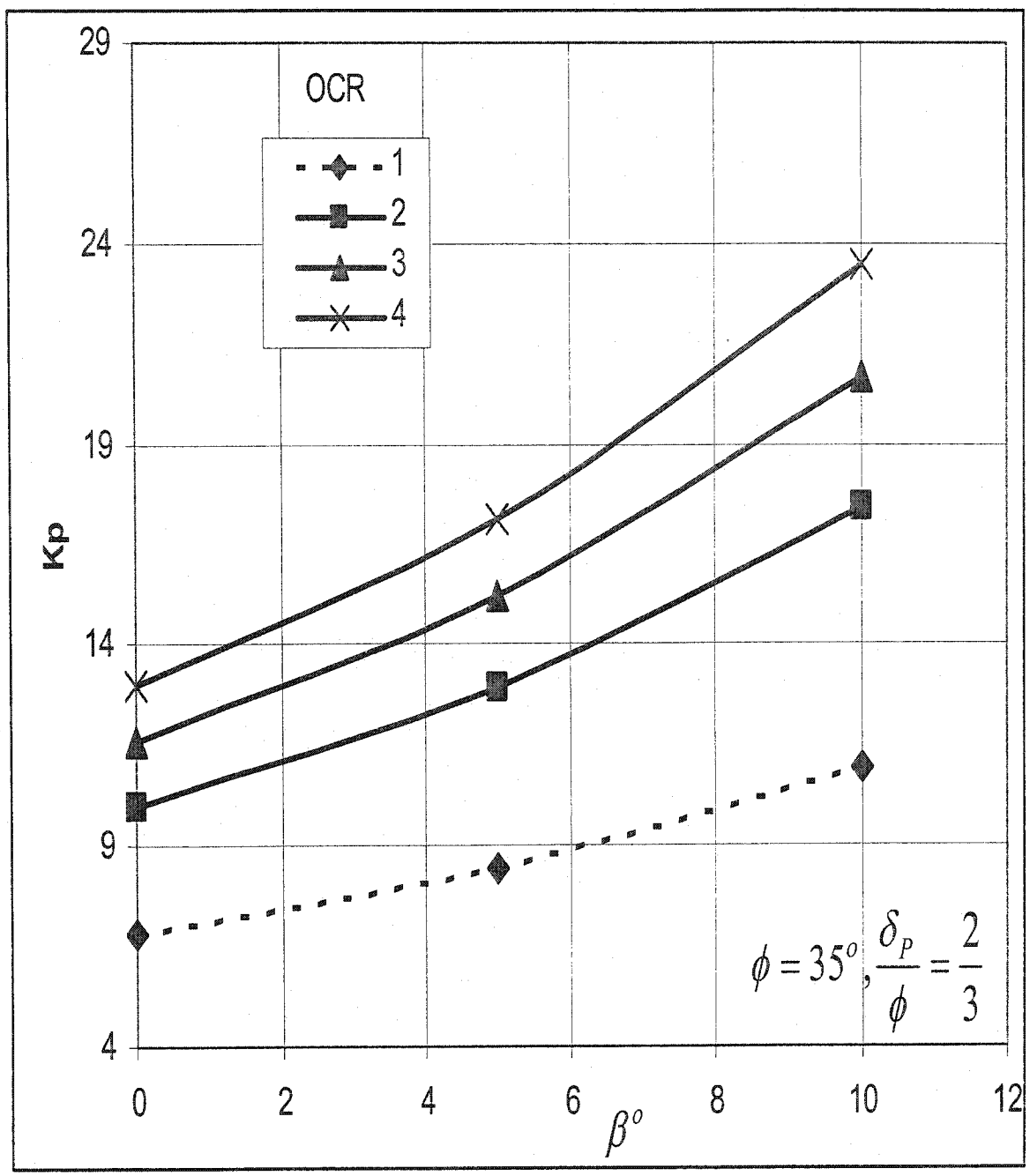

Figure 3.39: Coefficient of passive earth pressure for inclined homogeneous normally and overconsolidated backfill sand. $\phi = 35^o, \frac{\delta_P}{\phi} = \frac{2}{3}$.

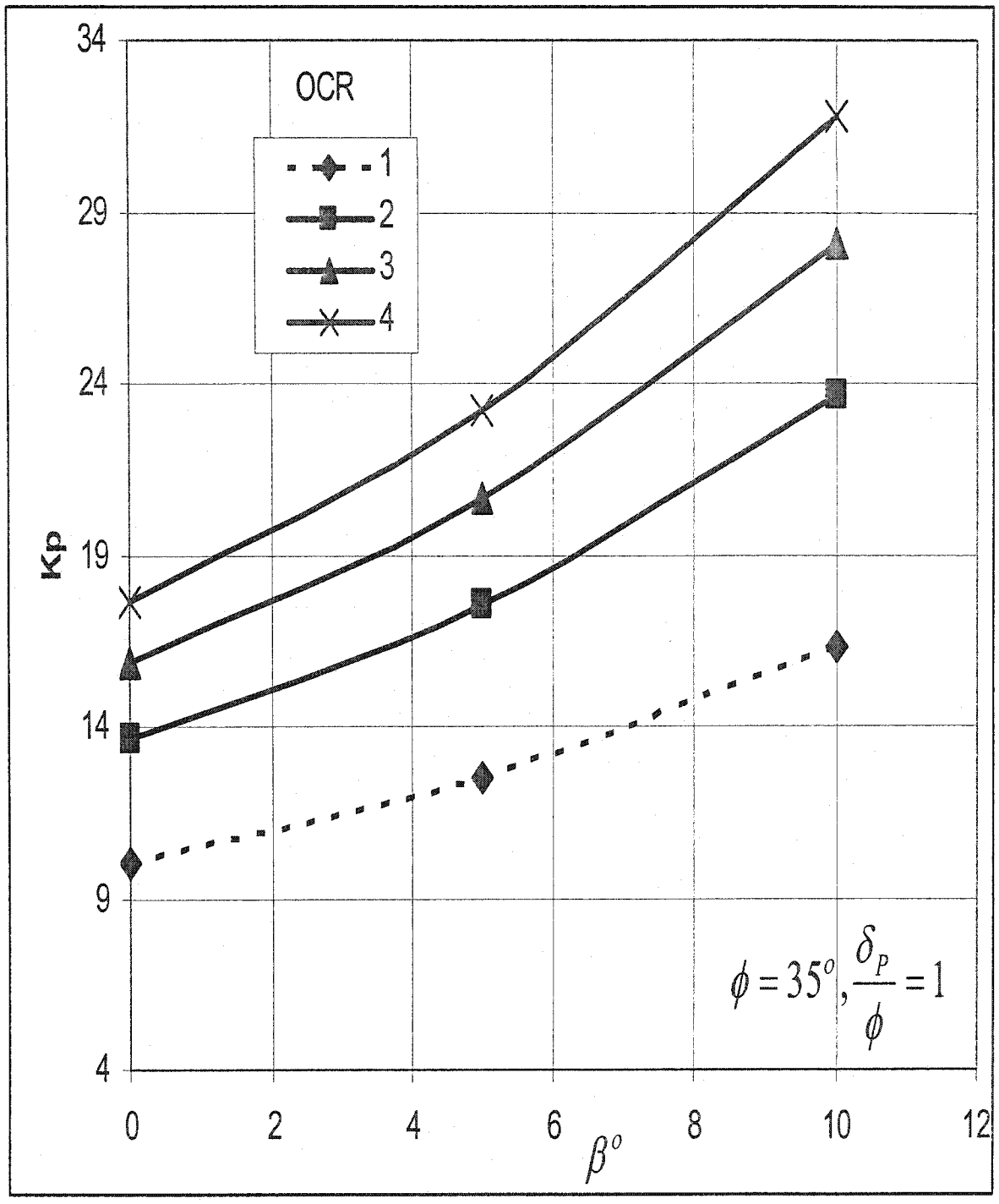

Figure 3.40: Coefficient of passive earth pressure for inclined homogeneous normally and overconsolidated backfill sand. $\phi = 35^o, \frac{\delta_P}{\phi} = 1$.

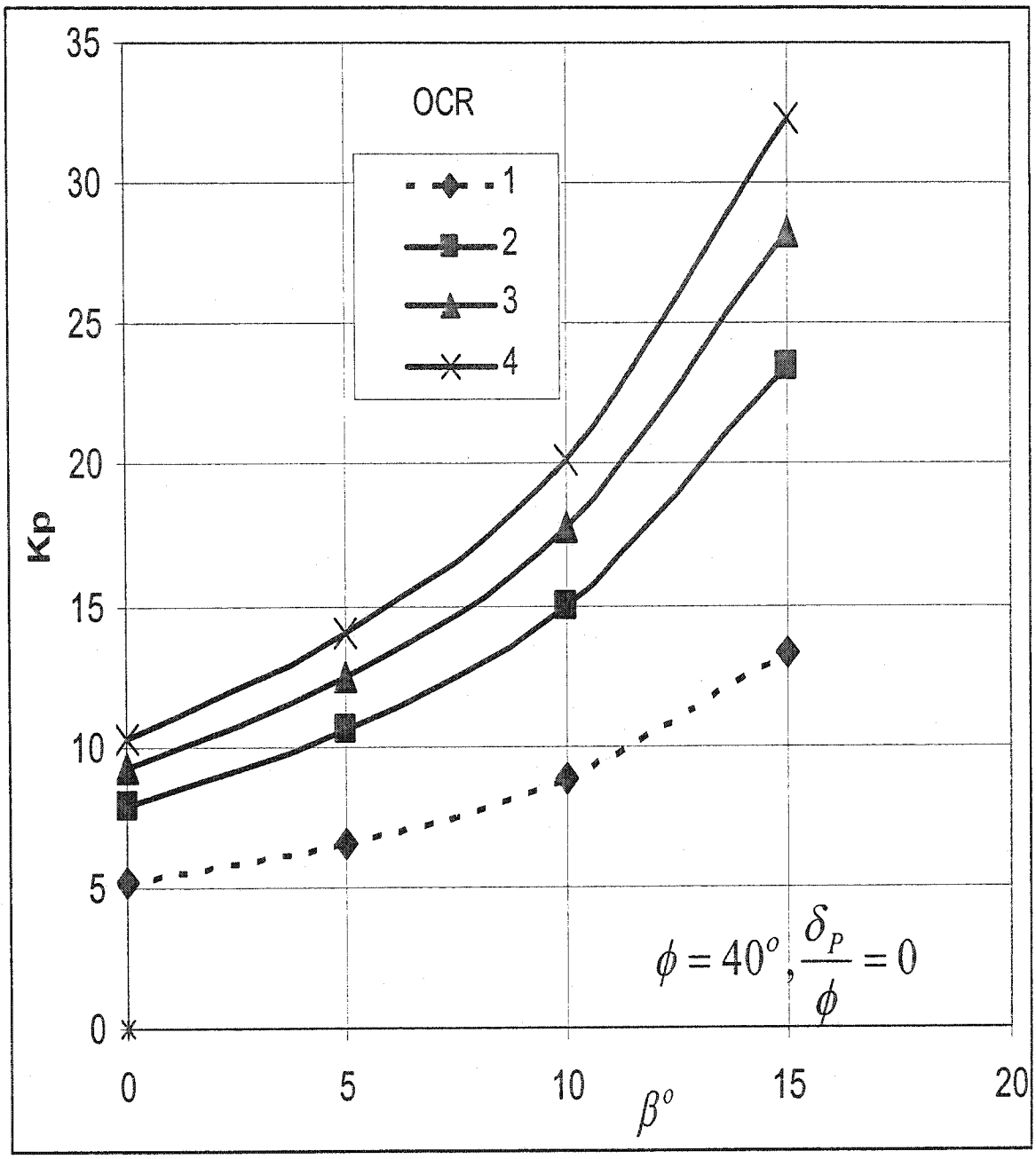

Figure 3.41: Coefficient of passive earth pressure for inclined homogeneous normally and overconsolidated backfill sand. $\phi = 40^o, \frac{\delta_P}{\phi} = 0$.

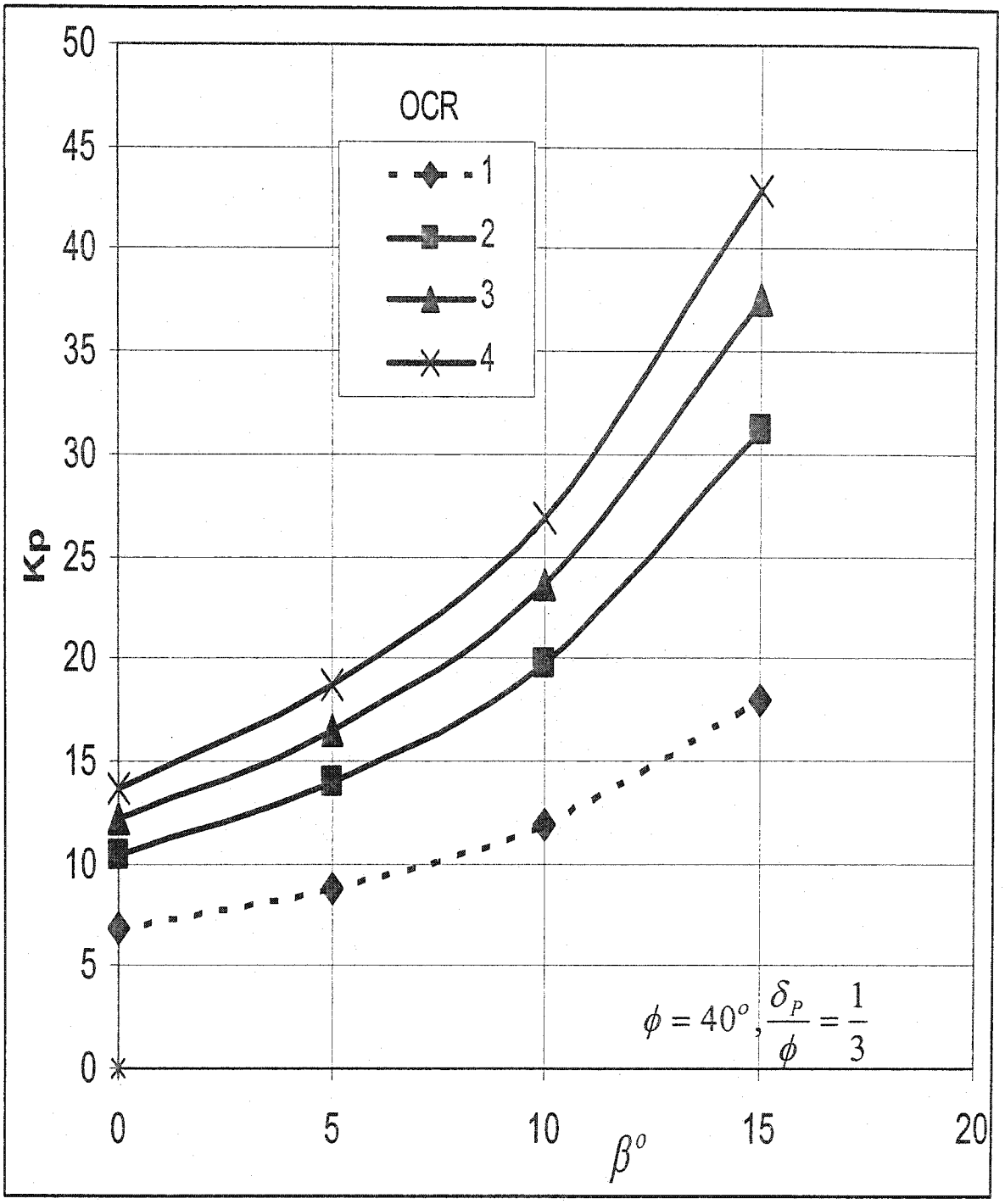

Figure 3.42: Coefficient of passive earth pressure for inclined homogeneous normally and overconsolidated backfill sand. $\phi = 40^o, \frac{\delta_P}{\phi} = \frac{1}{3}$.

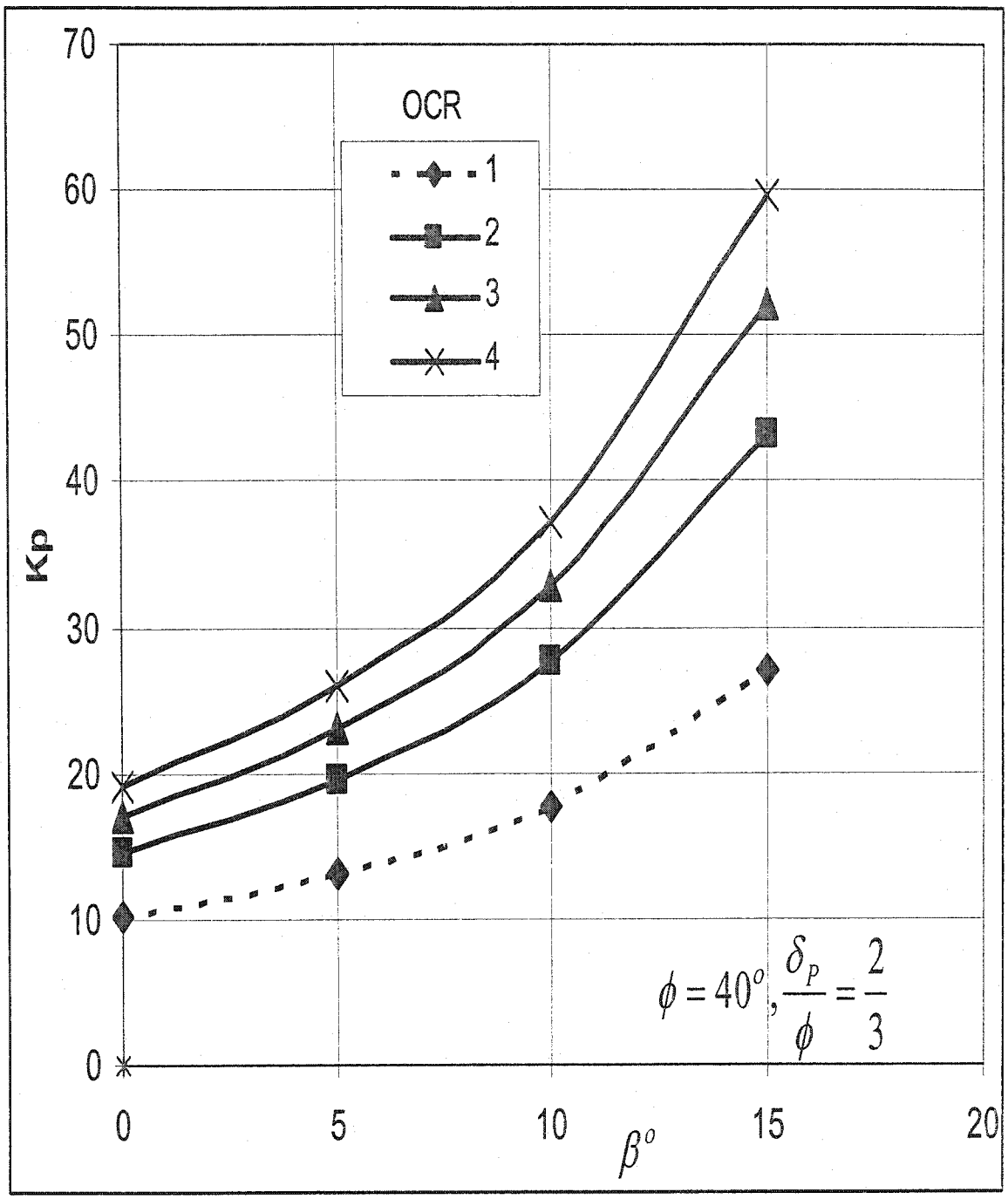

Figure 3.43: Coefficient of passive earth pressure for inclined homogeneous normally and overconsolidated backfill sand. $\phi = 40^o, \frac{\delta_P}{\phi} = \frac{2}{3}$.

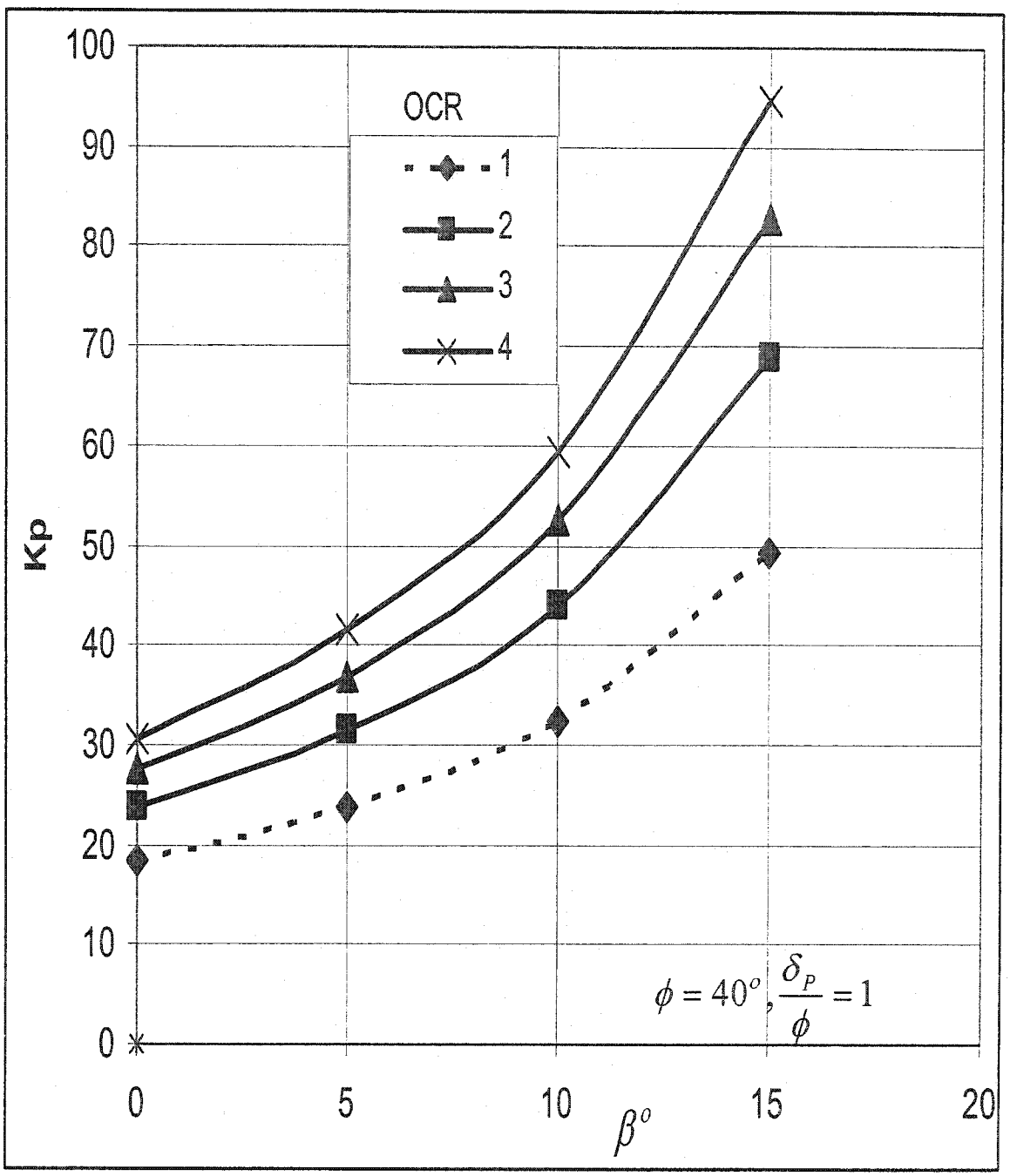

Figure 3.44: Coefficient of passive earth pressure for inclined homogeneous normally and overconsolidated backfill sand. $\phi = 40^o, \frac{\delta_P}{\phi} = 1$.

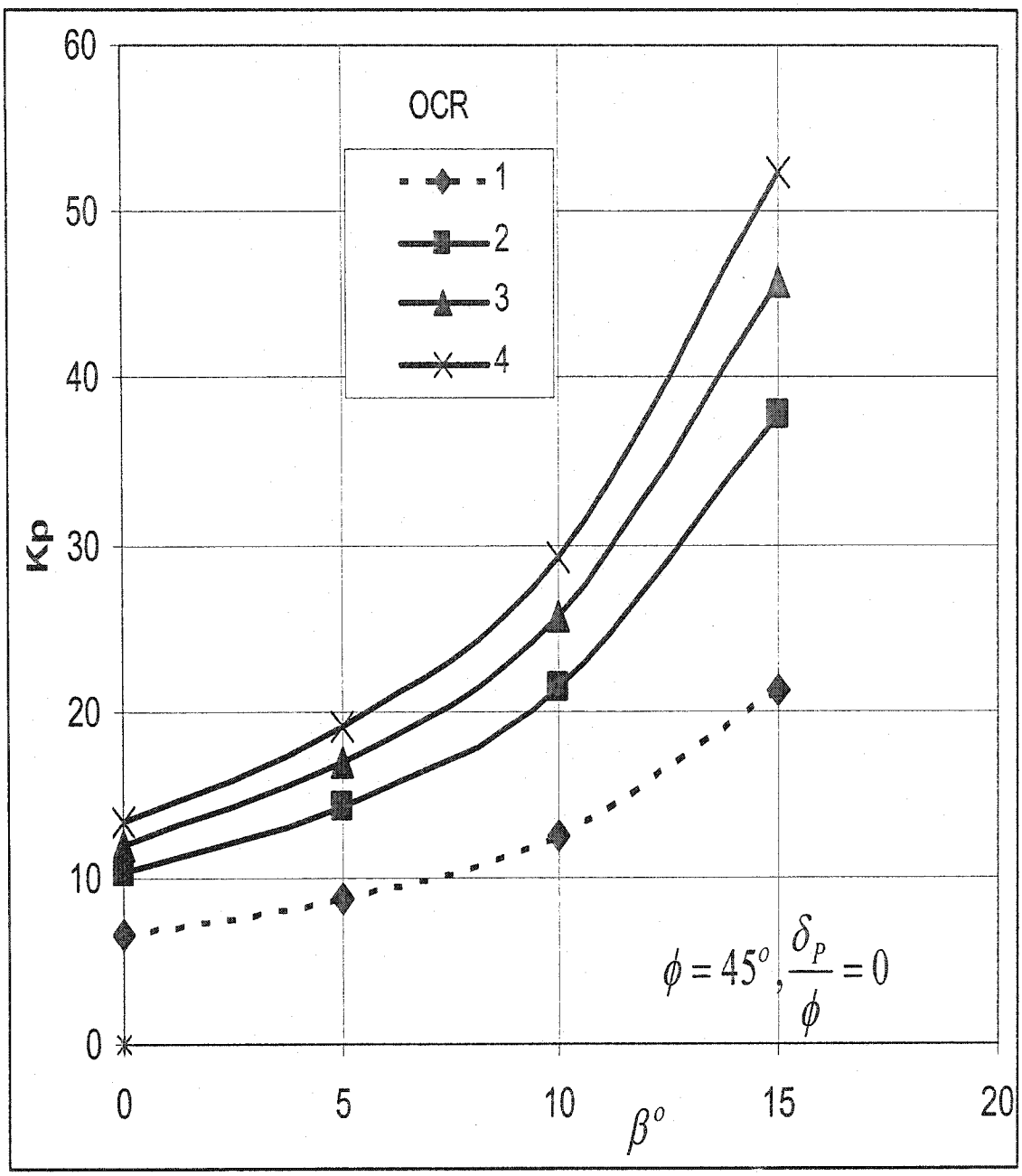

Figure 3.45: Coefficient of passive earth pressure for inclined homogeneous normally and overconsolidated backfill sand. $\phi = 45^o, \frac{\delta_P}{\phi} = 0$

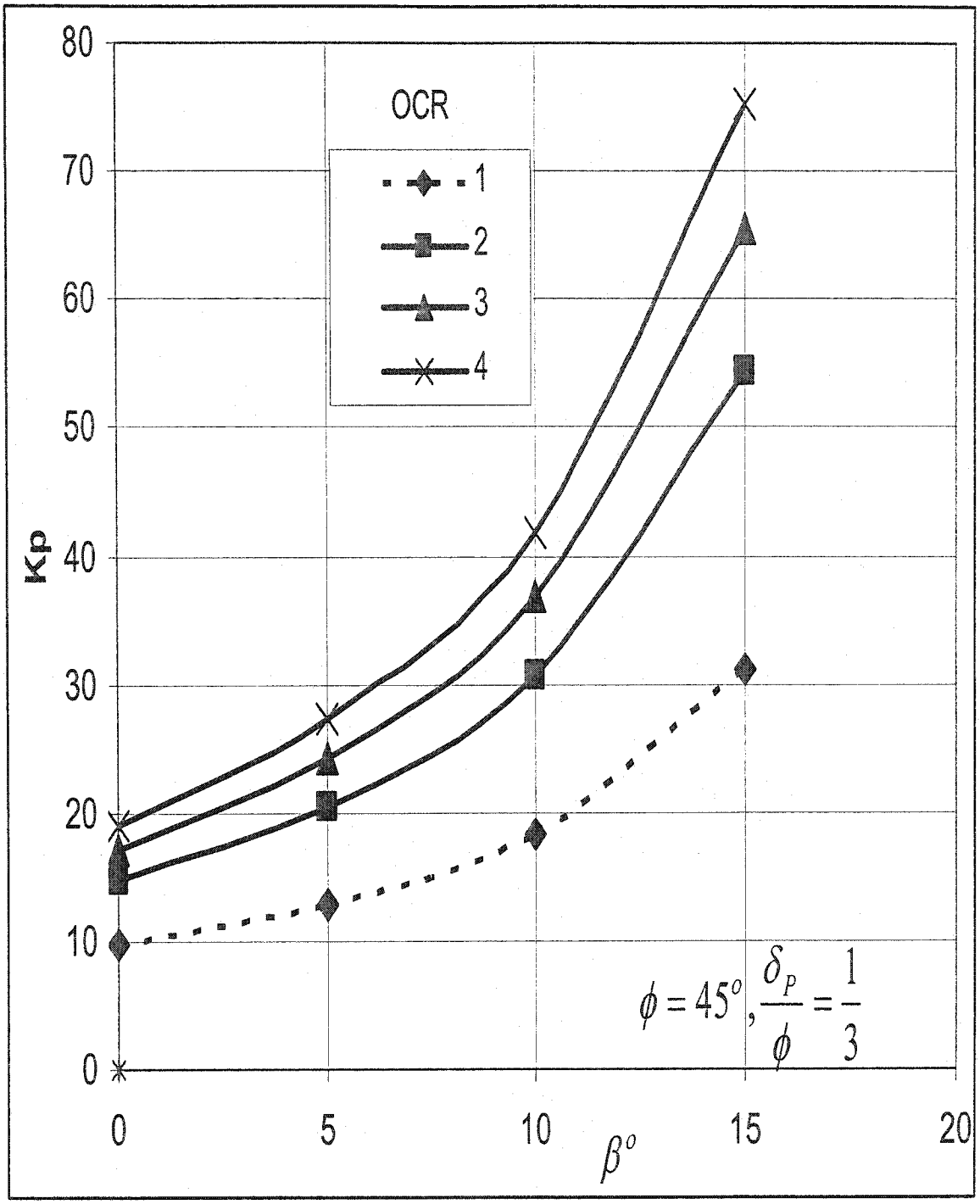

Figure 3.46: Coefficient of passive earth pressure for inclined homogeneous normally and overconsolidated backfill sand. $\phi = 45^o, \frac{\delta_P}{\phi} = \frac{1}{3}$.

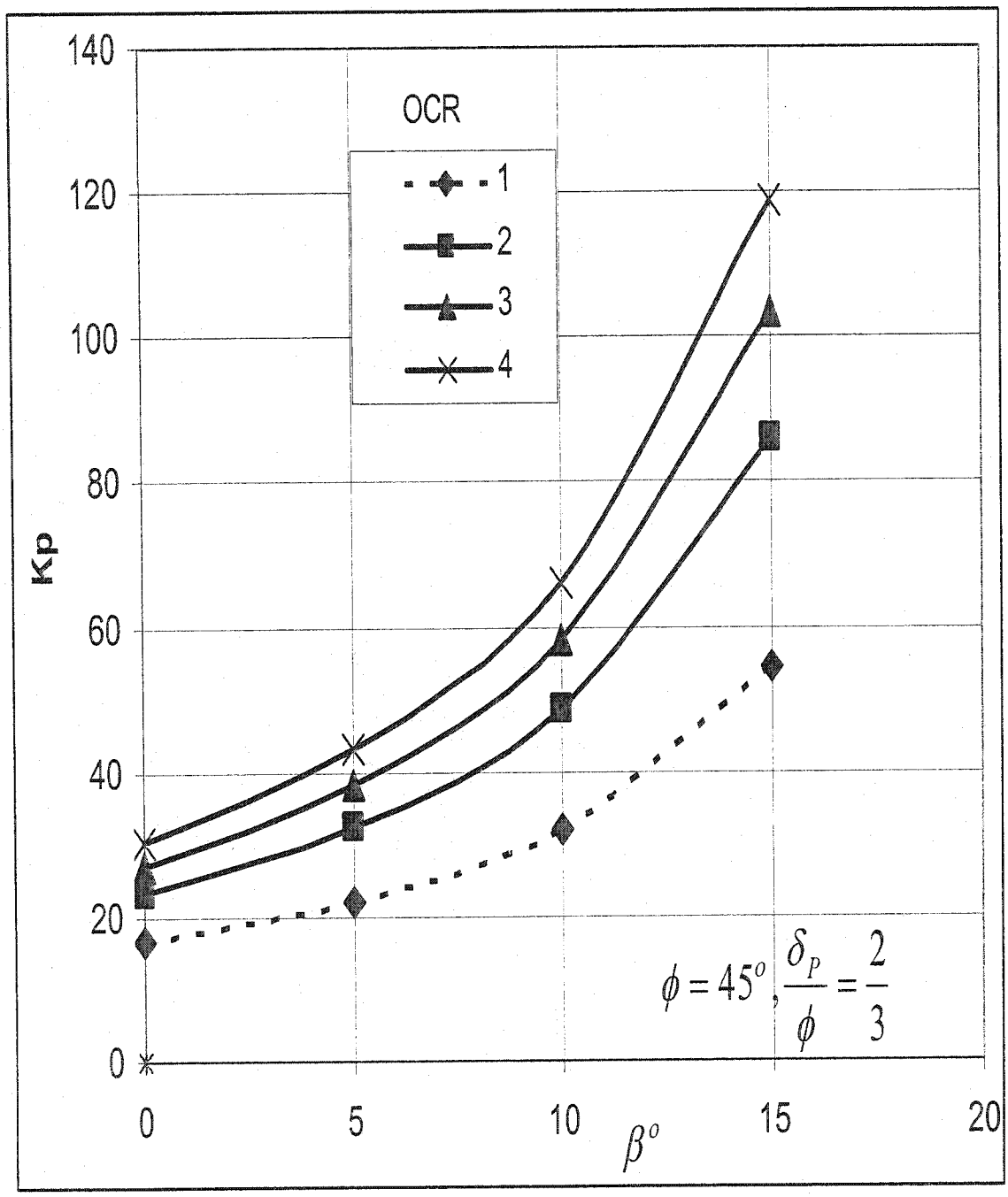

Figure 3.47: Coefficient of passive earth pressure for inclined homogeneous normally and overconsolidated backfill sand. $\phi = 45^o, \frac{\delta_P}{\phi} = \frac{2}{3}$.

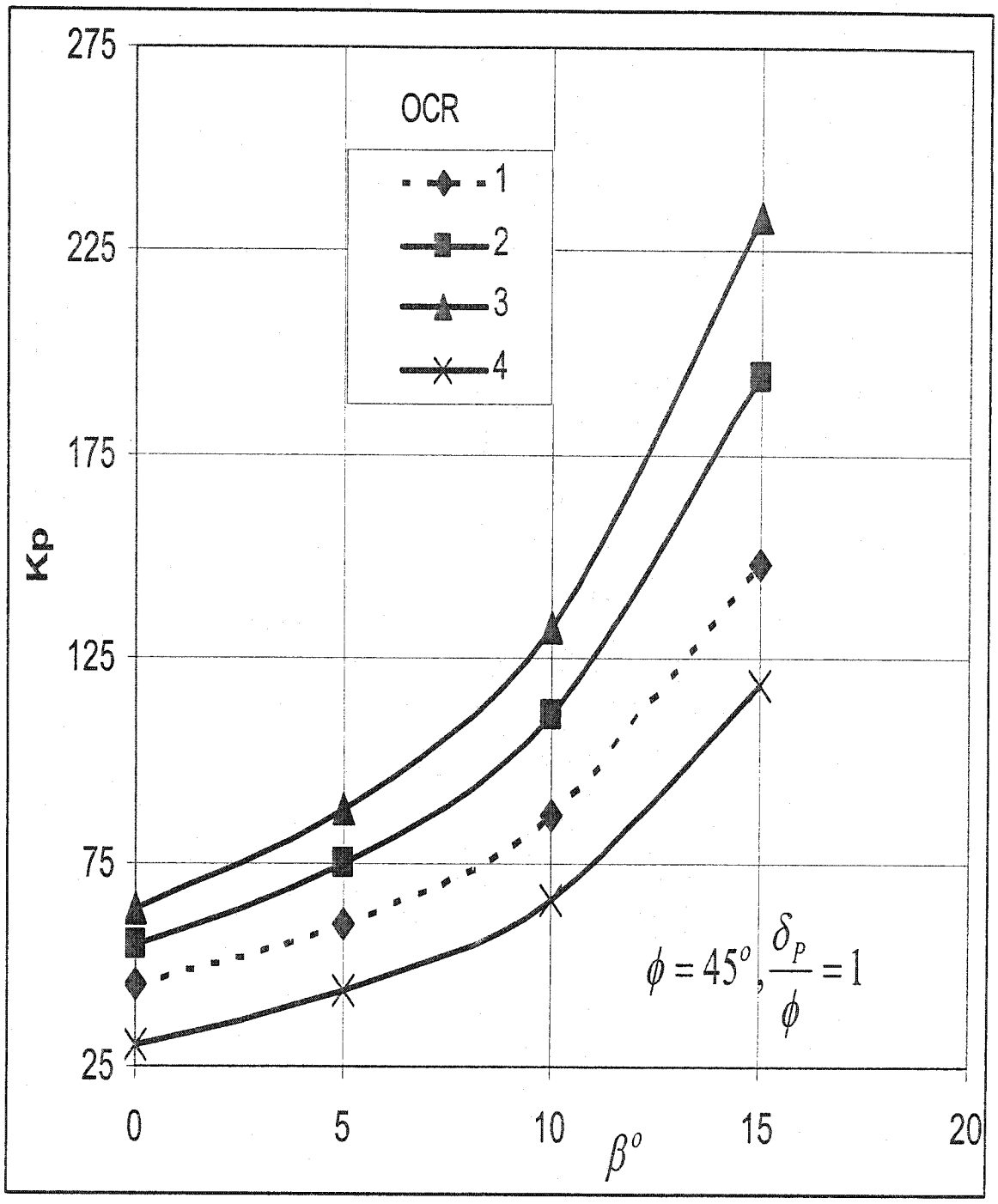

Figure 3.48: Coefficient of passive earth pressure for inclined homogeneous normally and overconsolidated backfill sand. $\phi = 45^o, \frac{\delta_P}{\phi} = 1$.

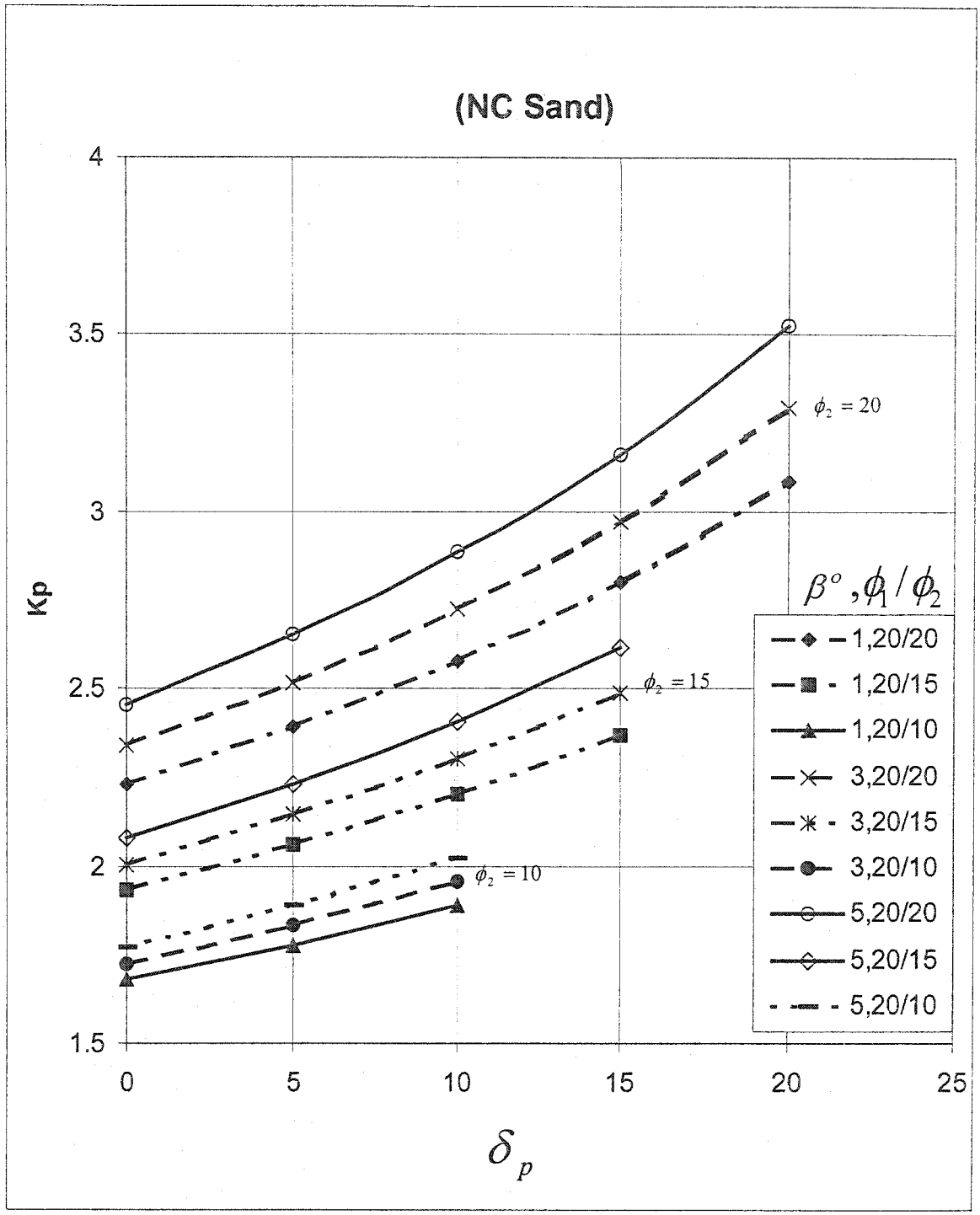

Figure 3.49: Coefficient of passive earth pressure for inclined backfill for normally consolidated sand.

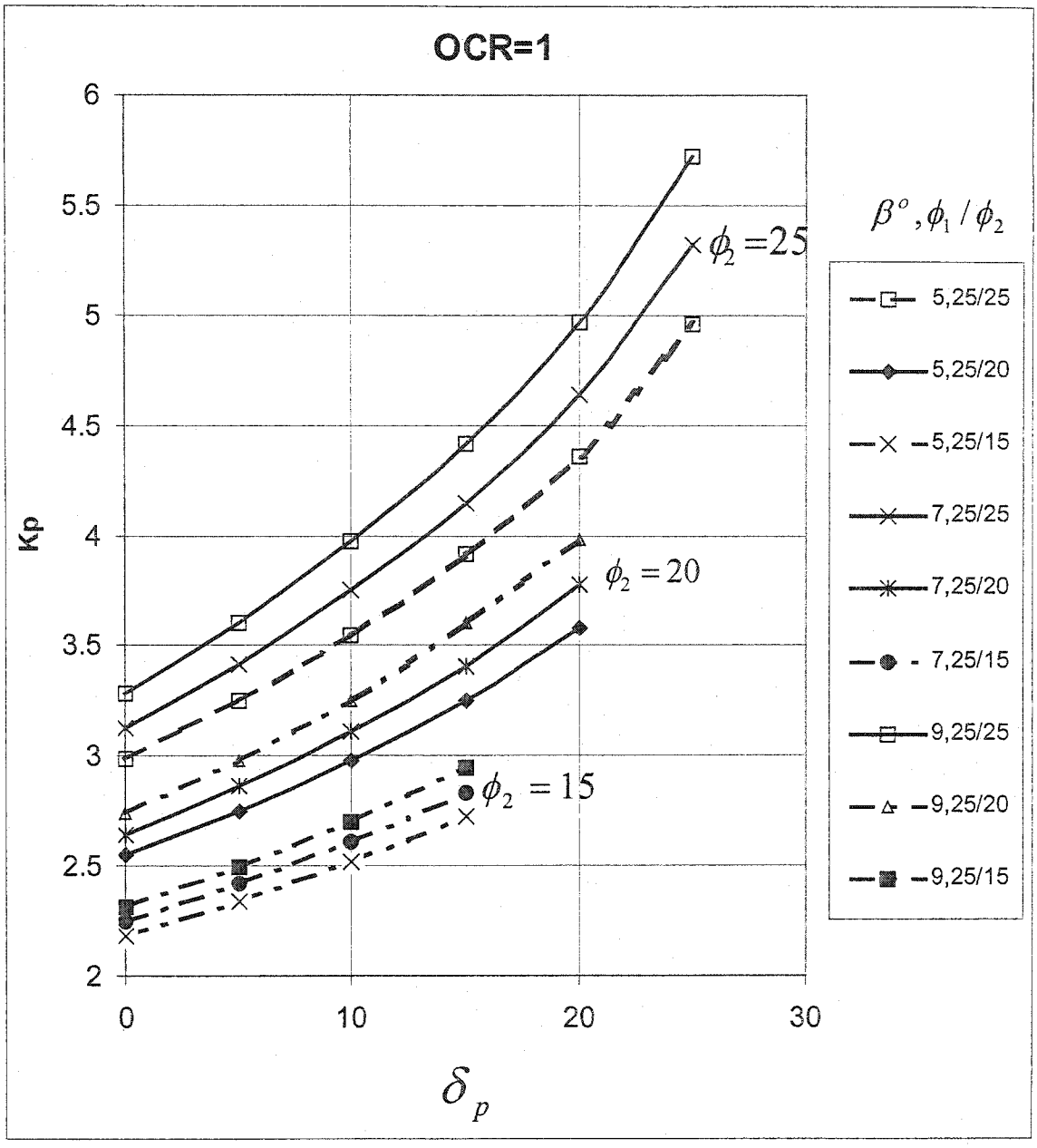

Figure 3.50: Coefficient of passive earth pressure for inclined backfill for normally consolidated sand.

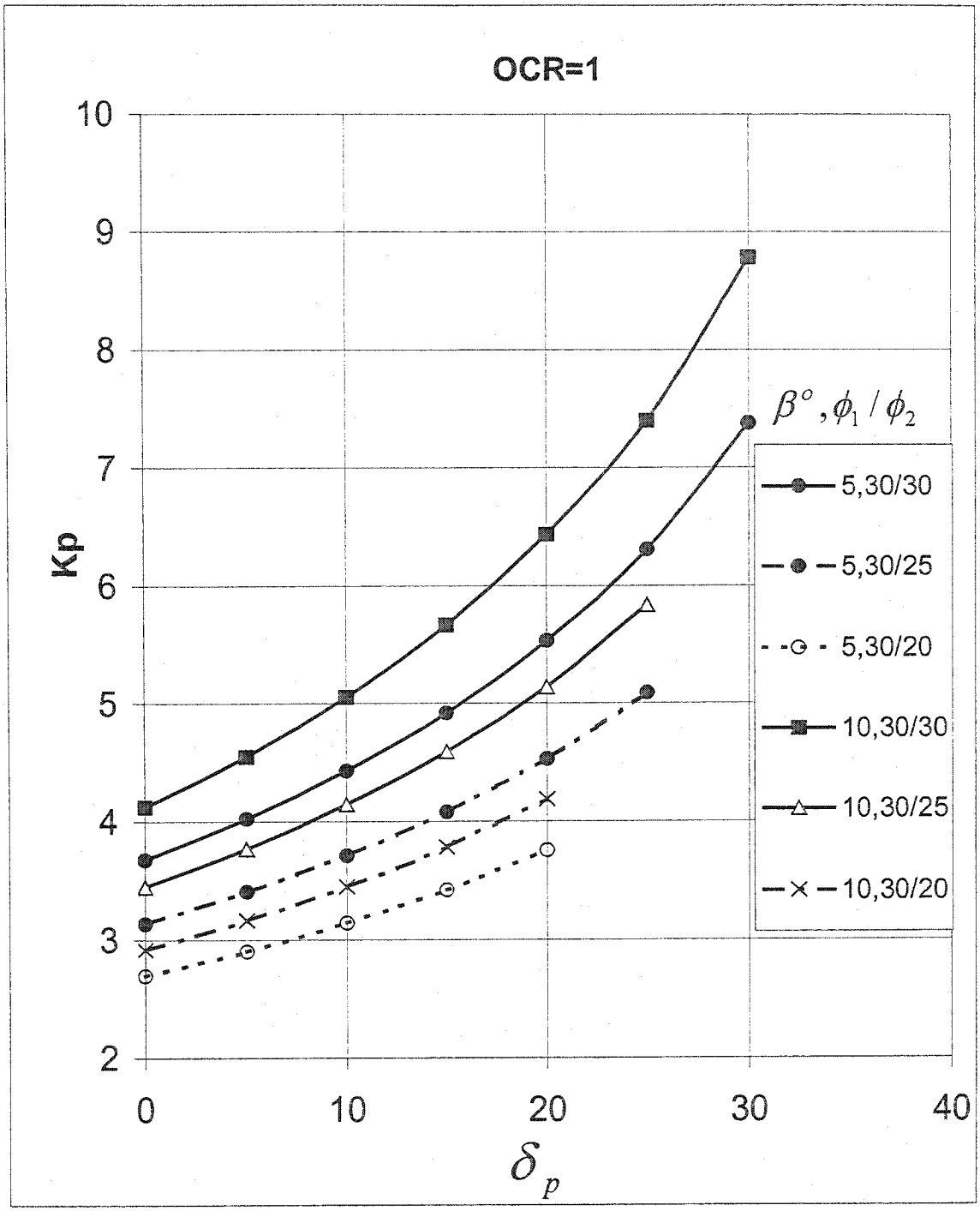

Figure 3.51: Coefficient of passive earth pressure for inclined backfill for normally consolidated sand.

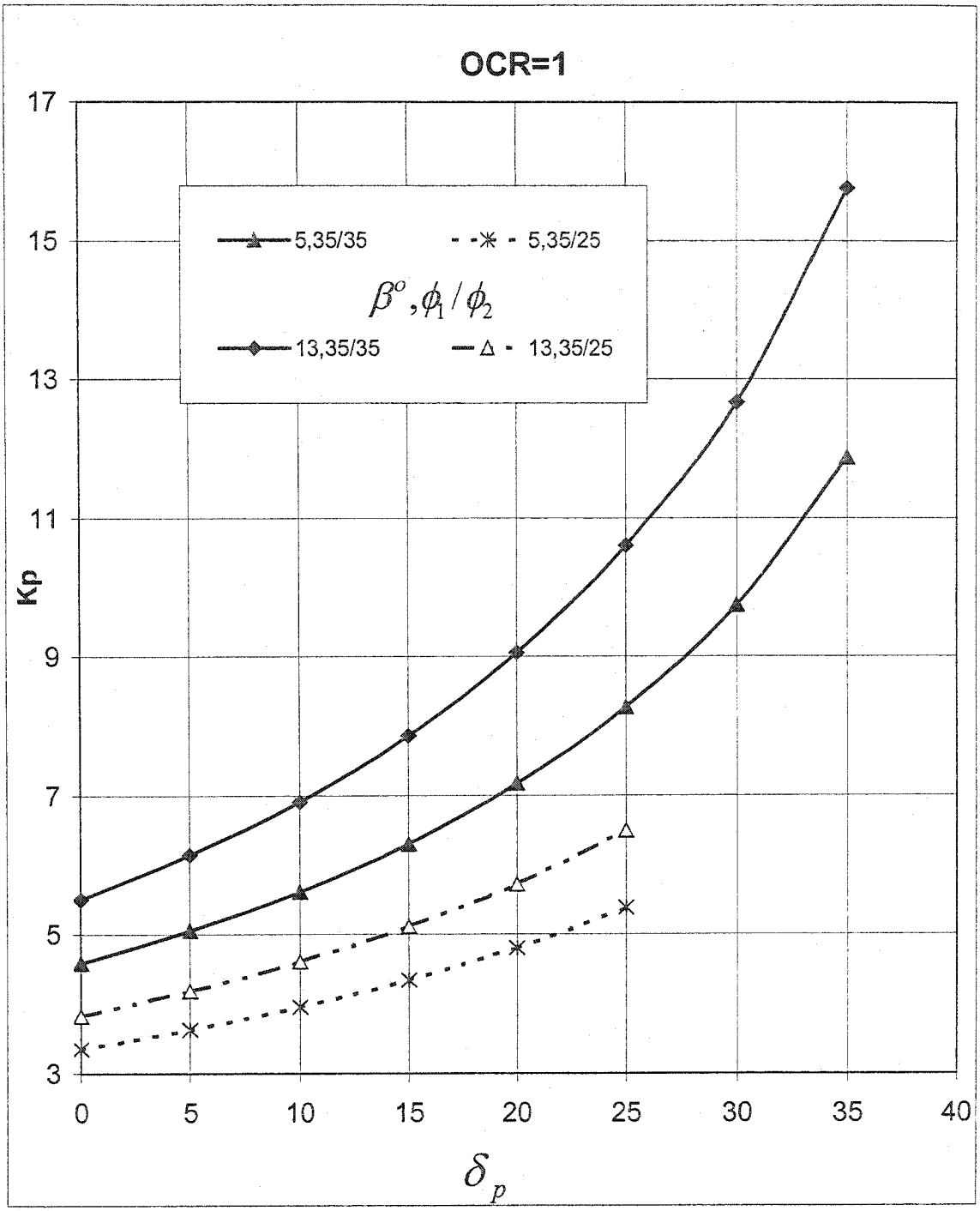

Figure 3.52: Coefficient of passive earth pressure for inclined backfill for normally consolidated sand.

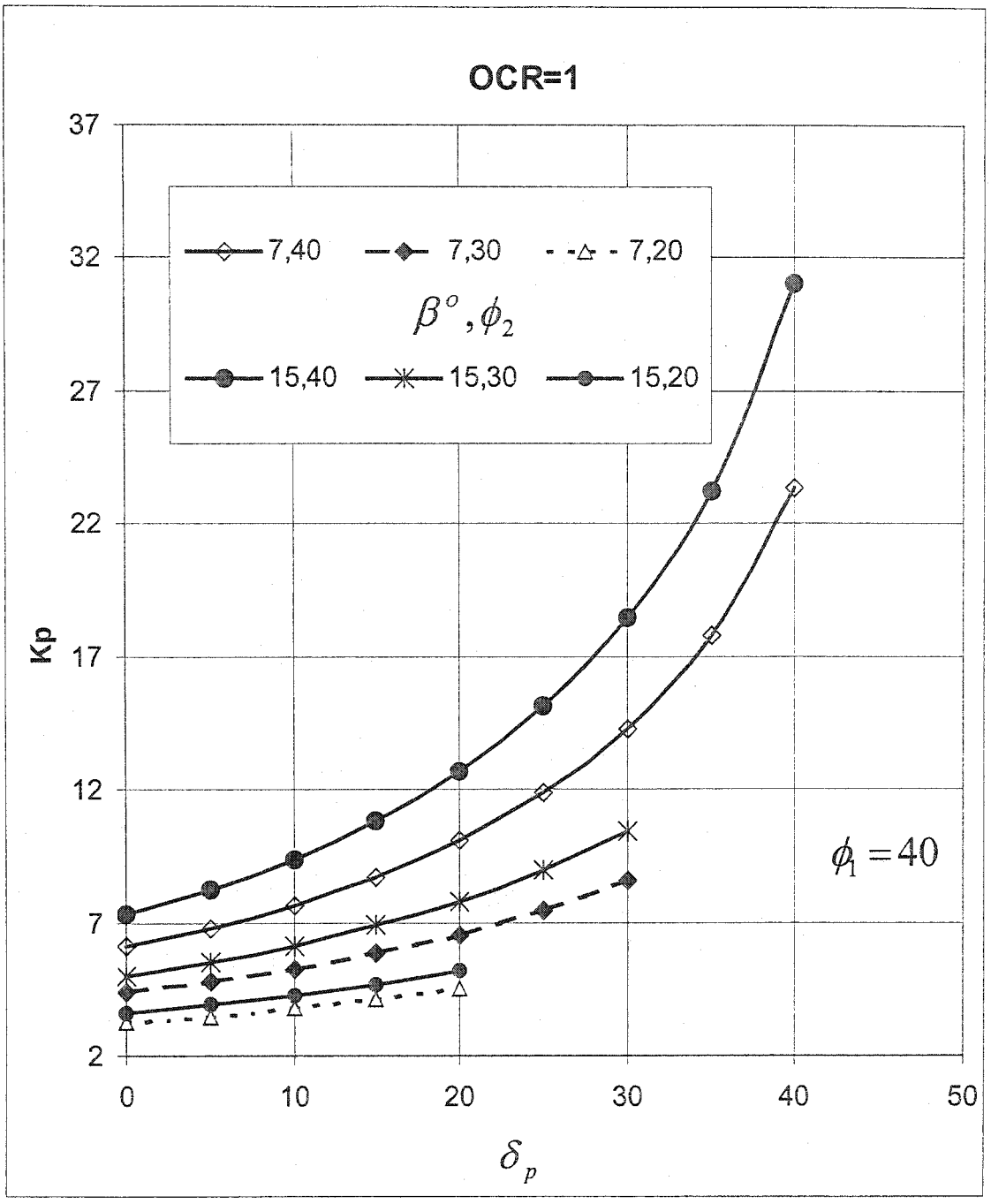

Figure 3.53: Coefficient of passive earth pressure for inclined backfill for normally consolidated sand.

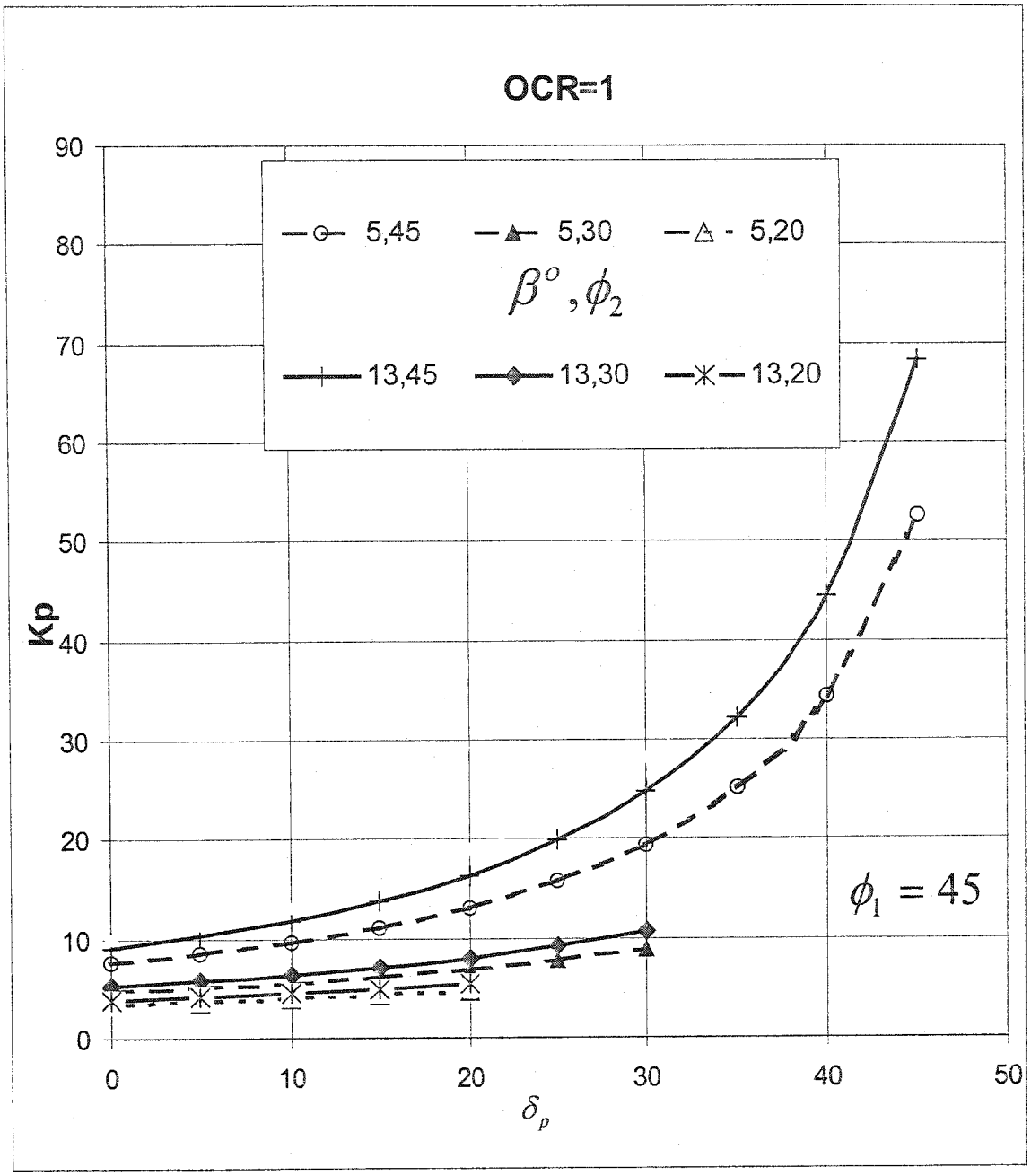

Figure 3.54: Coefficient of passive earth pressure for inclined backfill for normally consolidated sand.

CHAPTER 4

CONCLUSIONS

During the last half-century several methods have been proposed for calculation of earth pressure, especially for the passive case. Most are based on limit equilibrium involving assumptions regarding the shape of failure surface in the backfill. Furthermore, the problem of searching for the location of the critical failure surface of general shape has not been solved completely.

It is very important to mention that the passive earth pressure behind a retaining wall is affected directly by the strength of the sand backfill and the wall-soil fractional angle.

The orientation of the failure plane is significant in determining the coefficient of passive earth pressure, which depends on the inclination angles of the slice bases, this is a very important factor to estimate which affects all the results behind the interslice frictional angle which is assumed to increase through the slices toward the wall.

The stress history is a significant issue in passive earth pressure coefficient, which has a proportional relationship with the value of K_p.

Passive earth pressure coefficient in the case of homogeneous overconsolidated sands increase while increasing the internal frictional angle of the sands and it is a factor of overconsolidation. That means the stress history affects significantly the coefficient of passive earth pressure, which increases this coefficient while increasing the value of overconsolidation ratio (OCR).

For the case of two layers of different types of sands for normally consolidated case it appears that the passive earth pressure coefficients increased proportionally with

increasing of the soil-wall frictional angle (δ_p), the value of the composed internal frictional angle (ϕ_{new}), and the value of OCR. For the case of overconsolidated sands of two layers the passive earth pressure coefficient increases proportionally as increasing the soil-wall frictional angle (δ_p), the value of the composed internal frictional angle (ϕ_{new}), and the value of OCR, and the value of passive earth pressure coefficient K_p decreases as the lower layer internal frictional angle decreases while fixing the upper layer (strong layer) in the case of strong soil overlay weak sands, and as the lower layer internal friction angle increases to be close to the upper layer then Kp increases directly because it becomes more homogeneous. In the case of a weak soil overlaying a very strong layer of sands the coefficient of passive earth pressure remains approximately as that of the weak layer. It would be logical to infer that the passive earth pressure is related to the shearing resistance of soil along the rupture surface.

Backfill inclination upward the top of the wall increases the coefficient of passive earth pressure, as the inclination increases then the passive earth pressure increases.

Passive earth pressure is often presumed to resist the active movement of the wall. An overestimated factor of safety against sliding would put the design on the unsafe side.

Design charts were developed for engineering practice to predict the coefficient of passive earth pressure for homogeneous overconsolidated sand or overconsolidated sand backfill overlaying natural deposit.

RECOMMENDATIONS FOR FUTURE RESEARCH:

It should be noted that most of the design charts and tables based on theoretical solutions lack experimental tests. Therefore, it is important to design an experimental test to find the coefficient of passive earth pressure for the cases of normally consolidated and overconsolidated cohesionless soil of homogeneous and two layers of different types of sands for inclined backfill and inclined wall, as a general case in order to develop a theory that can calculate the passive earth pressure coefficient for these cases.

REFERENCES:

1. Braja. M.Das. (1998) Principles of Foundation Engineering, fourth Edition.
2. Brooker, E.W.and Ireland, H.O., (1965),"Earth Pressure at Rest Related to stress History". Canadian Geotechnical Journal, vol.2, No.1, P: 1-15.
3. Caquot, A.and Kerisel,J.,(1948),"Tables de poussée et butée". Gauthier-Vallars,Paris.
4. Coulomb, C.A., (1776),"Essai sur une application des régles des maximis et minimise à quelue problemés de statique". Mémoire Académie Royale des Sciences, 7, Paris.
5. Da-Yong and Qihu Qian (2000), Determination of passive earth pressure coefficients by the method of triangular slices. Canadian Geotechnical Journal.37: 485-491(2000).
6. Donald, H. Shield and Zeki, A. Tolunay (1972) Passive earth pressure for sand, Canadian Geotechnical Journal, 9,501 (1972).
7. James, R.G and Bransby, P.L., (1970),"Experimental and theoretical investigations of passive earth pressure problem'. Geotechnique 20, No.1, P: 17-37.
8. J.Duncan and L.Mokwa (2001) passive earth pressures: Theories and Tests. Journal of Geotechnical and Geoenvironmental Engineering. Vol.127, No.3, March 2001.
9. Hanna, A.M (1981),"Foundations on Strong Sand Overlying Weak Sands" ASCE vol.107 No.GT7 July 1981. P: 915-927.

10. Hanna, A.M., and Ghaly, A.M. (1990),"Effects of K_o and Overconsolidation on Uplift Capacity", ASCE, Vol.118 No.9SEP, P: 1449-1469.
11. Hanna, A.M., and Saad, N.S (2001),"Effect of Compaction Duration on the Induced Stress Levels in a Laboratory Prepared Sand Bed", ASTM, GTJODJ, Vol.24, December 2001,pp.430-438.
12. Hansen, J.B., (1953), "Earth Pressure Calculation". The Danish Technical Press, Institution of Danish Civil Engineers, Copenhagen.
13. Jyant Kumar (2001) Seismic pullout capacity of vertical anchors in sands. Indian Institute of Science, Bangalore-560012.
14. Khoury, R., (1994) "Passive Earth Pressure Behind a Retaining Wall for Normally Consolidated and Overconsolidated Cohesionless Soil". Thesis at Concordia University (1994).
15. Kumar, J., and Subba Rao (1997) Passive Pressure Coefficients, critical failure surface and its kinematic admissibility.Geotchnique 47, No 1:185-192.(1997).
16. Mayerhof, G.C, (1976),"Bearing Capacity and Settlement of Piles Foundations". Journal of Geotechnical Engineering Division, ASCE, vol. 102(GT3), P: 197-228.
17. Narain j.,Saran S. and Nandakumaran, P.,(1969),"Model study of passive pressure in sand". Journal of soil mechanics and foundations division proceeding of the ASCE.
18. Rankine, W.J.M., 1857. "On the stability of loose earth". Trans. Royal Soc., London, Vol. 147.

19. Riad Diab (1994), "Numerical Modeling of Passive Earth Pressure for Normally and Overconsolidated Sands", a thesis in the department of civil engineering, Concordia University.

20. Soubra, A.H., (2000), "Static and seismic passive earth pressure coefficients on rigid retaining structures." Canadian Geotechnical Journal .37: 463-478 (2000).

21. Soubra, A.H., and Regenass (2000), "Three-Dimensional Passive Earth Pressures by Kinematical Approach." Journal of Geotechnical and Geoenvironmental Engineering, Vol.126, No11, November, (2000).

22. Shields, D.H., and Tolunay, A.Z. (1972), "Passive Pressure Coefficients for sand by Terzaghi and Peck Method," Canadian Geotechnical Journal, vol.99, No. SM12.DEC.1973.

23. Shields, D.H., and Tolunay, A.Z. (1973), "Passive Pressure Coefficients by the Method of Slices", Journal of the Soil Mechanics and Foundations Division.

24. Terzaghi, K. (1948)"Theoretical Soil Mechanics in Engineering Practices". Wiley New -York.

25. Wang (2000), "Distribution of Earth Pressure on a Retaining Wall." Geotechnique 50, No 1: 83-88. (2000).

26. Worth (1975),"In-situ measurement of initial stresses and deformation characteristics". Proceeding Specialty Conference on In-situ Measurement of Soil Prperities. ASCE, Vol.2, P: 181-230.

27. Worth, C.P "General theories of earth pressure and deformation". Proceeding 5th European Conference on Soil Mechanics and Foundation Engineering, Madrid, vol.2, P: 33-52.

28. Yung, Ying and Chen (2002)," Passive earth pressure with critical state concept." Journal of geotechnical and geoenvironmental engineering. Vol 128. No.8. P: 651-659.

29. Da-Yong Zhu and Qihu Qian (2000) "Determination of passive earth pressure coefficients by the method of slices." Canadian Geotechnical Journal. Vol 37 P: 485-491.

APENDIX 1

MATLAB 6.1 PROGRAM FOR HOMOGENEOUS NORMALLY AND OVERCONSOLIDATED COHESIONLESS SOIL

```
clear
for OCR=1:1
   OCR=OCR
   %OCR=2.2;
for t=1:1:100
n=12;
lemda=t;
phi=pi*10/180;
phi2=phi;
phinew=atan((tan(phi)+tan(phi2))/2);
%OCR=2;
delta0=0;
deltap=0*pi/180;
delta(n)=deltap;
beta=((t-4)*phi/4)*0.39278*0;
theta0=((t/100)+.1)*((pi/4)-(phi/2));
r(t)=theta0;
%-(beta/2)-0.5*asin(sin(beta)/sin(phi)));
alpha0=(pi/2)-theta0-phi;
ratio=beta/phi;
for i=1:n
  theta(i)=(pi/2-theta0)*i/n + theta0;
  %theta(1)=theta0;
end
for i=1:n-1
 %delta(i)=((deltap-phi)*(theta(i)-theta0)/(pi/2-theta0))+phi+lemda*sin(pi*(theta(i)-
theta0)/(pi/2-theta0));
%delta(i)=(delta0+atan(-1*((tan(delta0)+tan(deltap)))*i/n));
delta(i) = delta0+(i/n)*deltap;
end
alphan=0.5*(acos(cos(phinew-deltap)-((sin(phinew-deltap))/tan(phinew)))-phinew-
deltap);
alpha(n)=alphan;
for i=1:10
  % alpha(i)=alphan-atan((tan(alpha0)-tan(alphan))*i/n);
  alpha(i)= ((i-10)/(.5*n))^2*(alpha0);
end
  for i=11:n-1
  alpha(i)= ((i-10)/(.5*n))^2*(alphan);
end
```

```
if OCR==1
   b=1;
elseif OCR==2
   b=1.35*cos(deltap)/cos(45*pi/180-phinew);
elseif OCR==3
   b=1.35*cos(deltap)/cos(45*pi/180-phinew);
else
   b=1.35*cos(deltap)/cos(45*pi/180-phinew);
end
k0=b*sqrt(OCR)*sin(theta0+alpha0)*sin(theta0+beta)*sin(alpha0+phi)/(sin(alpha0-
beta)*sin(theta0+alpha0+2*phi));
term1=sin(theta(1)+alpha(1))/(sin(theta0+alpha(1))*sin(theta(1)+alpha(1)+delta(1)+phi2)
);
term2=(k0)*sin(theta(1)+alpha(1))*sin(theta0+alpha(1)+delta(1)+phi2)/sin(theta0+alpha(
1));
term3=sin(theta(1)-theta0)*sin(alpha(1)+phi2);
k(1)=term1*(term2+term3);
%term4=sin(theta(2)+alpha(2))/sin(theta(1)+alpha(2))*sin(theta(2)+alpha(2)+delta(2)+ph
i);
%term5=(1/k(1))*(sin(theta(2)+alpha(2))*sin(theta(1)+alpha(2)+delta(1)+phi)/sin(theta(1
)+alpha(2));
%term6=sin(theta(2)-theta(1))*sin(alpha(2)+phi);
%k(2)=term4*term5+term6;
for i=2:n
term7=sin(theta(i)+alpha(i))/(sin(theta(i-
1)+alpha(i))*sin(theta(i)+alpha(i)+delta(i)+phi2));
term8=k(i-1)*sin(theta(i)+alpha(i))*sin(theta(i-1)+alpha(i)+delta(i-1)+phi2)/sin(theta(i-
1)+alpha(i));
term9=sin(theta(i)-theta(i-1))*sin(alpha(i)+phi2);
   k(i)=term7*(term8+term9);
end
kp(t)=k(n);
end
%deltap1=0:5:phi*180/pi;
%plot(deltap1,kp,'*')
kp=kp
end
plot(r,kp)
```

APENDIX 2

MATLAB 6.1 PROGRAM FOR TWO LAYERED NORMALLY AND OVERCONSOLIDATED COHESIONLESS SOIL

```
clear
for OCR=1:4
   OCR=OCR
   %OCR=2.2;
%for t=1:1:170
n=12;
%lemda=t;
phi=pi*15/180;
phi2=pi*10/180;
phinew=atan((tan(phi)+tan(phi2))/2);
%OCR=2;
delta0=0;
deltap=10*pi/180;
delta(n)=deltap;
beta=0;
theta0=(pi/4)-(phi/2);
%r(t)=theta0*180/pi;
%-(beta/2)-0.5*asin(sin(beta)/sin(phi)));
alpha0=(pi/2)-theta0-phi;
%ratio=beta/phi;
for i=1:n
  theta(i)=(pi/2-theta0)*i/n + theta0;
  %theta(1)=theta0;
end
for i=1:n-1
 %delta(i)=((deltap-phi)*(theta(i)-theta0)/(pi/2-theta0))+phi+lemda*sin(pi*(theta(i)-
theta0)/(pi/2-theta0));
%delta(i)=(delta0+atan(-1*((tan(delta0)+tan(deltap)))*i/n));
delta(i) = delta0+(i/n)*deltap;
end
alphan=0.5*(acos(cos(phinew-deltap)-((sin(phinew-deltap))/tan(phinew)))-phinew-
deltap);
alpha(n)=alphan;
for i=1:10
  % alpha(i)=alphan-atan((tan(alpha0)-tan(alphan))*i/n);
  alpha(i)= ((i-10)/(.5*n))^2*(alpha0);
end
```

```
  for i=11:n-1
  alpha(i)= ((i-10)/(.5*n))^2*(alphan);
end
if OCR==1
   b=1;
elseif OCR==2
  %b=(t/170)^2;
  b=1.35*cos(deltap)/cos(45*pi/180-phinew);
elseif OCR==3
   b=1.35*cos(deltap)/cos(45*pi/180-phinew);
else
   b=1.35*cos(deltap)/cos(45*pi/180-phinew);
end
k0=b*sqrt(OCR)*sin(theta0+alpha0)*sin(theta0+beta)*sin(alpha0+phi)/(sin(alpha0-
beta)*sin(theta0+alpha0+2*phi));
term1=sin(theta(1)+alpha(1))/(sin(theta0+alpha(1))*sin(theta(1)+alpha(1)+delta(1)+phi2)
);
term2=(k0)*sin(theta(1)+alpha(1))*sin(theta0+alpha(1)+delta(1)+phi2)/sin(theta0+alpha(
1));
term3=sin(theta(1)-theta0)*sin(alpha(1)+phi2);
k(1)=term1*(term2+term3);
%term4=sin(theta(2)+alpha(2))/sin(theta(1)+alpha(2))*sin(theta(2)+alpha(2)+delta(2)+ph
i);
%term5=(1/k(1))*(sin(theta(2)+alpha(2))*sin(theta(1)+alpha(2)+delta(1)+phi)/sin(theta(1
)+alpha(2));
%term6=sin(theta(2)-theta(1))*sin(alpha(2)+phi);
%k(2)=term4*term5+term6;
for i=2:n
term7=sin(theta(i)+alpha(i))/(sin(theta(i-
1)+alpha(i))*sin(theta(i)+alpha(i)+delta(i)+phi2));
term8=k(i-1)*sin(theta(i)+alpha(i))*sin(theta(i-1)+alpha(i)+delta(i-1)+phi2)/sin(theta(i-
1)+alpha(i));
term9=sin(theta(i)-theta(i-1))*sin(alpha(i)+phi2);

   k(i)=term7*(term8+term9);
end
%kp(t)=k(n);
%end
%deltap1=0:5:phi*180/pi;
%plot(deltap1,kp,'*')
kp=k(n)
end
%plot(r,kp)
```